ABSTRACT

Title of dissertation: APPLICATION OF THE
N-QUANTUM APPROXIMATION
TO THE PROTON RADIUS PROBLEM

Steven Cowen, Doctor of Philosophy, 2013

Dissertation directed by: Professor O.W. Greenberg
Department of Physics

This thesis is organized into three parts: 1. Introduction and bound state calculations of electronic and muonic hydrogen, 2. Bound states in motion, and 3. Treatment of soft photons. In the first part, we apply the N-Quantum Approximation (NQA) to electronic and muonic hydrogen and search for any new corrections to energy levels that could account for the 0.31 meV discrepancy of the proton radius problem. We derive a bound state equation and compare our numerical solutions and wave functions to those of the Dirac equation. We find NQA Lamb shift diagrams and calculate the associated energy shift contributions. We do not find any new corrections large enough to account for the discrepancy. In part 2, we discuss the effects of motion on bound states using the NQA. We find classical Lorentz contraction of the lowest order NQA wave function. Finally, in part 3, we develop a clothing transformation for interacting fields in order to produce the correct asymptotic limits. We find the clothing eliminates a trilinear interacting Hamiltonian term and produces a quadrilinear soft photon interaction term.

APPLICATION OF THE N-QUANTUM APPROXIMATION TO THE PROTON RADIUS PROBLEM

by

Steven Cowen

Dissertation submitted to the Faculty of the Graduate School of the
University of Maryland, College Park in partial fulfillment
of the requirements for the degree of
Doctor of Philosophy
2013

Advisory Committee:
Professor Rabindra Mohapatra, Chair/Advisor
Professor Kaustubh Agashe
Professor Zackaria Chacko
Professor William M. Goldman
Professor Stephen Wallace

Acknowledgments

I would like to thank my advisor, Professor O.W. Greenberg for giving me the opportunity to work on very interesting problems over the past few years. His advice and guidance were invaluable and it would have been impossible for me to reach this point without him.

I would also like to thank Professor Steve Wallace for his extremely helpful input.

I'd also like to thank my office colleagues for interesting and meaningful discussions over the years, as well as my family for supporting me through all of my efforts.

Table of Contents

List of Figures

Chapter 1: Introduction and Bound State Calculations of Electronic and Muonic Hydrogen

1.1 Introduction

The N-Quantum Approximation (NQA) is a procedure used for studying relativistic bound states with two or more constituents. It relies on the Haag expansion [1] to replace interacting fields in terms of asymptotic fields in operator equations of motion and in any other operator equation of interest. The introduction of asymptotic bound state fields into the Haag expansion allows us to interpret the Haag amplitudes as bound state wave functions and the final goal of the NQA is to derive an equation that can be used to solve for these wave functions and their associated eigenvalues. We will discuss the general procedure in more detail in section 1.3.

The NQA is an alternative to the Bethe-Salpeter (BS) equation, which is the more well known approach to studying relativistic bound states. They sometimes arrive at similar results, but their procedures are very different. The BS wave function for a 2-particle system is the transition amplitude of the two constituents

into a bound state where both constituents are allowed to be off shell,

$$\Psi_{BE} = \langle \Omega | \phi_1 \phi_2 | B \rangle \tag{1.1}$$

where ϕ_i are constituents and B is the bound state. In comparison, one of the NQA wave functions has one constituent on shell and one constituent off shell, and the other wave function has them reversed,

$$\Psi_{NQA_{2B}} = \langle \Omega | \phi_1 \phi_2^{in} | B \rangle, \tag{1.2}$$

$$\Psi_{NQA_{1B}} = \langle \Omega | \phi_1^{in} \phi_2 | B \rangle. \tag{1.3}$$

The derivation of the BS equation begins with the Dyson equation for the two particle Green function while the NQA's roots are, as stated above, in Haag's operator expansion. We will see in section 1.3.4 that in a certain approximation, the NQA can yield a QED spectator bound state equation which can be derived from the BS equation. We will discuss the advantages and disadvantages of both methods in section 1.3.

The NQA has been used in the past papers to study relativistic and non-relativistic bound states. A model for a bound state at rest composed of two scalars mediated by a third scalar was analyzed within the framework of the NQA in [2]. Other applications of the NQA, such as the study of symmetry breaking, scaling limits, and a deuteron model, can be found in [3], [4], and [5]. Some of the methods used in this thesis are discussed in great detail in [6]. In [6], a simplified bound

state equation is derived via the NQA. A QED bound state equation is solved in the non-relativistic limit after the Haag amplitude is reduced to 2×2 block form using an auxiliary condition which we will discuss in detail later. We will also be reducing the Haag amplitude to block form, but in a different way. The author of [6] also uses hyperboloidal harmonics to analyze the fully relativistic bound state equation. The mass shell delta functions introduced during the NQA procedure makes the use of hyperboloidal harmonics natural in this problem. After a coordinate transformation and some equation manipulation, a bound state equation that is numerically tractable arises. While this method of solving the bound state equation is elegant, we found that complications arise when this coordinate transformation is applied to a bound state equation that includes higher order QED contributions.

There are several other applications of the NQA that have not been fully explored. One such application is baryon spectroscopy. The Haag expansion for QCD constituents must be modified in order to take confinement into account. It may be possible to do this with projection operators that force QCD constituents to form color singlets. As shown in [7], a corollary of the use of these projection operators is confinement of the constituents. The non-perturbative nature of QCD makes truncating the Haag expansion difficult, but some kind of chiral constituent quark model such as the one given in [8] may solve some problems.

In this thesis, we focus on the application of the NQA to the simple case of the hydrogen atom, specifically muonic hydrogen. This is one of the most simple bound states in existence because the lepton is primarily bound through QED interactions. In electronic hydrogen, the proton is much more massive than the electron

($\frac{me}{mp} \approx 0.0005$) and extremely large compared to the binding energy, making the infinite proton mass limit useful. Terms with a proton mass in the denominator are suppressed. In muonic hydrogen, the proton mass is just about 9 times larger than the muon mass. Higher order terms that can be ignored in electronic hydrogen because of the proton's mass cannot necessarily be ignored in muonic hydrogen.

Both electronic and muonic hydrogen have been studied in great detail in many papers, for example [9], [10] , [11] , and [12], so we should explain our motivation for using the NQA to study an already well known bound state. In July 2010, a significant discrepancy between the derived proton radius from electronic hydrogen measurements and the proton radius found through muonic hydrogen measurements was discovered by Pohl et. al. in [14]. The proton radius enters the Lamb shift calculations as a parameter that characterizes the proton structure dependence of the energies involved:

$$\Delta E = 209.9779 - 5.2262 r_p^2 + 0.0347 r_p^3 \text{ meV}, \tag{1.4}$$

where r_p is given in fm. Using the accepted value of the proton radius, r_p yields a ΔE that differs from the value measured by Pohl et al. The amount of missing energy needed to account for the discrepancy is about 0.31 meV. One of the potential causes of this discrepancy is a problem in the QED calculations. The authors of [15] and [16] investigate this potential cause by reevaluating QED calculations in bound states, specifically in muonic hydrogen. This thesis also focuses on the QED aspects of the proton radius problem. We will discuss the findings of some of these papers

in more detail in the following section.

This thesis will begin with a summary of the proton radius problem in section 1.2 followed by some NQA preliminaries in section 1.3. In this third section, we will discuss the NQA in general and give some background into the asymptotic fields of the Haag expansion. We explain NQA diagrams, which are similar to Feynman diagrams, and the rules that can be used to write down expressions from the diagrams. We find the lowest order relativistic bound state equation for a hydrogen-like atom bound by Coulomb potential. We discuss our normalization scheme, and a way of relating the two lowest order bound state Haag amplitudes. We solve our equation numerically in momentum space and compare to solutions of the Dirac-Coulomb equation. We also discuss some of the magnetic splitting between levels of similar orbital angular momentum. The purpose of this third section is not to address the proton radius problem directly, but to explain how the NQA can be used to analyze simple bound states.

Section 1.4 is more directly related to the proton radius problem. We begin this section by discussing the NQA Lamb shift diagrams and how they can be reduced to diagrams resembling the well known vacuum polarization, self energy, and vertex Feynman diagrams for the Lamb shift. We go on to calculate some of the Lamb shift terms and compare with some of the more familiar results. We particularly pay attention to the vacuum polarization contribution, which is by far the largest contribution to the Lamb shift in muonic hydrogen. We work in momentum space for the entirety of this section.

The next section is dedicated to discussing the effects of bound states in mo-

tion. Motion of bound states most likely is not relevant to the proton radius problem, but there has been discussion on how to properly incorporate scattering data into the determination of the proton radius. In [17], Robson claims to be able to resolve the discrepancy between the proton radius from electron scattering and that from muonic hydrogen spectroscopy by stating that the electric form factor in the electron scattering analysis is not Lorentz invariant and must be modified. This modification results in the addition of a contribution to the proton mean square radius in the rest frame. This is a result of the Lorentz transformation of the mean square radius in the Breit frame of the electron scattering experiment to the rest frame. This addition does resolve the discrepancy between the muonic hydrogen spectroscopy results and the electron scattering results, but it fails to account for electronic hydrogen spectroscopy, which is more precise than electronic scattering. Additionally, if Robson's adjustment is applied in the comparison of the proton radius from electronic hydrogen spectroscopy to the proton radius from electronic scattering, a discrepancy between these two radii emerges. Still, the effects of motion on relativistic bound states is an interesting topic and one that is well suited for analysis within the NQA framework. Analysis of bound state motion is necessary to make electron scattering and muon scattering experiments useful in the search for a solution to the proton radius problem.

In the final section of this thesis, we discuss the proper handling of soft photons. Because of the long range Coulomb interaction, the asymptotic *in* and *out* states in QED do not technically exist. Instead, a certain dressing must be applied to a field before it has the proper asymptotic limit. Since the Haag expansion of

the NQA is based on expanding interacting fields in terms of *in* fields, it is very important to make sure properly dressed fields are used in our formulation of the bound state problem. A result of the dressing is a two-body interaction between charged particles with soft photons of momentum significantly less than αm_e. To make this relevant to the proton radius problem, we should investigate the effects of clothing constituents of bound states. It is possible that renormalization of QED already properly accounts for soft photon interactions, but the effects of soft photon interactions within the NQA framework have not been studied in detail.

1.2 Summary of the proton radius problem

An impressive experiment by Pohl et. al. [14] in 2010 found a major discrepancy between the accepted CODATA value of the proton radius and the proton radius found from muonic hydrogen spectroscopy. Pohl et. al. used pulsed laser spectroscopy to measure the Lamb shift ($2S^{F=1}_{1/2} - 2P^{F=2}_{3/2}$) of muonic hydrogen, and then used well known and accepted QED calculations to find a value for the proton radius. This radius was found to be 0.84184(67) fm, 5 standard deviations away from the CODATA value, 0.8768(69) fm. If the experiment was not flawed, which does not seem to be the case, we must either reevaluate the QED calculations, reexamine the current description of the proton structure and its influence on the Lamb shift, or introduce new particle interactions. It is also possible that the discrepancy is caused by more than one of these factors. In 2013, Antognini et al. [18] measured the same transition and found similar results. Antognini obtained a proton radius

that was 7 standard deviations smaller than the world average. Methods to resolve the problem have been proposed by several authors.

Carlson, Nazaryan and Griffioen [19] recalculated some structure dependent terms in the hyperfine splitting of muonic hydrogen. Their claim was that the usual structure dependent terms needed to be corrected because there are overlapping terms in the elastic and polarizability parts of the calculation. Their results are a minor change to the 2S-2P splitting, but not enough to explain the discrepancy.

Carroll, Thomas, Rafelski, and Miller [15] implemented a non-perturbative numerical approach. Their basic idea was to start with an effective Dirac equation and first guess a value for the eigenvalue. Then, they insert the eigenvalue into the equation and fix the boundaries of the wave function with assumed boundary conditions. They then integrated from both boundaries to some center value. The differences between the two values of these integrals was taken as a measure of error in the eigenvalue. The eigenvalue is adjusted and the process is repeated until the two integral values agree satisfactorily. Their results were in agreement with the accepted non-relativistic QED perturbative calculations and could not resolve the discrepancy.

Varger, Chiang, Keung, and Marfatia [20] attempted to resolve the problem by introducing new scalar, pseudoscalar, vector, and tensor flavor-conserving nonuniversal interactions. They conclude that low energy constraints from neutron scattering, the muon anomalous magnetic moment, and muonic atomic transitions, exclude any new spin-0, spin-1, or spin-2 particles as an explanation of the discrepancy, but that allowing a scalar and pseudoscalar boson with appropriately tuned couplings

might lead to cancellation and cause the theory to be within the low energy bounds while introducing a new muon coupling.

Authors have also investigated in great detail 2-photon exchange (2PE) and proton structure effects in muonic hydrogen. In [21], Chen and Dong consider corrections to the scattering amplitude in the process $l+p \rightarrow l+p$ from 2PE in a hadronic model where the intermediate states of the 2PE process are ground state nucleons or excitations. These corrections are vital in the use of muon-proton scattering data to find accurate form factors. The authors of [22] looked at 2PE contributions to the Lamb shift. The sum over nucleon excitations was done using virtual photo absorption data. They concluded that the discrepancy could not be caused by proton structure-dependent uncertainty alone.

Mohr, Griffith, and Sapirstein [23] developed a new framework in which to study muonic hydrogen using a variant of the Furry representation. The binding fields are three charged quarks contained within a spherical well. They used this model to calculate one- and two-photon exchange contributions to the Lamb shift, and their results were remarkably close to the typical Lamb shift expression using a model for the form factor of the proton.

A final interesting possible solution was proposed in [24] by Wang and Ni. They explained how the discrepancy can be resolved through the use of large extra dimensions (LED). A gravitational potential energy term due to the LED is set equal to the discrepancy, 0.31 meV. The LED potential depends on the number of extra dimensions, the radius of the extra dimensions (all taken to be the same), and the hard core radius (in the theory, a repulsive interaction at some radius is

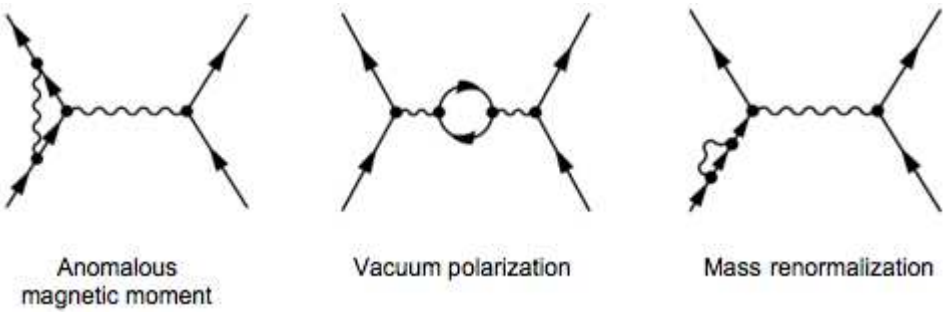

Figure 1.1: Lamb shift diagrams

needed for stability). The mass scale and size of the extra dimensions are related in this model. The authors concluded that an LED model with a hard core radius of 1 am, 0.1 am, or 0.02 am with 4 or more extra dimensions could account for the discrepancy without being inconstent with hydrogen and muonic spectroscopic data and muonium bounds.

Pohl's findings along with the subsequent papers on the proton radius problem motivates us to use the NQA to explore bound state properties. Our method will be be general enough to be applied to other two-body bound states such as muonium, positronium, and the $\bar{\mu}\mu$ system, although we do not discuss annihilation diagrams. Our ultimate goal is to take a similar approach as [15] and try to see if our way of calculating the Lamb shift results in any new energy contributions. We are hoping that either our method gives us some extra terms that other methods do not have, or perhaps we can calculate the Lamb shift in a more exact way in our framework. The usual diagrams used to calculate the Lamb shift are shown in Figure 1.1. The fermion lines on the left represent the electron or muon, and the line on the right is the proton. These diagrams are slightly different in the NQA. We will have more

diagrams with some of the lines being on-shell and others remaining off-shell. We discuss our framework for calculating the Lamb shift diagrams in more detail in section 1.4.

Before moving on to NQA preliminaries, we should briefly mention what we mean by "proton radius" and how it enters the Lamb shift. A detailed explanation of this calculation is given in [12], and we summarize these calculations here. In a non-relativistic framework, the Hamiltonian for the two-body static Coulomb problem can be split into two terms:

$$H \equiv H_0 + \Delta V_c \tag{1.5}$$

where

$$H_0 = \frac{p^2}{2\mu} - \frac{Z\alpha}{r} \tag{1.6}$$

and

$$\Delta V_c(r) = -Z\alpha \int d^3s \rho(s) \left(\frac{1}{|\mathbf{r} - \mathbf{s}|} - \frac{1}{r} \right) \tag{1.7}$$

where $\rho(s)$ is the charge density of the proton. $\Delta V_c(r)$ is treated as a perturbation and the well known Schrodinger-Coulomb solutions are the lowest order wave

functions. After applying perturbation theory, the energy correction found is [12]

$$\Delta E \approx \frac{2\pi Z\alpha}{3}|\phi_n(0)|^2\left(\langle r^2\rangle - Z\alpha\mu\langle r^3\rangle + \frac{(Z\alpha\mu)^2}{10}\langle r^4\rangle(5+\frac{1}{n^2}) + \ldots\right) \tag{1.8}$$

where

$$\langle r^n\rangle \equiv \int d^3r r^n \rho(r) \tag{1.9}$$

and $\phi_n(0)$ is the non-relativistic wave function at the origin. Since the wave function of the S-state at the origin differs from that of the P-state at the origin, this energy correction will have a significant effect on the $2S-2P$ Lamb shift.

1.3 N-quantum preliminaries and lowest order bound state equations

The following work can be found in [13]. In this section, we will develop a method to calculate the wave functions and energy levels of 2-body bound states. The main idea of the NQA is to expand the interacting fields that appear in the Lagrangian or Hamiltonian in terms of *in* fields. This method has been discussed in detail in [5, 6, 25, 26]. These *in* fields are related to eigenstates of the Hamiltonian with quantum numbers of freely moving asymptotic incoming particles. We assume that these fields form a complete set. The Haag expansion of the interacting fields in terms of *in* fields is generally an infinite series. For the purpose of approximation, we terminate this series, keeping only terms with a small number of *in* fields. Each term in the series contains an undetermined function of the relevant coordinates

known as a Haag amplitude. The goal of the NQA is to derive an equation, or a set of equations, that can be used to solve for these amplitudes. We accomplish this by taking the equations of motion for the interacting fields, expanding each of the fields in normal-ordered products of *in* fields, and normal ordering again. We remove residual *in* fields by contracting with external *in* fields. After all *in* fields are contracted, the results are bound state equations for the amplitudes. If only low order terms are used in the Haag expansions, these equations will be linear in the amplitudes. After some more simplifications, a spectator equation can be found that was first derived in [5].

Although they sometimes arrive at similar conclusions, the NQA is quite different than the Bethe-Salpeter method. The derivation of the Bethe-Salpeter equation begins with the Dyson equation for the two particle Green function, while the N-Quantum's roots are in Haag's operator expansion. Unlike the Bethe-Salpeter wave function, the position space Haag amplitudes depend only on three-vectors, although the equation is still relativistic. With the use of these amplitudes, the N-Quantum procedure avoids using a relative time coordinate while still maintaining a covariant formalism. The Haag amplitude is similar to a Bethe-Salpeter amplitude with one of the constituent's mass shell singularity removed and that constituent's momentum restricted to the mass shell.

One of the advantages of the NQA over some other QED bound state analyses is the independent introduction of mass parameters, rather than the use of a reduced mass. There are terms which cannot be expressed in terms of the simpler reduced mass alone, but must be written in terms of both masses independently. For this

reason, formulations such as the NQA and the Bethe-Salpeter equation are superior to the ordinary Dirac equation in describing bound states accurately. This is of particular importance in muonic hydrogen where the mass of the muon is only about 1/10th the proton mass.

1.3.1 Asymptotic fields and the Haag expansion

The collection of all possible *in* fields of a quantum field theory form a complete set once all of the relevant quantum numbers are specified. Because of this, we can use the *in* fields as the building blocks of our formulation and expand interacting fields in terms of them. The end results should be the same as the those produced by staying in the interacting picture. *in* fields are preferred over interacting fields because they obey the free equations of motion, have simple (anti-)commutation relations and obey these relations everywhere in space time. We acknowledge the difficulty that arises in this formulation when dealing with charged particles, where technically asymptotic limits do not exist. We discuss a modified "dressed" particle where asymptotic limits do exist in section 1.6, but ignore this complication in the next few sections.

As stated above, the Haag expansion involves expanding interacting fields in terms of normal ordered *in* fields with c-number coefficients known as Haag amplitudes. In the NQA, we expand these interacting fields in the operator equations of motion derived from some Lagrangian or Hamiltonian. After the *in* fields are contracted, the resulting set of equations can be used to solve for the Haag ampli-

tudes. This can be done numerically or, if simplifications are made, analytically. The amplitudes found at the end of the NQA serve the purpose of bound state wave functions.

The original Haag expansion did not include bound states. This modification was first made in [5]. The existence of these bound states are assumed. If a solution for the bound state can be found, then the bound state exists. As said earlier, the main advantages of using a Haag expansion formulation over the Bethe-Salpeter equation (discussed in [27]) are the lack of spurious solutions with negative norm amplitudes in the NQA, the three dimensional relativistic bound state equations of the NQA as opposed to the 4D equations of the BS equation, and the lack of a relative time coordinate in the NQA.

The infinite series of terms that results from the Haag expansion obviously creates problems when a finite number of calculations must be made. Luckily, in the case of QED (or any theory with a small coupling constant), it can be shown that the Haag amplitudes that are coefficients of terms with a greater number of constituent *in* fields contain higher powers of the coupling constant. The reason for this is that higher order Haag amplitudes contain more fundamental vertices. This is easily shown by finding expressions for the higher order amplitudes in terms of lower amplitudes via the equations of motion. We find an example of such expressions in section 1.4. The presence of higher powers of the coupling constant in higher Haag amplitudes allows us to truncate the series and calculate to some order in perturbation theory. We will discuss this truncation and the Haag terms that must be kept in order to calculate to a given order in the following sections.

1.3.2 Relativistic model of the hydrogen atom

We take the fundamental fermion fields to be $e_\alpha(x)$, $\mu_\alpha(x)$, $p_\alpha(x)$, for the electron, muon and proton, respectively. The photon vector potential is $A_\mu(x)$. The operator equations of motion for these fields derived from the QED Lagrangian are

$$(i\ \partial\!\!\!/ - m)e(x) = \frac{e}{2}[A\!\!\!/(x), e(x)]_+, \tag{1.10}$$

$$(i\ \partial\!\!\!/ - m_\mu)\mu(x) = \frac{e}{2}[A\!\!\!/(x), \mu(x)]_+, \tag{1.11}$$

$$(i\ \partial\!\!\!/ - M)p(x) = -\frac{e}{2}[A\!\!\!/(x), p(x)]_+, \tag{1.12}$$

$$\partial^\mu \partial \cdot A - \partial \cdot \partial A^\mu = \frac{e}{2}([\bar{e}(x), \gamma^\mu e(x)]_- + [\bar{\mu}(x), \gamma^\mu \mu(x)]_- - [\bar{p}(x), \gamma^\mu p(x)]_-), \tag{1.13}$$

where we have left out renormalization counter terms. Eq.(1.13) follows from the equation for the electromagnetic tensor,

$$\partial_\nu F^{\mu\nu}(x) = \frac{e}{2}([\bar{e}(x), \gamma^\mu e(x)]_- + [\bar{\mu}(x), \gamma^\mu \mu(x)]_- - [\bar{p}(x), \gamma^\mu p(x)]_-) \tag{1.14}$$

where $F^{\mu\nu}(x) = \partial^\mu A^\nu(x) - \partial^\mu A^\nu(x)$ and the masses of the electron, muon, proton, and hydrogen atom *in* states are m, m_μ, M, and M_i, respectively. The equations are symmetric under $e \leftrightarrow \mu,\ m \leftrightarrow m_\mu$ as well as $e \leftrightarrow p,\ m \leftrightarrow M$ and $\mu \leftrightarrow p,\ m_\mu \leftrightarrow M$ interchange. We will see a similar symmetry in our bound state equation for the Haag amplitudes. Since we are dealing with operators and will be expanding each operator field in terms of a series of normal ordered in fields, we have taken care to properly symmetrize the equations using anti-commutators and commutators. The

order of the fields matters greatly when dealing with operators because for fermonic contractions it affects which mass shell appears in a momentum space calculation. Properly symmetrizing ensures that we will have both the positive and the negative mass shells in our calculations.

We now expand the interacting fields in terms of *in* fields via the Haag expansion. As stated above, we truncate the series, keeping the first term involving the hydrogen bound-state *in* fields, h_i^{in}:

$$e(x) = e^{(in)}(x) + \sum_i \int d^3y d^3z : \bar{p}^{(in)}(y) f_{\bar{p}h,i}(x-y, x-z) i \overleftrightarrow{\frac{\partial}{\partial z^0}} h_i^{(in)}(z) :, \quad (1.15)$$

$$\bar{e}(x) = \bar{e}^{(in)}(x) + \sum_i \int d^3y d^3z : h_i^{(in)\dagger}(z) i \overleftrightarrow{\frac{\partial}{\partial z^0}} \bar{f}_{\bar{p}h}(x-y, x-z) p^{(in)}(y) :, \quad (1.16)$$

$$p(x) = p^{(in)}(x) + \sum_i \int d^3y d^3z f_{\bar{e}h}(x-y, x-z) : \bar{e}^{(in)}(y) i \overleftrightarrow{\frac{\partial}{\partial z^0}} h_i^{(in)}(z) :, \quad (1.17)$$

$$\bar{p}(x) = \bar{p}^{(in)}(x) + \sum_i \int d^3y d^3z : h_i^{(in)\dagger}(z) i \overleftrightarrow{\frac{\partial}{\partial z^0}} e^{(in)}(y) : \bar{f}_{\bar{e}h}(x-y, x-z), \quad (1.18)$$

$$\begin{aligned} A^\mu(x) = A^{(in)\mu}(x) + \int d^3y d^3z [: \bar{p}^{(in)}(y) f^\mu_{\bar{p}p}(x-y, x-z) p^{(in)}(z) : \\ + : \bar{e}^{(in)}(y) f^\mu_{\bar{e}e}(x-y, x-z) e^{(in)}(z) :] \\ + \sum_i \int d^3y d^3z d^3w : \bar{e}^{(in)}(y) \bar{p}^{(in)}(z) \\ \times f^\mu_{\bar{e}\bar{p}h}(x-y, x-z, x-w) i \overleftrightarrow{\frac{\partial}{\partial w^0}} h_i^{(in)}(w) :, \end{aligned} \quad (1.19)$$

where $\sum_i$ is the sum over the various hydrogen states, i.e. ground and excited states,

and

$$\bar{f}_{\bar{p}h}(x,y) = \gamma^0 f^\dagger_{\bar{p}h}(x,y)\gamma^0, \tag{1.20}$$

$$\bar{f}_{\bar{e}h}(x,y) = \gamma^0 f^\dagger_{\bar{e}h}(x,y)\gamma^0, \tag{1.21}$$

and we label each amplitude by the *in* fields of which they are coefficient functions.

In this section, we use spectroscopic notation for the states of the hydrogen atom that is adapted to treating the proton spin on the same basis as the electron spin. In a section 1.4, we will discuss other possible bases. We use F, L, and S for the total angular momentum, the orbital angular momentum, and the lepton+proton spin, respectively. We should note that only F is an exact quantum number, i.e. L and S are approximate quantum numbers which only become exact in nonrelativistic approximations. We label states as nL^F_S, where n is the principle quantum number. This notation differs from the typical spectroscopic notation where the orbital angular momentum, L, is coupled to the electron spin, S_e, and then this sum, $J = L + S_e$, is coupled to the proton spin to get F. States in this basis are labeled as nL^F_J. We discuss this in more detail in section 1.4.

Up to this point, we have been working only in position space. While position space calculations may be more intuitive and in some cases simplify calculations (which we will see in section 1.4.5), we move to momentum space now because contractions between momentum space fields involve delta functions rather than a more complicated S function. Working in momentum space also replaces differential equations with integral equations, although even in position space there would be

integrals. We discuss the position space formalism more in future sections. We use the usual 4D Fourier transforms to move to momentum space

$$e(x) = \int d^4q e(q) \exp(-iq \cdot x), \tag{1.22}$$

with analogous formulas for the other fields. For simplicity, we leave tildes off the Fourier-transformed fields. The momentum space equations are

$$(\not{q} - m)e(q) = \frac{e}{2} \int d^4k [\not{A}(k), e(q-k)]_+, \tag{1.23}$$

$$(\not{q} - m_\mu)\mu(q) = \frac{e}{2} \int d^4k [\not{A}(k), \mu(q-k)]_+, \tag{1.24}$$

$$(\not{p} - M)p(p) = -\frac{e}{2} \int d^4k [\not{A}(k), p(p-k)]_+, \tag{1.25}$$

$$-k^\mu k \cdot A(k) + k^2 A^\mu(k) = \frac{e}{2} \int d^4q' ([\bar{e}(q'), \gamma^\mu e(k-q')], \tag{1.26}$$

$$+ [\bar{\mu}(q'), \gamma^\mu \mu(k-q')] - [\bar{p}(q'), \gamma^\mu p(k-q')]), \tag{1.27}$$

where we have once again left out counter terms. The purpose of this section is to outline the NQA procedure and arrive at a simple result which can be compared to other well known bound state equations. For these reasons, we will be keeping diagrams with only one loop here and working in the Coulomb gauge. Just as we did with the position space equations of motion, we must move the Haag expansions into momentum space. The right hand side of the equation of motion for the electron has a factor of $e(q-k)A(k)$. We will be expanding these two fields using the Haag expansion and only keeping terms with the fields $: \bar{p}^{(in)} h^{(in)} :$ left after contractions.

Since we wish to produce diagrams with only 1 loop (we will discuss how to calculate these diagrams shortly), we only need to keep certain terms with up to three *in* fields in the Haag expansions for e and A. Schematically, the contractions we will have are $:\bar{p}\overbrace{p::\bar{p}}h:$, $:\overbrace{A::A}\bar{p}h:$, and $:\bar{p}h\overbrace{\bar{e}::e}:$ where the overbraces stand for contractions. We neglect any term that involves a contraction between bound state *in* fields because they are much higher order in the coupling constant. Some of these terms will involve higher order amplitudes which we will simplify and others are renormalization diagrams which we will largely ignore in this section, but discuss in more detail in section 1.4. The momentum space Haag expansion for the electron field is

$$\begin{aligned} e(q) &= e^{in}(q) + \sum_j \int d^4p d^4b \delta(p+q-b) f_{\bar{p}h_j}(p,b) : \bar{p}^{in}(p) h_j^{in}(b) : \\ &\quad + \int d^4p d^4b \delta(p+q+k-b) f^{\mu}_{A\bar{p}h_j}(p,k,b) : A_\mu(-k)\bar{p}^{in}(p) h_j^{in}(b) :, \qquad (1.28) \\ \bar{e}(q) &= \bar{e}^{in}(q) + \sum_j \int d^4p d^4b \delta(p+q-b) : h_j^{in\,\dagger}(b) p^{in}(p) : \bar{f}_{\bar{p}h_j}(p,b) : \\ &\quad + \int d^4p d^4b \delta(p+q+k-b) : h_j^{in\,\dagger}(b) p^{in}(p) A_\mu(k) : \bar{f}_{A\bar{p}h_j}(p,b) :, \qquad (1.29) \end{aligned}$$

where $\bar{f}_{\bar{p}h_i}(p,b) = \gamma^0 f^\dagger_{\bar{p}h_i}(p,b)\gamma^{0T}$.

In this parametrization, we have for the adjoint of our bound state wave function

$$\begin{aligned} \langle 0|\bar{e}(q)\bar{p}^{in}(p) h_i^{in\,\dagger}(b)|0\rangle &= \delta(q+p-b)\bar{f}_{\bar{p}h_i}(p,b)(\not{p}+M) \\ &\quad \times \theta(p^0)\delta(p^2-M^2)\theta(b^0)\delta(b^2-M_i^2). \qquad (1.30) \end{aligned}$$

There are analogous expressions for the muon and proton fields. For the photon field,

$$A^{\mu}(k) = A^{\mu\ in}(k) + \int d^4p d^4p' \delta(k-p-p')[: \bar{p}^{in}(p) f^{\mu}_{pp'}(p,p') p^{in}(p') : \\ - : \bar{e}^{in}(p) f^{\mu}_{ee'}(p,p') e^{in}(p') : - : \bar{\mu}^{in}(p) f^{\mu}_{\mu\mu'}(p,p') \mu^{in}(p') :] \\ + \sum_j \int d^4p d^4p' d^4b : \bar{e}^{in}(p) \bar{p}^{in}(p') f^{\mu}_{\bar{e}\bar{p}hj}(p,p',b) h^{in}_j(b) : . \tag{1.31}$$

We assume translational invariance for our position space Haag expansion and we demand Lorentz covariance for the momentum space expression as well. As an example, we determine how the amplitude $f_{\bar{p}h}$ transforms under a Lorentz transformation using this assumption. Focusing only on the term with the lowest order Haag amplitude on the right hand side of Eq.(1.28), we apply the Lorentz transformation operator, L, to both sides,

$$Le_{\alpha}(p)L^{-1} = \int d^4k d^4b \delta(p-k-b) f_{\bar{p}h\alpha\beta}(k,b) : L\bar{p}^{in}_{\beta}(k) L^{-1} L h^{in}(b) L^{-1} : \\ \Lambda_{\frac{1}{2}} e_{\alpha}(L^{-1}(p)) = \int dk db \delta(p-k-b) f_{\bar{p}h\alpha\gamma}(k,b) : \bar{p}^{in}_{\beta}(\Lambda^{-1}(k)) \Lambda^{-1}_{\frac{1}{2}\beta\gamma} h^{in}(\Lambda^{-1}(b)) : . \tag{1.32}$$

where Λ is a Lorentz transformation and $\Lambda_{\frac{1}{2}}$ is the spinor representation of the

Lorentz transformation. The Haag expanded electron field for the left hand side is

$$\begin{aligned} LHS &= \int d^4k d^4b \delta(\Lambda^{-1}(p) - k - b) \Lambda_{\frac{1}{2}\alpha\sigma} f_{\bar{p}h\sigma\beta}(k,b) : \bar{p}^{in}_{\beta}(k) h^{in}(b) : \\ &= \int d^4k d^4b \delta(p - \Lambda(k) - \Lambda(b)) \Lambda_{\frac{1}{2}\alpha\sigma} f_{\bar{p}h\sigma\beta}(k,b) : \bar{p}^{in}_{\beta}(k) h^{in}(b) : \end{aligned} \tag{1.33}$$

and the right hand side is

$$\begin{aligned} RHS &= \int d^4k d^4b \delta(p - k - b) f_{\bar{p}h\alpha\gamma}(k,b) : \bar{p}^{in}_{\beta}(\Lambda^{-1}(k)) \Lambda^{-1}_{\frac{1}{2}\beta\gamma} h^{in}(\Lambda^{-1}(b)) : \\ &= \int d^4k d^4b \delta(p - \Lambda(k) - \Lambda(b)) f_{\bar{p}h\alpha\gamma}(\Lambda(k), \Lambda(b)) : \bar{p}^{in}_{\beta}(k) \Lambda^{-1}_{\frac{1}{2}\beta\gamma} h^{in}(b) : \end{aligned} \tag{1.34}$$

We have used the delta function's invariance to arrive at Eq.(1.33) and we have changed coordinates to arrive at Eq.(1.35). Comparing both sides, we find

$$\begin{aligned} \Rightarrow \Lambda_{\frac{1}{2}\alpha\sigma} f_{\bar{p}h\sigma\beta}(k,b) &= \Lambda^{-1}_{\frac{1}{2}\beta\gamma} f_{\bar{p}h\alpha\gamma}(\Lambda(k), \Lambda(b)) \\ f_{\bar{p}h\alpha\beta}(k,b) &= \Lambda^{-1}_{\frac{1}{2}\alpha\delta} \Lambda^{-1}_{\frac{1}{2}\beta\gamma} f_{\bar{p}h\delta\gamma}(\Lambda(k), \Lambda(b)) \end{aligned} \tag{1.35}$$

We will discuss the transformation properties of the amplitudes further in our discussion of bound states in motion in section 1.5.

Contractions between two momentum space *in* fields are

$$\langle 0 | e^{in}_{\alpha}(p_1) \bar{e}^{in}_{\beta}(p_2) | 0 \rangle = (\not{p}_1 + m)_{\alpha\beta} \delta^{(+)}_m(p_1) \delta^4(p_1 + p_2) \tag{1.36}$$

$$\langle 0 | \bar{e}^{in}_{\beta}(p_2) e^{in}_{\alpha}(p_1) | 0 \rangle = -(\not{p}_1 + m)_{\alpha\beta} \delta^{(-)}_m(p_1) \delta^4(p_1 + p_2) \tag{1.37}$$

$$\langle 0 | A^{\mu\, in}(p_1) A^{\nu\, in}(p_2) | 0 \rangle = -g^{\mu\nu} \delta^{(+)}_0(p_1) \delta^4(p_1 + p_2) \tag{1.38}$$

where $\delta_m^{\pm}(p) = \theta(\pm p^0)\delta(p^2 - m)$ and there are similar contractions for the proton and muon fields. Plugging the momentum space Haag expansions, Eq. (1.28) and (1.31), into the electron equation of motion, Eq. (1.23), and contracting *in* fields until the only fields remaining are $: \bar{p}^{(in)} h^{(in)} :$ yields a bound state equation that still contains a higher order amplitude. We drop terms that will be eliminated in renormalization. We can "peel" the residual *in* fields off by contracting with external p^{in} and h^{in} fields. This is equivalent to replacing the proton field by a factor of $(\not{p} + M)$, where p is the momentum of the external field, and dropping the integrals over their momenta. The bound state equation found from the electron equation of motion is

$$
\begin{aligned}
(\not{b} - \not{p} - m) f_{\bar{p}h}(p,b)(\not{p} + M)^T = \\
&\frac{e^2}{2(2\pi)^3} \int d^4p' \delta_M(p') \gamma^\mu \frac{f_{\bar{p}h}(p',b)(\not{p}' + M)^T}{(p-p')^2} (\gamma_\mu)^T (\not{p} + M)^T \\
&+ \frac{e}{2(2\pi)^3} \int d^4p' \delta_m(p') \gamma^\mu (f^\mu_{\bar{e}\bar{p}h}(p',p,b)(\not{p}' + m)^T)^T (\not{p} + M)^T. \qquad (1.39)
\end{aligned}
$$

We can use the proton equation of motion to find an expression for the higher order amplitude, $f^\mu_{\bar{e}\bar{p}h}$, in terms of the lower order amplitude, $f_{\bar{e}h}$, by collecting terms proportional to $: \bar{e}^{in} \bar{p}^{in} h^{in} :$. We once again keep only the lowest order term in this approximation. The relation is

$$
f^\mu_{\bar{e}\bar{p}h}(p',p,b)(\not{p}' + m)^T = -e \frac{\gamma^\mu f_{\bar{e}h}(p',b)(\not{p}' + m)^T}{(b - p' - p)^2}. \qquad (1.40)
$$

A similar procedure can be used to find an equation for $f_{\bar{e}h}$ using the proton equation

of motion. Substituting and keeping the dominant mass shells, we finally arrive at the one-loop equations for the two main lowest order amplitudes for any state of the hydrogen atom:

$$(\not{b}-\not{p}-m)f_e(p,b) = \frac{e^2}{2(2\pi)^3}\int\frac{d^3p'}{2E_{p'}}\gamma^\mu\frac{f_e(p',b)}{(p-p')^2}(\gamma_\mu)^T(\not{p}+M)^T - \frac{e^2}{2(2\pi)^3}\int\frac{d^3p'}{2e_{p'}}\gamma^\mu\frac{f_p(p',b)^T}{(b-p'-p)^2}(\gamma_\mu)^T(\not{p}+M)^T, \quad (1.41)$$

$$(\not{b}-\not{q}-M)f_p(q,b) = \frac{e^2}{2(2\pi)^3}\int\frac{d^3q'}{2e_{q'}}\gamma^\mu\frac{f_p(q',b)}{(q-q')^2}(\gamma_\mu)^T(\not{q}+m)^T - \frac{e^2}{2(2\pi)^3}\int\frac{d^3q'}{2E_{q'}}\gamma^\mu\frac{f_e(q',b)^T}{(b-q'-q)^2}(\gamma_\mu)^T(\not{q}+m)^T, \quad (1.42)$$

where $f_e(p,b) \equiv f_{\bar{p}h}(p,b)(\not{p}+M)^T$, $f_p(q,b) \equiv f_{\bar{e}h}(q,b)(\not{q}+m)^T$, $E_p = \sqrt{\mathbf{p}^2+M^2}$, $e_q = \sqrt{\mathbf{q}^2+m^2}$, p is the energy momentum of the on shell proton, and $q = b-p$ is the energy momentum of the off shell electron. Due to the projection operators, the amplitudes satisfy certain subsidiary conditions. $f_e(p,b)$ obeys the condition $f_e(p,b)(\not{p}-M)^T = 0$ and $f_p(q,b)$ obeys $f_p(q,b)(\not{q}-m)^T = 0$. These subsidiary conditions are useful in reducing the amplitudes to a more tractable form when calculating eigenvalues and wave functions. We discuss this in subsection 1.3.5.

Unlike the Bethe-Salpeter approach, we have arrived at a pair of coupled equations that describe the bound state. They are symmetric under subscript $e \leftrightarrow p$ and mass $m \leftrightarrow M$ interchange. These two equations differ from those found in Refs. [31] and [32] where Bethe-Salpeter equations with one on shell particle are found, but we will show that in a certain approximation they reduce to their Bethe-Salpeter counterparts. As far as we know, the exact properties of Eqs. (1.41) and

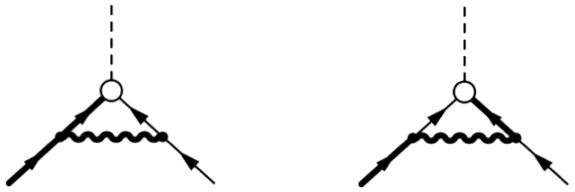

(a) (b)

Figure 1.2: Graphs for the right-hand side of the electron equation of motion. Heavy lines are off shell and light lines are on shell. The dashed line represents the bound state (hydrogen atom). The empty circle represents the amplitude f_e in panel (a) and f_p in panel (b). The left fermion line is the electron and the right line is the proton. Analogous graphs exist for the proton equation.

(1.42) are unexplored.

The terms on the right hand side of Eqs. (1.41) and (1.42) are expressed in diagrammatic form in Figures 1.2(a) and 1.2(b). Heavy lines are off shell and light lines are on shell. Point vertices represent the substitution of an off shell interacting field in terms of other interacting fields via the relevant equation of motion. These are the fundamental QED vertices. Circles indicate the use of the Haag expansion to express off shell interacting fields in terms of *in* fields with a Haag amplitude coefficient. We use similar diagrams in section 1.4 to show how higher order corrections are calculated.

We have arrived at the desired bound state equation through a somewhat arduous procedure. It would be useful for future calculations to develop a process for drawing and interpreting graphs, rather than contracting fields and simplifying more complicated expressions. The diagrams that are relevant to the preceding calculation must have one external off-shell electron line, an external on shell proton line, and an external on-shell bound state line. The two possible lowest order diagrams are

shown in Figure 2. The rules for analyzing the diagrams associated with the N-Quantum procedure are similar to Feynman rules, but they must also accommodate on-shell lines. The rules are:

1. Draw all possible relevant low order diagrams. In this case, these are diagrams with an "incoming" off-shell electron and on-shell proton and an "outgoing" on-shell bound state. Amplitude vertices should be distinct from normal vertices. Care must be taken to ensure the correct ordering of the following factors.

2. Write a factor of $\frac{1}{\not{p} - m}$ for any off-shell line not connected to an amplitude, where p is the momentum of the line and m is its mass (This factor is on the left hand side in Eq. (1.41)).

3. Write $e\gamma^{\mu}$ for every fermion-photon fundamental vertex.

4. Write nothing for any off shell line connected to an amplitude.

5. Write a factor of $\delta_m(p')f_i(p', b)$ for the bound state vertex, where p' is the 4-momentum of the on shell fermion line connected to the bound state vertex and m is its mass. Take a transpose.[1]

6. Write $-g_{\mu\nu}/k^2$ for every internal off shell photon line, where k is the momentum of the photon line.

7. Integrate over the internal on shell momentum with a factor of $(2\pi)^{-3}$.

8. Add a factor of $(\not{p}+m)^T$ for any on shell external fermion line, where m is the mass of the fermion.

9. Add a symmetry factor, in this case, $\frac{1}{2}$.

These rules must be slightly revised for more complicated diagrams, such as those including off shell internal fermion lines not connected to any amplitude.

In arriving at Eqs. (1.41) and (1.42), we have worked in Feynman gauge and we have kept only the dominant mass shell. The fully Lorentz covariant bound state equation has an energy integral over a full mass shell delta function. The opposite mass shell was also dropped in [6] in a section that uses the N-Quantum to study the hydrogen atom at rest. It is easy to see why the opposite mass shell is negligible. Looking at the momentum in the denominator, $k^2 \equiv (p-p')^2$, we find when the momentum p is on the opposite mass shell as p'

$$\begin{aligned} k^2 &= (E_p + E_{p'})^2 - (\mathbf{p}-\mathbf{p}')^2 \\ &\approx [\kappa_2\epsilon\left(1+\frac{(\frac{\mathbf{q}}{\kappa_2})^2 - \frac{2|\mathbf{b}|q_\parallel}{\kappa_2}}{2\epsilon^2}\right) + \kappa_2\epsilon\left(1+\frac{(\frac{\mathbf{q}'}{\kappa_2})^2 - \frac{2|\mathbf{b}|q_\parallel{}'}{\kappa_2}}{2\epsilon^2}\right)]^2 - (\mathbf{p}-\mathbf{p}')^2 \\ &= (2\kappa_2\epsilon)^2 + O(\alpha) \end{aligned}$$

where $\epsilon = \sqrt{\mathbf{b}^2 + (m_1+m_2)^2}$, $\kappa_2 = \frac{m_2}{m_1+m_2}$, $\mathbf{q}$ is the relative momentum, and $\mathbf{b}$ is the CM momentum. When the two momenta are on the same mass shell, we find

$$k^2 \approx -(\mathbf{k}_\perp^2 + \gamma^{-2}k_\parallel^2) \sim O(\alpha^2),$$

[1]The full mass shell function $\delta_m(p')$ is a result of symmetrization and specific to this example. For higher order terms, expressions will exist with higher order factors of $\delta_m^{(\pm)}(p)$. Symmetrization creates specific functions of the mass shell delta-functions such as $\Theta_1(p_1,p_2)$ found in Eq. (2.37).

a result which will be used section 1.5. The opposite mass shell term is suppressed by a factor of order $O(\frac{\alpha^2}{\epsilon^2})$ relative to the other mass shell and it does not have a pole at $\mathbf{p} = \mathbf{p}'$. While the negative mass shell does seem to be small compared to the positive shell, it may be important in the analysis of higher order contributions. We discuss the size of this omitted term in more detail in section 1.3.8.

1.3.3 Normalization of the wave functions

Finding solutions to the bound state equation will give us bound state wave functions and energy eigenvalues for the various states of the hydrogen atom, but if we wish to calculate higher order terms via some perturbative approach, it is necessary to properly normalize our wave functions. We discuss one possible normalization condition for our amplitudes here.

We once again employ the Haag expansion in our discussion of wave function normalization. The *in* (or *out*) fields of the Haag expansion diagonalize observables such as the Hamiltonian, the momentum operators, and charge operators. Via the Haag expansion, we can represent any conserved operator $\mathcal{O}$ that is a function of interacting fields in terms of asymptotic fields,

$$\sum_i \mathcal{O}[\xi_i] = \sum_i \mathcal{O}[\psi_i^{in}], \tag{1.43}$$

where ξ_i in an interacting field and ψ_i^{in} is an *in* field (*out* fields would be just as valid). We choose to use the operator for the number of electrons, N_e, to normalize the amplitude, $f_{\bar{p}h}(p, b)$. As before, the electron momentum is off-shell in this amplitude

while the proton momentum is on-shell. It is worth noting that we are neglecting weak interactions, so the number of electrons and muons is a conserved quantity which can be diagonalized when written in terms of asymptotic fields. In terms of interacting fields, the number operator is

$$N_e = \int e^\dagger(x) e(x) d^3x. \tag{1.44}$$

We take an expectation value of this operator with respect to a bound state with total bound state momenta b and b'. After Haag expanding the electron fields, the lowest order contribution to the electron number from the hydrogen atom in a given state comes from the terms in N_e that are bilinear in the hydrogen atom *in* field in that state. For higher order calculations, we would need to keep higher order amplitudes that also result in terms bilinear in the hydrogen *in* field after contractions, but we are only concerned with the lowest order term in these next few sections. Expanding the interacting electron field gives

$$\langle h(b)|N_e|h(b')\rangle = \int \frac{M d^3p}{E_p} \mathrm{Tr}[\bar{f}_{\bar{p}H_{j'}}(p,b')\gamma^0 f_{\bar{p}H_j}(p,b)] = 2E_b \delta(\mathbf{b}' - \mathbf{b}), \tag{1.45}$$

which fixes the normalization of the amplitudes.

1.3.4 Interchange of the on shell and off shell particles

In the previous section we arrived at a coupled equation for two Haag amplitudes. While this is enough to solve the problem numerically, it would be beneficial

to reduce the two equations to one equation in terms of one amplitude. Since the equations are not purely algebraic, it is difficult to simply solve for one amplitude in terms of the other and plug into the other equation. Instead, we can use the equal-time anticommutators for the interacting fields to relate the Haag amplitude with the lepton off shell to that with the proton off shell. Beginning with the equal-time anticommutator between the interacting electron and proton fields, $[e, p]_+ = 0$, we can once again Haag expand the two fields and group terms with the same *in* field coefficients (we can actually "peel off" these *in* fields by sandwiching them between appropriate asymptotic states and contracting). In this case, we are looking for terms with just the hydrogen *in* field after contractions. Once again, there will be higher order amplitudes present if we kept enough terms in the Haag expansion, but to the order we wish to calculate we are left with only two terms. The relation is

$$[f_{\bar{e}h,i}(q,b)(\frac{\not{q}+m}{2e_q})^T]_{\beta\alpha} + [f_{\bar{p}h,i}(p,b)(\frac{\not{p}+M}{2E_p})^T]_{\alpha\beta} = 0, \tag{1.46}$$

with the constraint $p + q = b$. We have arrived at a simple relation between the two lowest order bound state Haag amplitudes. The two amplitudes determine each other uniquely.

Using Eq. (1.46), we can simplify Eq. (1.41) to

$$(\not{b}-\not{p}-m)f_e(p,b) = \frac{e^2}{(2\pi)^3}\int \frac{d^3p'}{2E_{p'}}\gamma^\mu \frac{f_e(p',b)}{(p-p')^2}(\gamma_\mu)^T(\not{p}+M)^T, \tag{1.47}$$

which matches the Bethe-Salpeter equations of Refs. [31] and [32]. In the following

section we work in the rest frame of the bound state, $b = (M_{h_i}, \mathbf{0})$, to facilitate the calculations. This obviously breaks Lorentz covariance, but we will be able to compare our results with other well known bound state equations in the rest frame. To simplify things even further, we keep only the main mass shell and drop the magnetic interaction terms (we will examine these terms later). Comparisons of our results in the following sections will be to bound state equations involving only the Coulomb potential. The greatly simplified equation we study in the following section is

$$(\gamma^0 M_{H_i} - \not{p} - m) f_e(\mathbf{p}) = -\frac{e^2}{(2\pi)^3} \int \frac{d^3p'}{2E_{p'}} \gamma^0 \frac{f_e(\mathbf{p}')}{|\mathbf{p} - \mathbf{p}'|^2} (\gamma^0)^T (\not{p} + M)^T, \qquad (1.48)$$

where $f_e(\mathbf{p}) \equiv f_e(p; M_{h_i}, \mathbf{0})$.

1.3.5 Solution to bound-state equation

The purpose of the this section is to find a method for solving Eq. (1.48) which can be extended to solve Eqs. (1.41) and (1.42). For the sake of simplicity in this work, we will put off solving our more complicated coupled equations for a future paper. We acknowledge that we are solving an equation that has already been studied extensively in the literature, but our purpose is to develop the NQA framework for high-precision calculations. We therefore take an approach that differs from the typical perturbative method. The methods for finding higher order corrections are discussed in section 1.4.

We focus on binding due to the Coulomb interaction. We choose Coulomb

gauge to simplify our calculations and to allow comparison with the usual solution of the Dirac equation for the hydrogen atom. To keep the notation general for any two-particle system, we label the constituents m_1 and m_2 and the bound state m_b in this section. We solve the bound-state equation

$$(\gamma^0 m_b - \not{p} - m_1) f_e(\mathbf{p}) = \frac{e^2}{(2\pi)^3} \int \frac{d^3p'}{2E^{(2)}_{p'}} \gamma^0 V(\mathbf{p}, \mathbf{p}') f_e(\mathbf{p}') (\gamma^0)^T (\not{p} + m_2)^T, \quad (1.49)$$

where $m_b = m_1 + m_2 + \epsilon_i$, m_b is the energy of the hydrogen state, $\epsilon_i < 0$ is the binding energy of the atom, $V(\mathbf{p}, \mathbf{p}') = -1/|\mathbf{p} - \mathbf{p}'|^2$, and $E^{(i)}_p = \sqrt{p^2 + m_i^2}$. A similar equation is solved in Refs. [6, 26] in the non-relativistic limit. We solve the equation numerically without taking a non-relativistic limit.

We can think of m_2 as the mass of the proton and m_1 as the mass of the lepton, but the N-quantum equations that give Eq. (1.48) are symmetric under $m_1 \leftrightarrow m_2$ together with $e \leftrightarrow -e$ and our calculations reflect this.

Before solving this equation, we show that it reduces to the expected Dirac equation in the large-m_2 limit. The factor $(\not{p} + m_2)^T / 2E_{p'} \to (1 + \gamma^0)/2$ in the potential in Eq. (1.48) reduces the 4×4 system of equations to a 4×2 system with the usual Coulomb potential. From Eq. (1.48), using $q = b - p$, we find

$$(E\gamma^0 - \gamma \cdot \mathbf{q} - m_1 - \gamma^0 V) f_e = 0, \quad (1.50)$$

where V is the Coulomb potential. Because this equation comes from a covariant formulation, we have to multiply from the left by $\gamma^0 = \beta$ to get the usual form of

the Dirac equation for the hydrogen atom,

$$(\alpha \cdot \mathbf{q} + m_1\beta + V)f_e = Ef_e, \tag{1.51}$$

using $\gamma^0 = \beta$ and $\gamma^0\gamma^{\mathbf{i}} = \alpha^{\mathbf{i}}$.

1.3.5.1 Form of the matrix

To solve this equation, we break the 4×4 matrix down into four 2×2 matrices:

$$f_e(\mathbf{p}) = \begin{pmatrix} A(\mathbf{p}) & B(\mathbf{p}) \\ C(\mathbf{p}) & D(\mathbf{p}) \end{pmatrix}. \tag{1.52}$$

Next we introduce the partial wave expansion of the operators and the amplitude. Each of these 2×2 matrices can be written as a product of a spin-angle part and a radial function. For example, for a specific eigenstate we can write

$$A(\mathbf{p}) = \mathscr{Y}_{LS}^{Fm_F}(\Omega)g_L(p), \tag{1.53}$$

where $\mathscr{Y}_{LS}^{Fm_F}(\Omega)$ is the spin-angle function, $g_L(p)$ is a radial function, and $p = |\mathbf{p}|$. The most general solution is a sum over all possible eigenstates. The spin-angle function is given by

$$\mathscr{Y}_{LS}^{Fm_F}(\Omega) = \sum_{m_L}\langle LS; m_L\, m_F - m_L|Fm_F\rangle \boldsymbol{\phi}_{S\, m_F - m_L} Y_{Lm_L}(\theta,\phi). \tag{1.54}$$

where $\boldsymbol{\phi}_{S\,m_S}$ is the total spin state of the constituents, $Y_{Lm_L}(\theta,\phi)$ is a spherical harmonic, and $< LS; m_L\, m_F - m_L|Fm_F >$ is a Clebsch-Gordan coefficient. The spin state can be either a singlet or a triplet. We express these in terms of two-component Pauli spinors:

$$\boldsymbol{\phi}_{00} = \frac{1}{\sqrt{2}}[\psi(\uparrow)\otimes\chi(\downarrow) - \psi(\downarrow)\otimes\chi(\uparrow)] = \frac{1}{\sqrt{2}}\begin{pmatrix} 0 & 1 \\ -1 & 0 \end{pmatrix}, \tag{1.55}$$

$$\boldsymbol{\phi}_{11} = \psi(\uparrow)\otimes\chi(\uparrow) = \begin{pmatrix} 1 & 0 \\ 0 & 0 \end{pmatrix}, \tag{1.56}$$

$$\boldsymbol{\phi}_{1-1} = \psi(\downarrow)\otimes\chi(\downarrow) = \begin{pmatrix} 0 & 0 \\ 0 & 1 \end{pmatrix}, \tag{1.57}$$

$$\boldsymbol{\phi}_{10} = \frac{1}{\sqrt{2}}[\psi(\uparrow)\otimes\chi(\downarrow) + \psi(\downarrow)\otimes\chi(\uparrow)] = \frac{1}{\sqrt{2}}\begin{pmatrix} 0 & 1 \\ 1 & 0 \end{pmatrix}. \tag{1.58}$$

We expect our matrix wave function to be analogous to the direct product of an electron and a proton spinor,

$$\Phi \equiv \Psi_e \otimes \Psi_p^T = \begin{pmatrix} \psi_e \otimes \psi_p^T & \psi_e \otimes (\boldsymbol{\sigma}\cdot\mathbf{p}\psi_p)^T \\ (\boldsymbol{\sigma}\cdot\mathbf{p}\psi_e)\otimes\psi_p & (\boldsymbol{\sigma}\cdot\mathbf{p}\psi_e)\otimes(\boldsymbol{\sigma}\cdot\mathbf{p}\psi_p)^T \end{pmatrix}, \tag{1.59}$$

where Ψ_e and Ψ_p are free Dirac spinors for the electron and proton respectively, and ψ_e and ψ_p are their upper components. Our wave function must also satisfy the

auxiliary condition

$$f_e(\mathbf{p})(\not{p} - m_2)^T = 0. \tag{1.60}$$

With these two things in mind, we use the form

$$f_e(\mathbf{p}) = \begin{pmatrix} \mathscr{Y}_{LS}^{Fm_F} g_L(p)\mathbf{1} & S(p)\mathscr{Y}_{LS}^{Fm_F}(\boldsymbol{\sigma}\cdot\hat{\mathbf{p}})^T g_L(p) \\ \boldsymbol{\sigma}\cdot\hat{\mathbf{p}}\mathscr{Y}_{LS}^{Fm_F} h_L(p) & S(p)\boldsymbol{\sigma}\cdot\hat{\mathbf{p}}\mathscr{Y}_{LS}^{Fm_F}(\boldsymbol{\sigma}\cdot\hat{\mathbf{p}})^T h_L(p) \end{pmatrix}, \tag{1.61}$$

where $S(p) = p/(E_p^{(2)} + m_2)$, and $\hat{\mathbf{p}}$ is the unit vector in the direction of $\mathbf{p}$. We constructed this wave function to satisfy Eq. (1.60). This wave function is also a parity eigenstate,

$$\gamma^0 f_e(-\mathbf{p})\gamma^{0T} = (-1)^L f_e(\mathbf{p}). \tag{1.62}$$

1.3.5.2 The coupled radial integral equations

Use of Eq. (1.61) and the left-hand side (LHS) of Eq. (1.48) gives

$$\text{LHS} = \begin{pmatrix} L_{11} & L_{12} \\ L_{21} & L_{22} \end{pmatrix}, \tag{1.63}$$

where

$$L_{11} = [(m_b - E_p^{(2)} - m_1)g_L(p) + ph_L(p)]\mathscr{Y}_{LS}^{Fm_F},$$

$$L_{12} = S(p)[(m_b - E_p^{(2)} - m_1)g_L(p) + ph_L(p)]\mathscr{Y}_{LS}^{Fm_F}(\boldsymbol{\sigma}\cdot\hat{\mathbf{p}})^T,$$

$$L_{21} = -[pg_L(p) + (m_b + m_1 - E_p^{(2)})h_L(p)]\boldsymbol{\sigma}\cdot\hat{\mathbf{p}}\mathscr{Y}_{LS}^{Fm_F},$$

$$L_{22} = -S(p)[pg_L(p) + (m_b + m_1 - E_p^{(2)})h_L(p)]\boldsymbol{\sigma}\cdot\hat{\mathbf{p}}\mathscr{Y}_{LS}^{Fm_F}(\boldsymbol{\sigma}\cdot\hat{\mathbf{p}})^T.$$

The right-hand side (RHS) becomes

$$\text{RHS} = \begin{pmatrix} R_{11} & R_{12} \\ R_{21} & R_{22} \end{pmatrix}, \tag{1.64}$$

where

$$R_{11} = \int d^3p' \frac{V(\mathbf{p},\mathbf{p}')}{2E_{p'}^{(2)}}[(E_p^{(2)} + m_2)\mathscr{Y}'^{Fm_F}_{LS} + S(p')p\mathscr{Y}'^{Fm_F}_{LS}(\boldsymbol{\sigma}\cdot\hat{\mathbf{p}}')^T(\boldsymbol{\sigma}\cdot\hat{\mathbf{p}})^T]g_L(p'),$$

$$R_{12} = \int d^3p' \frac{V(\mathbf{p},\mathbf{p}')}{2E_{p'}^{(2)}}S(p)[(E_p^{(2)} + m_2)\mathscr{Y}'^{Fm_F}_{LS}(\boldsymbol{\sigma}\cdot\hat{\mathbf{p}})^T + S(p')p\mathscr{Y}'^{Fm_F}_{LS}(\boldsymbol{\sigma}\cdot\hat{\mathbf{p}}')^T]g_L(p'),$$

$$R_{21} = -\int d^3p' \frac{V(\mathbf{p},\mathbf{p}')}{2E_{p'}^{(2)}}[(E_p^{(2)} + m_2)\boldsymbol{\sigma}\cdot\hat{\mathbf{p}}'\mathscr{Y}'^{Fm_F}_{LS}$$

$$+ S(p')p\boldsymbol{\sigma}\cdot\hat{\mathbf{p}}'\mathscr{Y}'^{Fm_F}_{LS}(\boldsymbol{\sigma}\cdot\hat{\mathbf{p}}')^T(\boldsymbol{\sigma}\cdot\hat{\mathbf{p}})^T]h_L(p'),$$

$$R_{22} = -\int d^3p' \frac{V(\mathbf{p},\mathbf{p}')}{2E_{p'}^{(2)}}S(p)[(E_p^{(2)} + m_2)\boldsymbol{\sigma}\cdot\hat{\mathbf{p}}'\mathscr{Y}'^{Fm_F}_{LS}(\boldsymbol{\sigma}\cdot\hat{\mathbf{p}})^T$$

$$+ S(p')p\boldsymbol{\sigma}\cdot\hat{\mathbf{p}}'\mathscr{Y}'^{Fm_F}_{LS}(\boldsymbol{\sigma}\cdot\hat{\mathbf{p}}')^T]h_L(p'),$$

where $\mathscr{Y}'^{Fm_F}_{LS} = \mathscr{Y}^{Fm_F}_{LS}(\Omega')$. At this point, there is an apparent redundancy in the four equations. Right multiplying the upper right and lower right component equations by $\boldsymbol{\sigma} \cdot \hat{\mathbf{p}}$ and dividing by $S(p)$ results in the upper left and lower left component equations. Since we reduced the number of independent radial functions in our matrix to two by demanding that it satisfy the auxiliary condition, Eq. (1.60), we expected this redundancy. We focus only on the left components for the remainder of this discussion.

To keep this analysis general, we must find the action of the $\boldsymbol{\sigma} \cdot \mathbf{p}$ operators on the spin-angle functions,

$$\boldsymbol{\sigma} \cdot \mathbf{p} \mathscr{Y}^{Fm_F}_{LS} = \sum_{L'S'} C^{Fm_F}_{LSL'S'} \mathscr{Y}^{Fm_F}_{L'S'}, \tag{1.65}$$

$$\mathscr{Y}^{Fm_F}_{LS} (\boldsymbol{\sigma} \cdot \mathbf{p})^T = \sum_{L'S'} C^{T\,Fm_F}_{LSL'S'} \mathscr{Y}^{Fm_F}_{L'S'}, \tag{1.66}$$

where $C^{Fm_F}_{LSL'S'}$ are coefficients that can be determined explicitly and tabulated. $\boldsymbol{\sigma} \cdot \mathbf{p}$ is a pseudo-scalar operator and must change L by ± 1, i.e., $|L - L'| = 1$. Other

properties of these coefficients are

$$C^{Fm_F}_{L0L'S'} = -C^{T\,Fm_F}_{L0L'S'},$$

$$C^{Fm_F}_{L1L'0} = -C^{T\,Fm_F}_{L1L'0},$$

$$C^{Fm_F}_{L1L'1} = C^{T\,Fm_F}_{L1L'1},$$

$$C^{Fm_F}_{LSL'S'} = C^{Fm_F}_{L'S'LS},$$

$$\sum_{L'S'} C^{Fm_F}_{LSL'S'} C^{Fm_F}_{L'S'L''S''} = \delta_{LL''}\delta_{SS''},$$

$$\sum_{L'S'} C^{T\,Fm_F}_{LSL'S'} C^{T\,Fm_F}_{L'S'L''S''} = \delta_{LL''}\delta_{SS''}. \tag{1.67}$$

These properties are useful when using our general equations to determine specific cases. We have tabulated a few of them for some specific cases in appendix A.

The partial-wave expansion of the potential is

$$\begin{aligned} V(\mathbf{p},\mathbf{p}') &= \frac{1}{2\pi^2}\sum_{L=0}^{\infty}(2l+1)V_L(p,p')P_L(cos\theta_{pp'}) \\ &= \frac{2}{\pi}\sum_{L=0}^{\infty}\sum_{m_L=-L}^{L} V_L(p,p')Y^*_{Lm_L}(\Omega')Y_{Lm_L}(\Omega). \end{aligned} \tag{1.68}$$

With the orthogonality conditions,

$$\int_{-1}^{1} dx P_{L'}(x)P_L(x) = \frac{2}{2L+1}\delta_{LL'}$$

$$\int d\Omega Y^*_{Lm_L}(\Omega)Y_{L'm'_L}(\Omega) = \delta_{LL'}\delta_{m_Lm'_L}, \tag{1.69}$$

the components of the partial wave expansion in terms of the potential are,

$$V_L(p,p') = \pi^2 \int_{-1}^{1} dx P_L(x) V(\mathbf{p},\mathbf{p}'), \tag{1.70}$$

where $x = \cos\theta_{pp'}$. The orthogonality relation of the spin-angle functions,

$$\int d\Omega \, \mathrm{Tr}[\mathscr{Y}_{LS}^{Fm_F\dagger} \mathscr{Y}_{L'S'}^{Fm_F}] = \delta_{LL'}, \delta_{SS'} \tag{1.71}$$

are also useful.

Using Eq.(1.68) and Eq.(1.69) we find the left components on the right hand side

$$\begin{aligned} R_{11} = \frac{2}{\pi} \int \frac{dp' p'^2}{2E_{p'}^{(2)}} [(E_p^{(2)} + m_2) V_L(p,p') \mathscr{Y}_{LS}^{Fm_F} \\ + S(p') p \sum_{L'S'} \sum_{L''S''} C^{T\,Fm_F}_{LSL'S'} C^{T\,Fm_F}_{L'S'L''S''} V_{L'}(p,p') \mathscr{Y}_{L''S''}^{Fm_F}] g_L(p') \end{aligned} \tag{1.72}$$

$$\begin{aligned} R_{21} = -\frac{2}{\pi} \int \frac{dp' p'^2}{2E_{p'}^{(2)}} [(E_p^{(2)} + m_2) \sum_{L'S'} C^{Fm_F}_{LSL'S'} V_{L'}(p,p') \mathscr{Y}_{L'S'}^{Fm_F} \\ + S(p') p (\sum_{L'S'} \sum_{L''S''} \sum_{L'''S'''} C^{Fm_F}_{LSL'S'} C^{T\,Fm_F}_{L'S'L''S''} C^{T\,Fm_F}_{L''S''L'''S'''} V_{L''}(p,p') \mathscr{Y}_{L'''S'''}^{Fm_F})] h_L(p') \end{aligned} \tag{1.73}$$

We remove the spin-angle functions by multiplying the top left by $(\mathscr{Y}_{LS}^{jm_j})^\dagger$ and the bottom left by $(\boldsymbol{\sigma}\cdot\hat{\mathbf{p}}\mathscr{Y}_{LS}^{jm_j})^\dagger$, taking a trace, and integrating over Ω using Eq.(1.71).

The resulting equations are

$$(m_b - E_p^{(2)} - m_1)g_L(p) + ph_L(p) =$$
$$\frac{2}{\pi}\int \frac{dp'p'^2}{2E_{p'}^{(2)}}[(E_p^{(2)} + m_2)V_L(p,p') + S(p')p\sum_{L'S'}(C^{T^{Fm_F}}_{LSL'S'})^2 V_{L'}(p,p')]g_L(p') \quad (1.74)$$

$$-pg_L(p) - (m_b + m_1 - E_p^{(2)})h_L(p) =$$
$$-\frac{2}{\pi}\int \frac{dp'p'^2}{2E_{p'}^{(2)}}[(E_p^{(2)} + m_2)\sum_{L'S'}(C^{Fm_F}_{LSL'S'})^2 V_{L'}(p,p')$$
$$+ S(p')p\sum_{L'S'}\sum_{L''S''}\sum_{L'''S'''} C^{Fm_F}_{LSL'S'}C^{T^{Fm_F}}_{L'S'L''S''}C^{T^{Fm_F}}_{L''S''L'''S'''}C^{Fm_F}_{LSL'''S'''}V_{L''}(p,p')]h_L(p'). \quad (1.75)$$

Substituting $m_b = \epsilon + m_1 + m_2$ gives

$$\epsilon g_L(p) = (E_p^{(2)} - m_2)g_L(p) - ph_L(p)$$
$$+\frac{2}{\pi}\int \frac{dp'p'^2}{2E_{p'}^{(2)}}[(E_p^{(2)} + m_2)V_L(p,p') + S(p')p\sum_{L'S'}(C^{T^{Fm_F}}_{LSL'S'})^2 V_{L'}(p,p')]g_L(p') \quad (1.76)$$

$$\epsilon h_L(p) = (E_p^{(2)} - m_2 - 2m_1)h_L(p) - pg_L(p)$$
$$+\frac{2}{\pi}\int \frac{dp'p'^2}{2E_{p'}^{(2)}}[(E_p^{(2)} + m_2)\sum_{L'S'}(C^{Fm_F}_{LSL'S'})^2 V_{L'}(p,p')$$
$$+ S(p')p\sum_{L'S'}\sum_{L''S''}\sum_{L'''S'''} C^{Fm_F}_{LSL'S'}C^{T^{Fm_F}}_{L'S'L''S''}C^{T^{Fm_F}}_{L''S''L'''S'''}C^{Fm_F}_{LSL'''S'''}$$
$$\times V_{L''}(p,p')]h_L(p') \quad (1.77)$$

1.3.5.3 Specific cases of the bound state equation

As shown earlier, our equation reduces to the Dirac Coulomb equation in the large-m_2 limit. Here we show this reduction for each partial wave. The last term in both equations goes to zero and the equation simplifies to

$$\epsilon g_L(p) = -p h_L(p) + \int dp' p'^2 v_L(p,p') g_L(p') \tag{1.78}$$

$$\epsilon h_L(p) = -2m_1 h_L(p) - p g_L(p) + \int dp' p'^2 \sum_{L'S'} (C^{Fm_F}_{LSL'S'})^2 v_{L'}(p,p') h_L(p') \tag{1.79}$$

where $v_L(p,p') = \frac{2}{\pi} V_L(p,p')$. Again, we find the momentum space Dirac equation for an electron moving in a Coulomb potential.

We can use Eq.(1.67) along with some general properties of the coefficients to simplify our equations in some specific cases. For the case where $S = 0$, S' must be 1, and we can use Eq.(1.67) to greatly simplify the sums in the last term of the second equation. The result is

$$\begin{aligned}\epsilon g_L(p) = {} & (E_p^{(2)} - m_2) g_L(p) - p h_L(p) \\ & + \frac{2}{\pi} \int \frac{dp' p'^2}{2E_{p'}^{(2)}} [(E_p^{(2)} + m_2) V_L(p,p') + S(p') p \sum_{L'} (C^{T\,Fm_F}_{L0L'1})^2 V_{L'}(p,p')] g_L(p')\end{aligned} \tag{1.80}$$

$$\begin{aligned}\epsilon h_L(p) = {} & (E_p^{(2)} - m_2 - 2m_1) h_L(p) - p g_L(p) \\ & + \frac{2}{\pi} \int \frac{dp' p'^2}{2E_{p'}^{(2)}} [(E_p^{(2)} + m_2) \sum_{L'} (C^{Fm_F}_{L0L'1})^2 V_{L'}(p,p') + S(p') p V_L(p,p')] h_L(p').\end{aligned} \tag{1.81}$$

For $S = 1$, $L = J$, we know $L' = J \pm 1$ and $S' = 1$. Our simplified equations are

$$\epsilon g_L(p) = (E_p^{(2)} - m_2) g_L(p) - p h_L(p) + \frac{2}{\pi} \int \frac{dp' p'^2}{2E_{p'}^{(2)}} [(E_p^{(2)} + m_2) V_L(p,p') + S(p') p \sum_{L'} (C^{T^{Fm_F}}_{L1L'1})^2 V_{L'}(p,p')] g_L(p') \tag{1.82}$$

$$\epsilon h_L(p) = (E_p^{(2)} - m_2 - 2m_1) h_L(p) - p g_L(p) + \frac{2}{\pi} \int \frac{dp' p'^2}{2E_{p'}^{(2)}} [(E_p^{(2)} + m_2) \sum_{L'S'} (C^{Fm_F}_{L1L'1})^2 V_{L'}(p,p') + S(p') p V_L(p,p')] h_L(p'). \tag{1.83}$$

Finally, we have the case where $S = 1$ and $L = J - 1$. In this case L' must be equal to J, and the remaining sum of the squared coefficients over S' is 1. The simplified equations are

$$\epsilon g_L(p) = (E_p^{(2)} - m_2) g_L(p) - p h_L(p) + \frac{2}{\pi} \int \frac{dp' p'^2}{2E_{p'}^{(2)}} [(E_p^{(2)} + m_2) V_L(p,p') + S(p') p V_J(p,p')] g_L(p') \tag{1.84}$$

$$\epsilon h_L(p) = (E_p^{(2)} - m_2 - 2m_1) h_L(p) - p g_L(p) + \frac{2}{\pi} \int \frac{dp' p'^2}{2E_{p'}^{(2)}} [(E_p^{(2)} + m_2) V_J(p,p') + S(p') p \sum_{S'} \sum_{L''} \sum_{S'''} C^{Fm_F}_{L1JS'} C^{T^{Fm_F}}_{JS'L''1} C^{T^{Fm_F}}_{L''1JS'''} C^{Fm_F}_{L1JS'''} V_{L''}(p,p')] h_L(p'). \tag{1.85}$$

Note that even without the inclusion of a hyperfine spin-spin coupling term there is a difference between the nS_0^0 and the nS_1^1 equations. The former's state

equations, found from Eq.(1.80) and Eq.(1.81), are

$$\epsilon g_0(p) = (E_p^{(2)} - m_2)g_0(p) - ph_0(p) + \frac{2}{\pi}\int \frac{dp'p'^2}{2E_{p'}^{(2)}}[(E_p^{(2)} + m_2)V_0(p,p') + S(p')pV_1(p,p')]g_0(p') \tag{1.86}$$

$$\epsilon h_0(p) = (E_p^{(2)} - m_2 - 2m_1)h_0(p) - pg_0(p) + \frac{2}{\pi}\int \frac{dp'p'^2}{2E_{p'}^{(2)}}[(E_p^{(2)} + m_2)V_1(p,p') + S(p')pV_0(p,p')]h_0(p') \tag{1.87}$$

and the latter's, found from Eq.(1.84) and Eq.(1.85), are

$$\epsilon g_0(p) = (E_p^{(2)} - m_2)g_0(p) - ph_0(p) + \frac{2}{\pi}\int \frac{dp'p'^2}{2E_{p'}^{(2)}}[(E_p^{(2)} + m_2)V_0(p,p') + S(p')pV_1(p,p')]g_0(p') \tag{1.88}$$

$$\epsilon h_0(p) = (E_p^{(2)} - m_2 - 2m_1)h_0(p) - pg_0(p) + \frac{2}{\pi}\int \frac{dp'p'^2}{2E_{p'}^{(2)}}[(E_p^{(2)} + m_2)V_1(p,p') + S(p')p(\frac{1}{9}V_0(p,p') + \frac{8}{9}V_2(p,p'))]h_0(p'). \tag{1.89}$$

Because $p \sim \alpha\mu$, where μ is the reduced mass, the terms containing $S(p')$ are very small. For this reason the splitting between the energy levels of these two states created by the dissimilarity in the equations is very small. For large m_2, the potential terms with $S(p')$ are smaller by a factor that is $O(\alpha^2(m_1/m_2)^2)$.

1.3.5.4 Corrections to the approximation using the reduced mass

The NQA introduces both the light and heavy particle masses independently, rather than introducing the heavy-particle mass via the reduced mass. In the small-p approximation, the NQA coincides with the reduced mass approximation, but for larger momenta the reduced-mass approximation fails. We show this by examining the kinetic terms in the bound-state equations,

$$\begin{bmatrix} E_p^{(2)} - m_2 & -p \\ -p & E_p^{(2)} - m_2 - 2m_1 \end{bmatrix} \begin{bmatrix} g \\ h \end{bmatrix} = \epsilon \begin{bmatrix} g \\ h \end{bmatrix}. \tag{1.90}$$

The eigenvalue of this equation is

$$\epsilon = \sqrt{p^2 + m_2^2} - m_2 + \sqrt{p^2 + m_1^2} - m_1 \approx \frac{p^2}{2\mu} - \frac{m_1^3 + m_2^3}{8m_1^3 m_2^3} p^4.$$

For the Dirac equation the kinetic terms are

$$\begin{bmatrix} 0 & -p \\ -p & -2\mu \end{bmatrix} \begin{bmatrix} g \\ h \end{bmatrix} = \epsilon \begin{bmatrix} g \\ h \end{bmatrix}. \tag{1.91}$$

The eigenvalue for the Dirac equation is

$$\epsilon = \sqrt{p^2 + \mu^2} - \mu \approx \frac{p^2}{2\mu} - \frac{p^4}{8\mu^2},$$

where $\mu = m_1 m_2/(m_1 + m_2)$ is the reduced mass. (This result was found earlier by Raychaudhuri. [26]) We note that there are further mass dependencies in the

potential term, but do not discuss them here.

1.3.6 Numerical results

We briefly discuss some of our numerical results here. The purpose of this section is to show that our procedure and numerical calculations yield results that are consistent with standard calculations. We are aware that solutions to Eq. (1.47) are already well known, and we merely intend to show that our procedure does not return any erroneous results.

We solved the integral equation numerically for several states. We used a grid with 1200 points per equation and converted the integral eigenvalue equations into matrix eigenvalue equations. We handled the singularities at $p = p'$ in the kernels with Lande subtractions [28]. We excluded momenta close to infinity to avoid infinities in our discretized integral equation. The wave functions are extremely close to zero well before our cutoff is imposed. We made our equations dimensionless by dividing by m_1 and expressed the coupled equation in terms of the dimensionless parameter $\xi = m_2/m_1$. Our results agree with those of the Dirac-Coulomb equation with the reduced mass. With a higher precision we expect our results to differ from the Dirac-Coulomb equation, because our equation contains effects of the proton spin that are not found in the Dirac equation.

We found a rough estimate of our uncertainty by finding the eigenvalues with 800, 1000, and 1200 grid points and analyzing the stability of the eigenvalues. We conservatively estimated our uncertainty to be 0.01 meV for electronic hydrogen and

2 meV for muonic hydrogen.

We give comparisons of the NQA electronic hydrogen eigenvalues and Dirac-Coulomb eigenvalues for the nS_0^0 states in table 1.1 (a). These values are nearly identical and the results indicate that we may have overestimated our uncertainty.

We give the same comparisons for muonic hydrogen in table 1.1 (b). These values are similar, but differ significantly for the lower eigenvalues. The NQA energies in the ground- and next lowest-states are higher than the Dirac energies by 21 meV and 4 meV, respectively. It is possible that our numerical calculations failed for these two particular eigenvalues, or we may have underestimated the uncertainty. A higher degree of precision is needed to investigate such concerns.

Using the same method of estimating the uncertainty as before, we conservatively take our uncertainty to be 0.01 meV. As in the case of muonic hydrogen, there are some discrepancies in the first two eigenvalues. The first and second values are larger than the Dirac energies by 0.16 and .03 meV respectively. The higher eigenvalues are consistent with the Dirac energies.

We also calculated the energies of the nS_1^1 states. They are identical to those shown in tables 1.1 (a) and (b) for some nS_0^0 states. We need higher precision to study the energy splitting in these states caused by the differences in the NQA equations.

n	NQA	Dirac
1	-13.59847	-13.59847
2	-3.39963	-3.39963
3	-1.51094	-1.51094
4	-0.84990	-0.84990
5	-0.54394	-0.54394
6	-0.37774	-0.37773
7	-0.27752	-0.27752

(a) Electronic hydrogen nS_0^0

n	NQA	Dirac
1	-2.528506	-2.528527
2	-0.632130	-0.632134
3	-0.280946	-0.280947
4	-0.158032	-0.158033
5	-0.101141	-0.101141
6	-0.070236	-0.070236
7	-0.051602	-0.051602

(b) Muonic hydrogen nS_0^0

n	NQA	Dirac
2	-3.39963	-3.39963
3	-1.51094	-1.51094
4	-0.84991	-0.84990
5	-0.54394	-0.54394
6	-0.37774	-0.37773
7	-0.27753	-0.27752
8	-0.21248	-0.21248

(c) Electronic hydrogen nP_1^0

n	NQA	Dirac
2	-0.632132	-0.632134
3	-0.280947	-0.280947
4	-0.158033	-0.158033
5	-0.101141	-0.101141
6	-0.070238	-0.070236
7	-0.051604	-0.051602
8	-0.039510	-0.039508

(d) Electronic hydrogen nP_1^0

n	NQA	Dirac
2	-3.39958	-3.39958
3	-1.51093	-1.51093
4	-0.84990	-0.84990
5	-0.54394	-0.54394
6	-0.37774	-0.37773
7	-0.27752	-0.27752
8	-0.21248	-0.21247

(e) Electronic hydrogen nP_1^2

n	NQA	Dirac
2	-0.632125	-0.632125
3	-0.280945	-0.280945
4	-0.158032	-0.158031
5	-0.101141	-0.101140
6	-0.070237	-0.070236
7	-0.051604	-0.051602
8	-0.039510	-0.039508

(f) Electronic hydrogen nP_1^2

Table 1.1: Energy eigenvalues for electronic and muonic hydrogen states. The table on the left is for electronic hydrogen in units of eV and the right table is for muonic hydrogen in units of keV. Dirac eigenvalues are for the Dirac-Coulomb equation with the reduced mass. NQA values are numerically calculated from the NQA integral equations with a Coulomb potential.

To get a feel for the splitting in the $L = 1$ levels, we also calculated eigenvalues nP_1^0 and nP_1^2 states. These states were chosen because it is clear the spin of the lepton is anti-aligned with the orbital angular momentum in the first case and aligned with the orbital angular momentum in the second case, allowing us to compare to similar states of the Dirac equation. The results are shown in tables 1.1 (c), (d), (e), and (f). To our degree of precision there is no significant difference between NQA and Dirac eigenvalues in these states. Once again the closeness of the two sets of values for electronic hydrogen suggests an overestimation of uncertainty.

The full coupled NQA equations are symmetric under $m_1 \leftrightarrow m_2$. We used an approximation to get the final form of the equations used in these numerical calculations. This approximation obscures the mass interchange symmetry, but it should still be present to some degree. To check this, we interchanged masses and calculated a few of the eigenvalues for electronic hydrogen, where the mass interchange creates more of a drastic change to the equations than in muonic hydrogen. We recovered the same eigenvalues shown in the tables up to 1 or 2 sigmas.

We also found evidence that our precision is not high enough for the final terms in Eq. (1.76) and Eq. (1.77) to have a significant effect on the eigenvalues. We calculated ground state and $n = 1$ eigenvalues without these terms and the values were not appreciably different. This is another motivation for improving our precision in the future.

In addition to eigenvalues, we compared our wave functions with Dirac equation solutions. Specifically, we compared the momentum space radial wave function of the upper components of the Dirac equation solutions with our function $g_L(p)$.

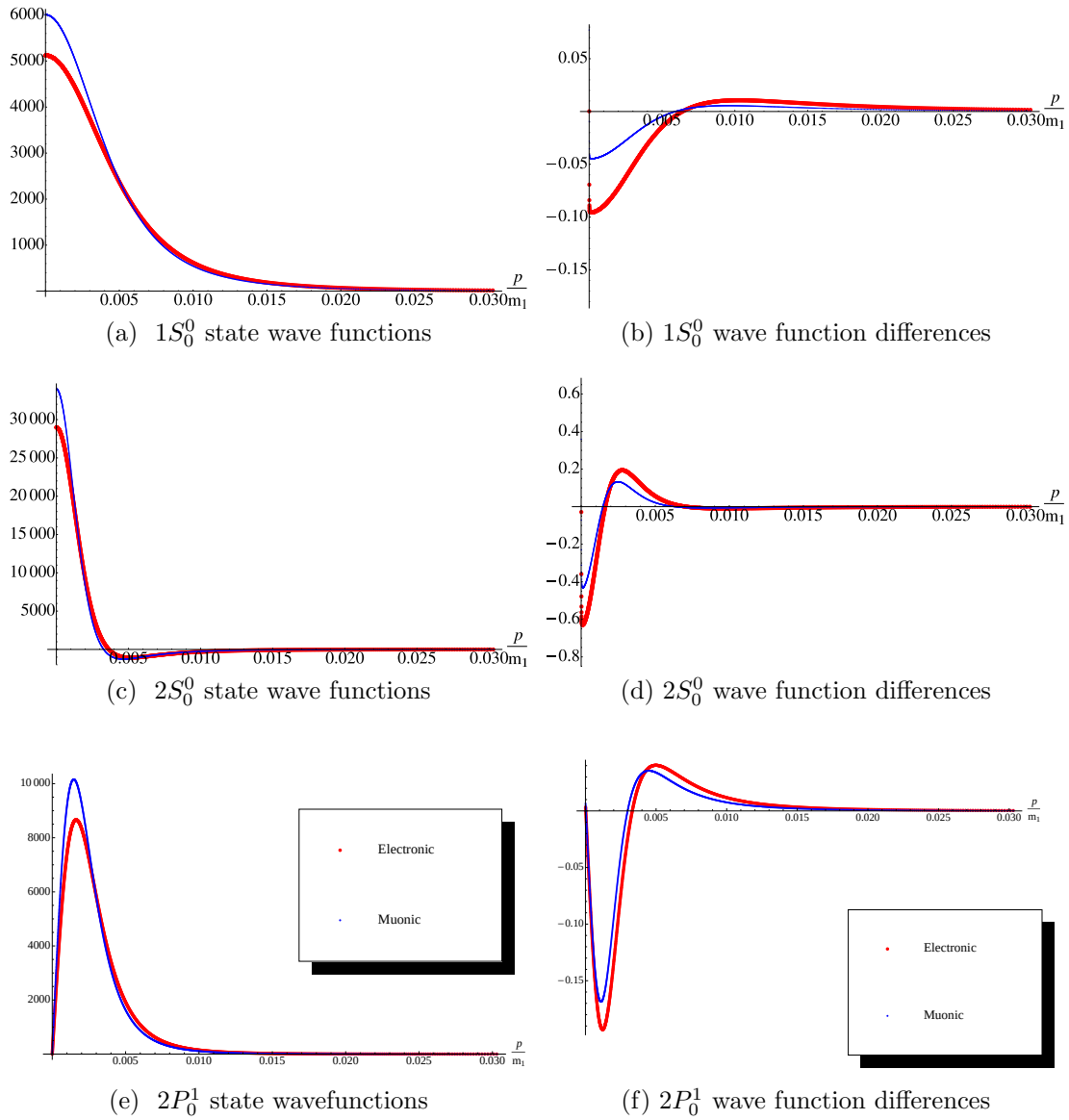

(a) $1S_0^0$ state wave functions

(b) $1S_0^0$ wave function differences

(c) $2S_0^0$ state wave functions

(d) $2S_0^0$ wave function differences

(e) $2P_0^1$ state wavefunctions

(f) $2P_0^1$ wave function differences

Figure 1.3: Plots on the left are NQA momentum space wave functions for certain electronic and muonic hydrogen states. Plots on the right are differences between NQA wave functions and Dirac-Coulomb wave functions for certain electronic and muonic hydrogen states. Thick red lines represent electronic hydrogen wave functions or differences and thin blue lines represent muonic hydrogen wave functions or differences.

Once again we make comparisons for both muonic and electronic hydrogen. Comparisons for two states are shown in Figure 1.3. Plots on the left hand side are the NQA wave functions as a function of p/m_1 for three electronic and muonic hydrogen states. Plots on the right hand side are differences between the NQA wave functions and

Dirac-Coulomb wave functions for the same electronic and muonic hydrogen states. We plotted the muonic and electronic wave functions and differences for each state on the same set of axes in order to make direct comparisons between electronic and muonic hydrogen. As is the case for Dirac-Coulomb wave functions, NQA muonic wave functions are larger for smaller momenta and smaller for large momenta than their electronic counterparts. It is clear from the right plots that muonic hydrogen wave functions are more consistent with Dirac-Coulomb wave functions. The NQA solutions are less than the Dirac wave functions for small momenta and greater for larger momenta.

We also show the NQA wave function for positronium and the difference between the NQA wave function and Dirac-Coulomb wave function for the positronium $1S_0^0$ state in Figures 1.4a and 1.4b, respectively. Strangely, unlike electronic and muonic hydrogen, the NQA wave function is greater than the Dirac solution for small momenta and less than the Dirac wave function for larger momenta. The positronium NQA solution seems to be as consistent with the Dirac solution as the electronic hydrogen wave function is with its Dirac counterpart, but the muonic hydrogen wave function is more consistent with the Dirac solution.

The differences shown on the right in Figure 1.3 are small compared to the size of the wave functions themselves, therefore we can conclude that we have found wave functions that are fairly consistent with Dirac wave functions, as well as eigenvalues that are all within 2 sigmas except for the $1S_0^0$ state. It is worth noting that we introduced the heavy particle mass independently in the NQA equations, yet the results compare nicely with Dirac equation results with the reduced mass.

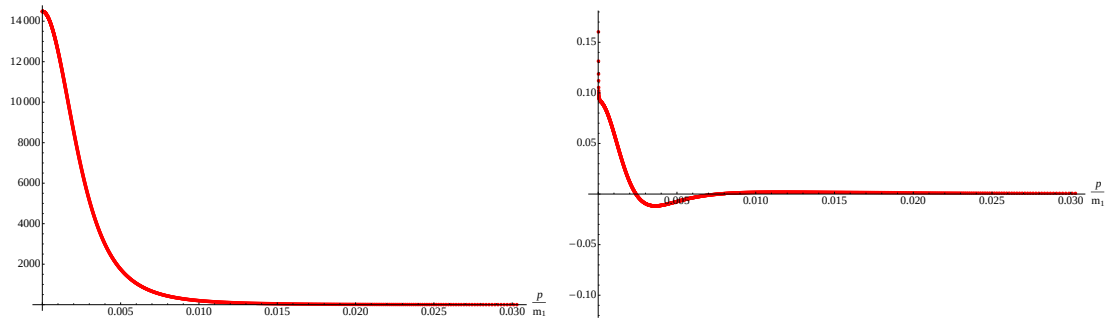

(a) NQA positronium $1S_0^0$ state wave function (b) Positronium $1S_0^0$ wave function difference

Figure 1.4: The left plot is the momentum space NQA wave function for positronium in the $1S_0^0$ state. The right plot is a difference between the NQA wave function and the Dirac-Coulomb wave function for positronium in the $1S_0^0$ state.

1.3.7 Framework for higher order contributions

In this section, we briefly show how to calculate higher order contributions to the bound state energy, specifically Lamb shift terms. We will explain how to extend our formalism to include the corrections here, but we will save the actual calculation for section 1.4. The usual diagrams used to calculate the Lamb shift perturbatively are shown in Figure 1.1.

The energy contributions of these diagrams are typically calculated with respect to zeroth order wave functions of solutions to equations such as Eq. (1.48). We intend to calculate the analogs of these diagrams within the framework of the NQA. We can incorporate these terms in our integral equations and use the numerical techniques described above to find a less perturbative solution, or we can employ our own perturbative technique.

Three examples of NQA Lamb shift diagrams are shown in Figure 1.6. The external off shell line at the lower left of each diagram is assumed to be the electron.

Figure 1.5: Examples of NQA Lamb shift diagrams

These terms will be added to the right hand side of Eq. (1.41). In any diagram, every loop that does not contain an NQA amplitude must have one on shell line. With this rule, there are 2 permutations of the vacuum polarization diagram, 3 of the anomalous magnetic moment diagram, and 2 of the mass renormalization diagram. The diagrams shown in Figure 1.5 involve the amplitude f_e, but there are similar diagrams involving f_p where the line directly to the lower left of the circle is the on shell line and the line directly to the circle's lower right is off shell. This means that there are a total of 4 diagrams for vacuum polarization, 6 for the anomalous magnetic moment, and 4 for mass renormalization. We also must find similar diagrams to add to the right hand side of Eq. (1.42) where the external off shell line is the proton.

The NQA seems to be more complicated than the standard procedure where there is only 1 Feynman diagram for each Lamb shift contribution, but diagrams of the same type are very similar and it is not necessary to calculate each diagram independently. Additionally, the mass shell delta functions that appear in the NQA simplify calculations.

1.3.8 Magnetic contributions

We dropped the magnetic contributions of our original bound state equation, Eq. (1.47). In this section we will show how to calculate them in our framework and find the expected S-state splitting. We will treat the magnetic terms as perturbations about our lowest order bound state equation, Eq. (1.48) We first work out

$$\gamma^i f_e(\mathbf{p}')\gamma^{iT} = \begin{pmatrix} M_{11} & M_{12} \\ M_{21} & M_{22} \end{pmatrix} \tag{1.92}$$

where

$$\begin{aligned} M_{11} &= -S(p')\sigma^i \boldsymbol{\sigma}\cdot\hat{\mathbf{p}}' \mathscr{Y}'^{jm_j}_{LS} (\boldsymbol{\sigma}\cdot\hat{\mathbf{p}}')^T \sigma^{iT} h_L(p') \\ &= -S(p') \sum_{L'S'} \sum_{L''S''} C^{TJM}_{LSL'S'} C^{JM}_{L'S'L''S''} T_{S''} \mathscr{Y}'^{jm_j}_{L''S''} h_L(p'), \end{aligned} \tag{1.93}$$

$$\begin{aligned} M_{12} &= -\sigma^i \boldsymbol{\sigma}\cdot\hat{\mathbf{p}}' \mathscr{Y}'^{jm_j}_{LS} \sigma^{iT} h_L(p') \\ &= -\sum_{S'L'} C^{JM}_{LSL'S'} T_{S'} \mathscr{Y}'^{jm_j}_{L'S'} h_L(p'), \end{aligned} \tag{1.94}$$

$$\begin{aligned} M_{21} &= S(p')\sigma^i \mathscr{Y}'^{jm_j}_{LS} (\boldsymbol{\sigma}\cdot\hat{\mathbf{p}}')^T \sigma^{iT} g_L(p'), \\ &= S(p') \sum_{S'L'} C^{TJM}_{LSL'S'} T_{S'} \mathscr{Y}'^{jm_j}_{L'S'} g_L(p') \end{aligned} \tag{1.95}$$

$$\begin{aligned} M_{22} &= \sigma^i \mathscr{Y}'^{jm_j}_{LS} \sigma^{iT} g_L(p') \\ &= T_S \mathscr{Y}'^{jm_j}_{LS} g_L(p'), \end{aligned} \tag{1.96}$$

where $T_1 = 1$ and $T_0 = -3$. With this notation, the magnetic terms in Eq. (1.47) can be written as

$$-\frac{e^2}{(2\pi)^3}\int \frac{d^3p'}{2E_{p'}}\gamma^i \frac{f_e(p',b)}{(p-p')^2}(\gamma^i)^T(\not{p}'+M)^T = \frac{2}{\pi}\int \frac{dp'p'^2}{2E_p}V(\mathbf{p},\mathbf{p}')\begin{pmatrix} A & B \\ C & D \end{pmatrix} \tag{1.97}$$

where

$$A = (E_p + m_2)M_{11} + pM_{12}(\boldsymbol{\sigma}\cdot\hat{\mathbf{p}})^T \tag{1.98}$$

$$B = -pM_{11}(\boldsymbol{\sigma}\cdot\hat{\mathbf{p}})^T - pS(p)M_{12} \tag{1.99}$$

$$C = (E_p + m_2)M_{21} + pM_{22}(\boldsymbol{\sigma}\cdot\hat{\mathbf{p}})^T \tag{1.100}$$

$$D = -pM_{21}(\boldsymbol{\sigma}\cdot\hat{\mathbf{p}})^T - pS(p)M_{22} \tag{1.101}$$

and

$$V(\mathbf{p},\mathbf{p}') = -\frac{4\pi\alpha}{(\mathbf{p}-\mathbf{p}')^2}. \tag{1.102}$$

We will discuss perturbation theory within the NQA in more detail in section 1.4.2. Here we will just say that we must left multiply by $f^\dagger\gamma^0$,

$$f_e^\dagger(\mathbf{p})\gamma^0\begin{pmatrix} A & B \\ C & D \end{pmatrix} = \begin{pmatrix} f_{11}^\dagger A - f_{21}^\dagger C & f_{11}^\dagger B - f_{21}^\dagger D \\ f_{12}^\dagger A - f_{22}^\dagger C & f_{12}^\dagger B - f_{22}^\dagger D \end{pmatrix} \tag{1.103}$$

where

$$f_{11}^{\dagger} = \mathscr{Y}^{\dagger}{}_{LS}^{jm_j} g_L(p),$$

$$f_{12}^{\dagger} = S(p)(\boldsymbol{\sigma}\cdot\hat{\mathbf{p}})^T \mathscr{Y}^{\dagger}{}_{LS}^{jm_j} g_L(p),$$

$$f_{21}^{\dagger} = \mathscr{Y}^{\dagger}{}_{LS}^{jm_j} (\boldsymbol{\sigma}\cdot\hat{\mathbf{p}}) h_L(p),$$

$$f_{22}^{\dagger} = S(p)(\boldsymbol{\sigma}\cdot\hat{\mathbf{p}})^T \mathscr{Y}^{\dagger}{}_{LS}^{jm_j} (\boldsymbol{\sigma}\cdot\hat{\mathbf{p}}) h_L(p),$$

and we must take a trace over this matrix to find the energy contribution. Taking into account that the function h is $O(p)$ smaller than g, it is clear that the top left term is the dominant contribution. The dominant contributions to the energy shift are

$$\Delta E_m = \frac{2}{\pi(2\pi)^3} \int \frac{p^2 p'^2 dp dp'}{2E_p^{(2)}} (T_1 + T_2 + T_3 + T_4) \tag{1.104}$$

where

$$T_1 = -\mathscr{Y}^{\dagger jm_j}_{LS}\sigma^i(\boldsymbol{\sigma}\cdot\hat{\mathbf{p}}')\mathscr{Y}'^{jm_j}_{LS}(\boldsymbol{\sigma}\cdot\hat{\mathbf{p}}')^T\sigma^{iT}h_L(p')g_L(p)(E_p+m_2)S(p')$$
$$= -\mathscr{Y}^{\dagger jm_j}_{LS}\sum_{L'S'}\sum_{L''S''}C^{TJM}_{LSL'S'}C^{JM}_{L'S'L''S''}T_{S''}\mathscr{Y}'^{jm_j}_{L''S''}h_L(p')g_L(p)(E_p+m_2)S(p') \tag{1.105}$$

$$T_2 = -\mathscr{Y}^{\dagger jm_j}_{LS}\sigma^i(\boldsymbol{\sigma}\cdot\hat{\mathbf{p}}')\mathscr{Y}'^{jm_j}_{LS}\sigma^{iT}(\boldsymbol{\sigma}\cdot\hat{\mathbf{p}})^T p h_L(p')g_L(p)$$
$$= -\sum_{S''L''}C^{TJM}_{LSL''S''}\mathscr{Y}^{\dagger jm_j}_{L''S''}\sum_{S'L'}C^{JM}_{LSL'S'}T_{S'}\mathscr{Y}'^{jm_j}_{L'S'}p h_L(p')g_L(p) \tag{1.106}$$

$$T_3 = -\mathscr{Y}^{\dagger jm_j}_{LS}(\boldsymbol{\sigma}\cdot\hat{\mathbf{p}})\sigma^i\mathscr{Y}'^{jm_j}_{LS}(\boldsymbol{\sigma}\cdot\hat{\mathbf{p}}')^T\sigma^{iT}(E_p+m_2)S(p')h_L(p)g_L(p')$$
$$= -\sum_{S''L''}C^{JM}_{LSL''S''}\mathscr{Y}^{\dagger jm_j}_{L''S''}\sum_{S'L'}C^{TJM}_{LSL'S'}T_{S'}\mathscr{Y}'^{jm_j}_{L'S'}(E_p+m_2)S(p')h_L(p')g_L(p) \tag{1.107}$$

$$T_4 = -\mathscr{Y}^{\dagger jm_j}_{LS}(\boldsymbol{\sigma}\cdot\hat{\mathbf{p}})\sigma^i\mathscr{Y}'^{jm_j}_{LS}\sigma^{iT}(\boldsymbol{\sigma}\cdot\hat{\mathbf{p}})^T p h_L(p)g_L(p')$$
$$= -\sum_{L'S'}\sum_{L''S''}C^{TJM}_{LSL'S'}C^{JM}_{L'S'L''S''}\mathscr{Y}^{\dagger jm_j}_{L''S''}\mathscr{Y}'^{jm_j}_{LS}T_S p h_L(p)g_L(p'). \tag{1.108}$$

(Had we calculated in a more conventional way, we would have found terms in which the spin couplings were more apparent:

$$\sum_i T_i = -\frac{1}{4}[-\mathbf{k}^2\mathscr{Y}^{\dagger jm_j}_{LS}\sigma^i\mathscr{Y}'^{jm_j}_{LS}\sigma^{iT} + (\boldsymbol{\sigma}\cdot\mathbf{k})\mathscr{Y}'^{jm_j}_{LS}(\boldsymbol{\sigma}\cdot\mathbf{k})^T + (\mathbf{p}+\mathbf{p}')^2\mathscr{Y}'^{jm_j}_{LS}$$
$$+ 2i\boldsymbol{\sigma}\cdot\mathbf{p}\times\mathbf{p}'\mathscr{Y}'^{jm_j}_{LS} + 2i\mathscr{Y}'^{jm_j}_{LS}\boldsymbol{\sigma}^T\cdot\mathbf{p}\times\mathbf{p}']g_L(p')g_L(p) \tag{1.109}$$

where $\mathbf{k} = \mathbf{p} - \mathbf{p}'$.)

We expand the potential in a spherical basis, do the prime and unprimed

angular integrals, and take a trace to find

$$T_1 = -\sum_{L'S'} C^{TJM}_{LSL'S'} C^{JM}_{L'S'LS} T_S V_L h_L(p') g_L(p)(E_p + m_2) S(p') \tag{1.110}$$

$$T_2 = -\sum_{S'L'} C^{TJM}_{LSL'S'} C^{JM}_{LSL'S'} T_{S'} V_{L'} \mathscr{Y}^{jm_j}_{L'S'} p h_L(p') g_L(p) \tag{1.111}$$

$$T_3 = -\sum_{S'L'} C^{JM}_{LSL'S'} C^{TJM}_{LSL'S'} T_{S'} V_{L'} (E_p + m_2) S(p') h_L(p) g_L(p') \tag{1.112}$$

$$T_4 = -\sum_{L'S'} C^{TJM}_{LSL'S'} C^{JM}_{L'S'LS} T_S V_L p h_L(p) g_L(p') \tag{1.113}$$

Taking a non-relativistic limit, we substitute $h(p) \approx -\frac{p g_L(p)}{2m_1}$ to find

$$T_1 = \frac{1}{2m_1} \sum_{L'S'} C^{TJM}_{LSL'S'} C^{JM}_{L'S'LS} T_S V_L p'^2 g_L(p') g_L(p) \tag{1.114}$$

$$T_2 = \frac{1}{2m_1} \sum_{S'L'} C^{TJM}_{LSL'S'} C^{JM}_{LSL'S'} T_{S'} V_{L'} \mathscr{Y}^{jm_j}_{L'S'} p p' g_L(p') g_L(p) \tag{1.115}$$

$$T_3 = \frac{1}{2m_1} \sum_{S'L'} C^{JM}_{LSL'S'} C^{TJM}_{LSL'S'} T_{S'} V_{L'} p p' g_L(p') g_L(p) \tag{1.116}$$

$$T_4 = \frac{1}{2m_1} \sum_{L'S'} C^{TJM}_{LSL'S'} C^{JM}_{L'S'LS} T_S V_L p^2 g_L(p) g_L(p'). \tag{1.117}$$

and the sum of the terms is just

$$T = \frac{1}{2m_1} \sum_{L'S'} C^{TJM}_{LSL'S'} C^{JM}_{L'S'LS} [(p'^2 + p^2) T_S V_L + 2pp' T_{S'} V_{L'}] g_L(p) g_L(p') \tag{1.118}$$

We now calculate the splitting for muonic hydrogen between the 2^0S_0 and the

2^1S_1 states. We have for the sums over the coefficients

$$\sum_{L'S'}(C^{T\,1M}_{01L'S'}C^{1M}_{L'S'01}T_1V_0 - C^{T\,0M}_{00L'S'}C^{0M}_{L'S'00}T_0V_0) = \frac{1}{3}V_0 - 3V_0 = -\frac{8}{3}V_0 \tag{1.119}$$

and

$$(\sum_{L'S'}C^{T\,1M}_{01L'S'}C^{JM}_{L'S'01}T_{S'}V_{L'} - \sum_{L'S'}C^{T\,0M}_{00L'S'}C^{0M}_{L'S'00}T_{S'}V_{L'}) = \frac{5}{3}V_1 - (-V_1) = \frac{8}{3}V_1. \tag{1.120}$$

With these, the splitting can be written as

$$\Delta E_S = \frac{8}{6\pi m_1 m_2(2\pi)^3}\int p^2 p'^2 dpdp'(-(p^2+p'^2)V_0 + 2pp'V_1)g_L(p)g_L(p') \tag{1.121}$$

$$= -\frac{8}{6\pi m_1 m_2(2\pi)^3}\pi^2\int p^2 p'^2 dpdp'dx(\mathbf{p}-\mathbf{p}')^2 V(\mathbf{p},\mathbf{p}')g_L(p)g_L(p') \tag{1.122}$$

$$= \frac{8\pi\alpha 4\pi}{3m_1 m_2(2\pi)^3}\int p^2 p'^2 dpdp'dx g_L(p)g_L(p') \tag{1.123}$$

which is consistent with Pachuki when the anamolous magnetic moment of the proton ($\kappa = 1.792847337(29)$) and muon ($a_\mu = 0.001166$) is taken into account. This hyperfine splitting between the S-states can be found via the usual perturbative approach with a HFS quasi-potential [29]

$$V(\mathbf{k}) = \frac{8\pi\alpha}{3m_1 m_2}\frac{\boldsymbol{\sigma_1}\cdot\boldsymbol{\sigma_2}}{4}(1+\kappa). \tag{1.124}$$

Since the states we are using are different from the usual ones, their fine and hyperfine structure are broken up in a different way, although their energy levels should

be the same as those of the usual basis.

1.3.9 Other mass shell

We have neglected the contribution from the opposite mass shell in our calculation. This other term has the form

$$\frac{e^2}{(2\pi)^3}\int \frac{d^3p'}{2E^{(2)}_{p'}} V_s(\mathbf{p},\mathbf{p}')\gamma^0 f(\mathbf{p}')(\gamma^0)^T(\not{p}'+m_2)^T \tag{1.125}$$

where

$$V_s(\mathbf{p},\mathbf{p}') = \frac{1}{(E^{(2)}_p + E^{(2)}_{p'})^2 - (\mathbf{p}-\mathbf{p}')^2}. \tag{1.126}$$

This potential does not have a singularity at $\mathbf{p}=\mathbf{p}'$. This allows us to avoid using Lande subtraction in any numerical calculation.

We can get a rough estimate for the size of this term relative to the dominant mass shell term by approximating

$$V_s \approx \frac{1}{4m_2^2}, \tag{1.127}$$

and estimating the dominant mass shell potential as

$$V = -\frac{1}{(\mathbf{p}-\mathbf{p}')^2} \sim \frac{1}{(\alpha\mu)^2}. \tag{1.128}$$

We see that the opposite mass shell term is $O(\alpha^2(\frac{\mu}{m_2})^2)$ smaller than than the usual

term. In the case of electronic hydrogen, this is approximately $O(\alpha^2(\frac{m_1}{m_2})^2) \approx 10^{-11}$. For muonic hydrogen it is about a factor of 10^{-6}.

If we wish to go beyond a crude estimation, we can calculate perturbatively in a non-relativistic limit. A useful normalization condition for our non-relativistic wavefunctions is

$$\int d^3p \mathrm{Tr}[f(\mathbf{p})^\dagger f(\mathbf{p})] = 1. \tag{1.129}$$

Using the form of $f(\mathbf{p})$ given in (1.52), we find

$$\begin{aligned}
\int d^3p \mathrm{Tr}[f(\mathbf{p})^\dagger f(\mathbf{p})] = \int d^3p \mathrm{Tr}[&\mathscr{Y}^{\dagger JM}_{LS} \mathscr{Y}^{JM}_{LS} g^*(p)g(p) + (\boldsymbol{\sigma}\cdot\hat{\mathbf{p}}\mathscr{Y}^{JM}_{LS})^\dagger \boldsymbol{\sigma}\cdot\hat{\mathbf{p}}\mathscr{Y}^{JM}_{LS} \\
&\times h^*(p)h(p) \\
&+ S(p)^2((\mathscr{Y}^{JM}_{LS}(\boldsymbol{\sigma}\cdot\hat{\mathbf{p}})^T)^\dagger \mathscr{Y}^{JM}_{LS}(\boldsymbol{\sigma}\cdot\hat{\mathbf{p}})^T g^*(p)g(p) \\
&+ (\boldsymbol{\sigma}\cdot\hat{\mathbf{p}}\mathscr{Y}^{JM}_{LS}(\boldsymbol{\sigma}\cdot\hat{\mathbf{p}})^T)^\dagger \boldsymbol{\sigma}\cdot\hat{\mathbf{p}}\mathscr{Y}^{JM}_{LS}(\boldsymbol{\sigma}\cdot\hat{\mathbf{p}})^T h^*(p)h(p))] \\
= \int d^3p \mathrm{Tr}[&\mathscr{Y}^{\dagger JM}_{LS} \mathscr{Y}^{JM}_{LS}](1+S(p)^2)(g^*(p)g(p) + h^*(p)h(p)) \\
= \int dp p^2 &(1+S(p)^2)(g^*(p)g(p) + h^*(p)h(p))
\end{aligned} \tag{1.130}$$

With this, our normalization condition becomes

$$\int dp p^2 (1+S(p)^2)(g^*(p)g(p) + h^*(p)h(p)) = 1. \tag{1.131}$$

$S(p)^2$ is $O(\alpha^2(\frac{\mu}{m_2})^2)$, so the condition is approximately

$$\int dpp^2(g^*(p)g(p) + h^*(p)h(p)) = 1. \tag{1.132}$$

To enforce this condition, we must multiply the radial wave functions $g(p)$ and $f(p)$ by some normalization constant.

Before applying perturbation theory, we must alter the form of our equation slightly. A Hamiltonian formalism is desirable for a perturbative approach. To get this form, we simply left multiply our bound state equation by γ^0. In the usual perturbative process, we have $\epsilon = \epsilon_0 + \epsilon_1 + \ldots$, and $f(\mathbf{p}) = f_0(\mathbf{p}) + f_1(\mathbf{p}) + \ldots$ where ϵ_0 and $f_0(\mathbf{p})$ are the eigenvalue and wave function of the equation without the perturbative term, respectively. To find the contribution of the opposite mass shell to our energy eigenvalue, we compute

$$\epsilon_1 = \frac{e^2}{(2\pi)^3}\int \frac{d^3pd^3p'}{2E^{(2)}_{p'}} V_s(\mathbf{p},\mathbf{p}')\mathrm{Tr}[f_0^\dagger(\mathbf{p})f_0(\mathbf{p}')(\gamma^0)^T(\not{p}' + m_2)^T] \tag{1.133}$$

We once again expand the potential into partial waves

$$\begin{aligned} V_s(\mathbf{p},\mathbf{p}') &= \frac{1}{2\pi^2}\sum_{L=0}^{\infty}(2l+1)V_L(p,p')P_L(cos\theta_{pp'}) \\ &= \frac{2}{\pi}\sum_{l=0}^{\infty}\sum_{m_L=-L}^{L} V_L(p,p')Y^*_{Lm_L}(\Omega')Y_{Lm_L}(\Omega). \end{aligned} \tag{1.134}$$

After taking the trace and the doing the angular integration, we find

$$\epsilon_1 = \frac{2e^2}{\pi(2\pi)^3}\int \frac{dpdp'p^2p'^2}{2E^{(2)}_{p'}}[A+B+C+D] \tag{1.135}$$

where

$$A = (E^{(2)}_{p'}+m_2)[V_L g^*(p)g(p') + \sum_{L'S'} C^{JM}_{LSL'S'}C^{JM}_{LSL'S'}V_{L'}h^*(p)h(p')] \tag{1.136}$$

$$\begin{aligned} B = S(p')p[&\sum_{L'S'} C^{TJM}_{LSL'S'}C^{TJM}_{LSL'S'}V_{L'}g^*(p)g(p') \\ &+ \sum_{L'S'}\sum_{L''S''}\sum_{L'''S'''} C^{TJM}_{LSL'S'}C^{JM}_{L'S'L''S''}C^{TJM}_{LSL'''S'''}C^{JM}_{L''S''L'''S'''}V_{L''}h^*(p)h(p')] \end{aligned} \tag{1.137}$$

$$C = S(p)p[V_L g^*(p)g(p') + \sum_{L'S'} C^{JM}_{LSL'S'}C^{JM}_{LSL'S'}V_{L'}h^*(p)h(p')] \tag{1.138}$$

$$\begin{aligned} D = S(p)S(p')(E^{(2)}_p - m_2)[&\sum_{L'S'} C^{TJM}_{LSL'S'}C^{TJM}_{LSL'S'}V_{L'}g^*(p)g(p') \\ &+ \sum_{L'S'}\sum_{L''S''}\sum_{L'''S'''} C^{TJM}_{LSL'S'}C^{JM}_{L'S'L''S''}C^{TJM}_{LSL'''S'''}C^{JM}_{L''S''L'''S'''}V_{L''}h^*(p)h(p')]. \end{aligned} \tag{1.139}$$

Clearly A is the most significant contribution. We drop the other terms and focus on calculating the A term numerically. Before finding a value for the integral, we can put it into a more numerically tractable form by substituting $p \to m_1 p$, and $p' \to m_1 p'$ to eliminate the mass dependence of the integral. We can write the

energy contribution as

$$\epsilon_1 = \frac{2m_1e^2}{\pi(2\pi)^3}\int \frac{dpdp'p^2p'^2}{2\mathscr{E}^{(2)}_{p'}}(\mathscr{E}^{(2)}_{p'}+1)[v_L G^*(p)G(p') + \sum_{L'S'} C^{JM}_{LSL'S'}C^{JM}_{LSL'S'}v_{L'}H^*(p)H(p')] \tag{1.140}$$

where $v_L(p,p') = m_1^2 V_L(m_1p, m_1p')$, $G_L(p) = m_1^{3/2}g_L(m_1p)$, $\mathscr{E}^{(2)}_p = \sqrt{(p/\xi)^2+1}$, and $\xi = m_2/m_1$. We solved this integral numerically in Mathematica with 1200 sampling points. We found

$$\begin{aligned} \epsilon_1 &= 4.2\times10^{-10}\text{ meV} \qquad \text{for electronic hydrogen} \\ \epsilon_1 &= 2.3\times10^{-3}\text{ meV} \qquad \text{for muonic hydrogen} \end{aligned} \tag{1.141}$$

This is certainly not large enough to account for the 0.31 meV discrepancy of the proton radius problem, but it is an example of an energy correction that is much more significant for muonic hydrogen than electronic hydrogen. It might be possible that a QED correction that has been overlooked can account for the discrepancy without significantly altering the well known electronic hydrogen energy splittings.

1.3.10 Section summary

We used the NQA in one-loop order to calculate the energy levels and bound-state amplitudes of ordinary and muonic hydrogen, as well as the wave functions of positronium. We used the NQA systematically to find a relation between wave functions with the light particle off shell and the heavy particle off shell and to

find normalization conditions for our amplitudes. Our formalism was general and could be applied to any 2-particle weakly bound state. We also examined how magnetic contributions could be calculated in the NQA and made a connection with an accepted result. Finally, we calculated the energy contribution from the opposite mass shell and concluded that it is negligible.

In the following section, we will derive integral equations that include higher-order corrections. While it is possible to solve these equations numerically without using perturbation theory by simply including some of the energy correction terms, the program would need to calculate with an extremely high precision for the corrections to be noticeable. Instead, we will use perturbation theory to add corrections to the electron-photon vertex and to the photon propagator to include the terms that lead to the Lamb shift. We will compute the Lamb shift of both electronic and muonic hydrogen. We will carry these calculations to sufficient order to compare our results with the usual methods to see if our methods resolve the muonic hydrogen anomaly.

1.4 N-quantum Lamb shift calculations of muonic hydrogen

1.4.1 Diagrams

Our goal is to calculate the Lamb shift corrections within the framework of the NQA. The Lamb shift has three contributions: electron vacuum polarization, vertex correction, and a self-energy term. It is usually calculated perturbatively in QED and we also employ a perturbative approach using the NQA.

As shown in the previous section, the NQA makes use of the Haag expansion, an expansion of the interacting fields in terms of asymptotic in fields. The Haag expansions must be truncated at some point to make it finite. This is justified because the higher order amplitudes (amplitudes with more lines connected to them) contain more powers of the coupling constant. In this section we keep more of the higher order terms dropped in the previous section. As before, our method involves first plugging in the Haag expansions into the lepton and proton equations of motion and contracting in fields. This results in fundamental diagrams involving higher order amplitudes. We have shown all the diagrams needed for the Lamb shift (to the order we wish to calculate) in Figure D.1. While the diagrams shown come from the electron equation of motion, there are similar diagrams associated with the proton equation of motion. We have kept only the diagrams necessary to produce terms that involve just one or two virtual photons.

Equations for the higher order amplitudes can be found by the same method of plugging the Haag expansion into the equations of motion and contracting to find equations for the relevant amplitudes in terms of other amplitudes. An example of this is Eq. (1.40). This process results in a set of coupled equations for the amplitudes which, in principle, can be solved for the amplitudes and energy eigenvalues. Solving such a set of equations should give accurate results, but in practice is difficult, even numerically. The next pragmatic step is to express all of the higher order amplitudes in terms of the lowest level amplitudes via perturbation theory. There are two lowest order amplitudes: one for the proton going to hydrogen and a positron *in* fields and another for the electron going to hydrogen and antiproton *in*

fields. These two amplitudes are themselves related via the commutation relation of the interacting fields given in Eq. (1.46). All higher order amplitudes can be expanded in terms of these two. A diagrammatic example of such an expansion is shown in Figure D.2. The ellipsis indicate in this figure indicate that there are additional terms that resemble the drawn diagrams but with different lines off- or on-shell.

These expansions can be plugged into the original Figure D.1 diagrams to produce Feynman-like diagrams. Examples of these diagrams is shown in Figure D.5. This figure shows the diagrams that result from the expansion of the diagram shown in Figure D.1a. The key difference between NQA diagrams and Feynman diagrams is NQA diagrams always include on-shell lines and Haag amplitudes. Similar to Feynman diagrams, there are rules that can be followed to write expressions associated with NQA diagrams. We discussed a simplified version of these rules in section 1.3.2. The final NQA diagrams contain self energy corrections, vacuum polarization terms, vertex corrections, and crossed and uncrossed two photon exchange diagrams.

It should be noted that diagrams of any one of these categories (self energy, vacuum polarization, vertex corrections, crossed and uncrossed diagrams) can come from several different fundamental diagrams. The diagrams should be regrouped into their appropriate Lamb shift category before further calculation. An example of such a regrouping is shown in Figure D.6. This figure shows all the NQA diagrams for the lepton vertex correction. The first two diagrams come from Figure D.1b, the next two from Figure D.1c, the next one from Figure D.1e, and the last one from Figure D.1g.

1.4.2 Perturbation theory in the NQA

After finding all the diagrams in terms of the two lowest order amplitudes and using the commutation relation of the interacting fields to write one lowest order amplitude in terms of the other via Eq. (1.46), we arrive at a bound state equation with many terms that are small compared to the 1-photon exchange terms. After grouping these terms and integrating over some of the mass shell delta functions, we arrive at the bound state equation,

$$
\begin{aligned}
(\not{b} - \not{p} - m) f_e(p,b) = {} & \frac{e^2}{(2\pi)^3} \int d^4q D_R(p-q) \delta_{m_2}(q) \gamma^\mu f_e(q,b) (\gamma_\mu)^T (\not{p} + m_2)^T \\
& + \frac{1}{(2\pi)^3} \int d^4q T^e(p-q) D_R(p-q) \delta_{m_2}(q) \gamma^\mu f_e(q,b) (\gamma_\mu)^T (\not{p} + m_2)^T \\
& - \frac{1}{(2\pi)^3} \int d^4q \bar{S}^e((p-q)^2) D_R(p-q) \delta_{m_2}(q) (p-q)_\nu m^{\mu\nu} f_{ph}(q,b) (\gamma_\mu)^T (\not{p} + m_2)^T \\
& + \frac{1}{(2\pi)^3} \int d^4q T^p(p-q) D_R(p-q) \delta_{m_2}(q) \gamma^\mu f_e(q,b) (\gamma_\mu)^T (\not{p} + m_2)^T \\
& - \frac{1}{(2\pi)^3} \int d^4q \bar{S}^p((p-q)^2) D_R(p-q) \delta_{m_2}(q) \gamma^\mu f_e(q,b) (p-q)_\nu (m_p^{\mu\nu})^T (\not{p} + m_2)^T \\
& + 2\text{PE}, \qquad (1.142)
\end{aligned}
$$

where

$$T^e(p) = -\bar{\Pi}^e(p^2) + \bar{\Pi}^e(0) + \bar{R}^e(p^2) - \bar{R}^e(0) - \bar{S}^e(p^2) + \bar{S}^e(0), \qquad (1.143)$$

$$m_e^{\mu\nu} = \frac{1}{4m_e}(\gamma^\mu\gamma^\nu - \gamma^\nu\gamma^\mu), \qquad (1.144)$$

$D(p)$ is the retarded photon propagator,

$$D_R(p) = \frac{1}{(p^0 + i\epsilon)^2 - \mathbf{p}^2}, \tag{1.145}$$

and the functions $\bar{\Pi}^e(p^2)$, $\bar{R}^e(p^2)$, and $\bar{S}^e(p^2)$ are the end result of the radiative correction calculations to the electron current,

$$-\bar{\Pi}^e(p^2) + \bar{\Pi}^e(0) = \frac{e^2}{12\pi^2}\left(\frac{4m_1^2}{p^2} - \frac{5}{3} + \left(1 - \frac{2m_1^2}{p^2}\right)\sqrt{1 - \frac{2m_1^2}{p^2}}\log\frac{1 + \sqrt{1 + \frac{4m_1^2}{p^2}}}{|1 - \sqrt{1 + \frac{4m_1^2}{p^2}}|}\right) \tag{1.146}$$

$$\bar{R}^e(p^2) - \bar{R}^e(0) = -\frac{e^2}{12\pi^2}\frac{p^2}{m^2}\left(\log\frac{m_1}{m_{ph}} - \frac{1}{8}\right) + \ldots \tag{1.147}$$

$$\bar{S}^e(p^2) = \frac{e^2}{8\pi^2} - \frac{e^2}{48\pi^2}\frac{p^2}{m_1^2} + \ldots \tag{1.148}$$

where the ellipses stands for terms higher order in $\frac{p^2}{m_1^2}$. m_{ph} is the photon mass which we will eventually set to 0 after renormalization. $\bar{T}^p$ and $\bar{S}^p$ are the same as $\bar{T}^e$ and $\bar{S}^e$ with $m_1 \to m_2$. These functions also appear in the standard analysis of radiative corrections (See [30]). 2PE stands for crossed and uncrossed 2-photon exchange terms. The 2-photon exchange diagrams contain proton structure corrections and will be dealt with separately. There are radiative corrections to both the proton and electron currents. The most significant corrections are those to the electron current and we focus on them in the following discussion.

As with the magnetic and opposite mass-shell contributions, we treat these smaller terms as a perturbation to the lowest order bound state equation with one

Coulomb photon exchange. We first left multiply by γ^0 to get the equation into a Hamiltonian form. Schematically, we have

$$(H_0 + H_{f,hf} + H_{LS})f = Ef \tag{1.149}$$

where

$$H_0 f = (\gamma^0\gamma^i p_i + \gamma^0 m)f(p,b) - \frac{e^2}{(2\pi)^3}\int d^4q D_R(p-q)\delta_{m_2}(q)f_e(q,b)(\gamma^0)^T(\not{p}+M)^T, \tag{1.150}$$

$$H_{f,hf} f = \frac{e^2}{(2\pi)^3}\int d^4q D_R(p-q)\delta_{m_2}(q)\gamma^0\gamma^i f_e(q,b)(\gamma^i)^T(\not{p}+M)^T, \tag{1.151}$$

and

$$\begin{aligned} H_{LS} f = {} & \frac{1}{(2\pi)^3}\int d^4q T^e(p-q)D_R(p-q)\delta_{m_2}(q)\gamma^\mu f_e(q,b)(\gamma_\mu)^T(\not{p}+M)^T \\ & - \frac{1}{(2\pi)^3}\int d^4q \bar{S}^e((p-q)^2)D_R(p-q)\delta_{m_2}(q)(p-q)_\nu m^{\mu\nu} \\ & \times f_{ph}(q,b)(\gamma_\mu)^T(\not{p}+M)^T. \end{aligned} \tag{1.152}$$

Our focus in this section will be on the Lamb shift term. The energy corrections of this section are corrections to the eigenvalues found in section 1.3.6. Our wave function is a bispinor, so we must left multiply by $\bar{f}$, integrate over the on shell

momentum p, and take a trace to find our expectation value:

$$E_L = \frac{1}{(2\pi)^3}\int \frac{d^4q d^3p}{2E_p^{(2)}} T^e(p-q) D_R(p-q)\delta_{m_2}(q)\mathrm{Tr}[\bar{f}_e(p,b)\gamma^\mu f_e(q,b)(\gamma_\mu)^T(\not{p}+m_2)^T]$$
$$- \frac{\mu_e}{(2\pi)^3}\int \frac{d^4q d^3p}{2E_p^{(2)}} \bar{S}^e((p-q)^2) D_R(p-q)\delta_{m_2}(q)(p-q)_\nu$$
$$\times \mathrm{Tr}[\bar{f}_e(p,b) m_e^{\mu\nu} f_e(q,b)(\gamma_\mu)^T(\not{p}+m_2)^T]. \quad (1.153)$$

1.4.3 Basis for f

There are three possible ways we can couple the angular momentum in the problem. The first is to couple the two spins and then couple the total spin to the orbital angular momentum. This way leads to a more symmetric wave function and makes some of the momentum space partial wave calculations more straightforward. This approach was taken in section 1.3.5. The downside to this approach is that the actual energies of the measured states are not close to the eigenvalues of a wave function with quantum numbers S (total spin), L (orbital angular momentum) and F, which are the relevant parameters in this basis (It should be noted that L is only an approximate quantum number). This is due to the significant mass difference in the constituents. A linear combination of wave functions in this basis is needed for hydrogen with significant weighting on each term. For electronic hydrogen, the difference between the masses is large enough to make this basis less useful, but in muonic hydrogen the muon is only about 1/10th as massive as the proton, making the bound state more symmetric and making this basis a bit more useful. Still, this basis is best suited for a completely symmetric bound state like positronium.

The second basis involves coupling the lepton spin to the orbital angular momentum and then coupling this angular momentum, J, to the proton spin. This basis is not as symmetric and not as well suited for a partial wave expansion in momentum space (although this can still be done), however, the actual energies of the full bound state equation are very close to the energy eigenvalues of the wave functions in this basis. This is due to the relative large mass of the proton. A linear sum of functions is still necessary, but one term will be weighted most significantly.

The final way of coupling momenta is to couple the proton spin with the orbital angular momentum and then couple this sum to the lepton momentum. It is unlikely that this basis will be useful for any kind of calculation.

For our Lamb shift calculations, we choose the second basis. This is the basis used in most of the literature and the actual energy levels are usually labeled by the J, L, and F corresponding to the state with the closest energy. In the CM frame, our amplitude can be written as

$$f^{F_z}_{FJL}(\mathbf{p}) = \sum_{J_z} < F, F_z | J, J_z, 1/2, F_z - J_z > \psi^{J_z}_{JL}(\mathbf{p}) \otimes u^{F_z - J_z\,T}(-\mathbf{p}) \qquad (1.154)$$

where

$$u^s(\mathbf{p}) = \sqrt{E_p^{(2)} + m_2} \begin{pmatrix} \chi^s \\ \frac{\boldsymbol{\sigma}\cdot\mathbf{p}}{E_p^{(2)}+m_2}\chi^s \end{pmatrix}, \qquad (1.155)$$

where we have chosen the Dirac basis and χ^s is a Pauli spinor. The free proton

spinor is normalized so that

$$u^{s\dagger}(p)u^{s'}(p) = \delta^{ss'}2E_p^{(2)} \tag{1.156}$$

$$\bar{u}^{s}(p)u^{s'}(p) = \delta^{ss'}2m_2. \tag{1.157}$$

We also have

$$\psi^{J_z}_{JL_a}(\mathbf{p}) = \begin{pmatrix} \mathscr{Y}^{J_z}_{JL}(\hat{\mathbf{p}})g_L(p) \\ \\ \frac{\boldsymbol{\sigma}\cdot\mathbf{p}}{E_p^{(1)}+m_1}\mathscr{Y}^{J_z}_{JL}(\hat{\mathbf{p}})h_L(p) \end{pmatrix}, \tag{1.158}$$

where the spin angle functions are defined as

$$\mathscr{Y}^{J_z}_{J=L\pm1/2,L} = \pm\sqrt{\frac{L\pm J_z+1/2}{2L+1}}Y_L^{J_z-1/2}\chi^{+} + \sqrt{\frac{L\mp J_z+1/2}{2L+1}}Y_L^{J_z+1/2}\chi^{-}. \tag{1.159}$$

The whole wave function is normalized so that

$$\int \frac{d^3p}{2E_p^{(2)}}\mathrm{Tr}[\bar{f}^{F_z}_{FJL}(\mathbf{p})f^{F_z}_{FJL}(\mathbf{p})] = \int dpp^2\left(g_L^*(p)g_L(p) + \frac{E_p^{(1)}-m_1}{E_p^{(1)}+m_1}h_L^*(p)h_L(p)\right) = 1. \tag{1.160}$$

1.4.4 Lowest order Lamb shift terms in NQA framework

The two primary contributions to the Lamb shift are electron vacuum polarization and vertex correction (although we will also calculate corrections due to the self interaction of the lepton). In electronic hydrogen, the vertex correction smears out the electron position over a range of about 0.1 fermi. This causes the electron spin factor to be slightly different from 2 and creates a slight weakening of the force

on the electron when it is very close to the nucleus. Since the 2S level penetrates to the nucleus, it will have a slightly higher energy than the 2P level due to this contribution.

In the vacuum polarization we are dealing with in this section, a lepton/anti-lepton (usually an electron/positron) pair is created that effectively screens the bound lepton from the nucleus. This reduces the nuclear charge felt by the bound lepton. At short distances from the nucleus, the bare charge is still seen, thus the 2S is of lower energy than the 2P due to this effect.

The size of the vacuum polarization contribution is much larger in muonic hydrogen because the Compton wavelength of the electron (and positron) produced in vacuum polarization, which determines the spatial distribution of the electron, is comparable to the Bohr radius of muonic hydrogen, causing much overlap between the vacuum polarization charge density and the muonic hydrogen wave function. In electronic hydrogen, the effect of vacuum polarization is less than that of the vertex correction. For this reason, the 2S is lower than 2P in muonic hydrogen and higher in electronic hydrogen. We will deal with electron vacuum polarization separately in the following section.

It is important to make a connection with the literature before attempting to calculate any new corrections that arise within our framework. To make these connections, we will focus on only the most significant components of our matrix wave function in the following subsections.

1.4.4.1 Electron vacuum polarization for muonic hydrogen

As stated above, vacuum polarization for muonic hydrogen is the dominant contribution to the Lamb shift. Our vacuum polarization contribution is

$$E_{vac} = \frac{e^2}{(2\pi)^3}\int \frac{d^3qd^3p}{2E_p^{(2)}}(-\Pi((p-q)^2)+\Pi(0))D_R(p-q)\delta_{m_2}(q) \times \mathrm{Tr}[\bar{f}_e(p,b)\gamma^\mu f_e(q,b)(\gamma_\mu)^T(\not{p}+m_2)^T]. \quad (1.161)$$

We focus on the larger γ^0 term and take the large m_2 limit:

$$E_{vac} = \frac{e^2}{(2\pi)^3}\int \frac{d^4qd^3p}{4E_q^{(2)}E_p^{(2)}}(-\Pi(-(\mathbf{p}-\mathbf{q})^2)+\Pi(0))D_R(\mathbf{p}-\mathbf{q}) \times \mathrm{Tr}[\bar{f}_e(p,b)\gamma^0 f_e(q,b)\frac{1+\gamma^0}{2}]. \quad (1.162)$$

We approximate the amplitude as a direct product of the Dirac-Coulomb wave function for the electron with a free proton spinor, as shown above. We can take the upper components of the Dirac-Coulomb wave function as a Pauli spinor with the non-relativistic Schroedinger wave function: $\tilde{\psi}(\mathbf{p})$. Performing the trace gives

$$E_{vac} = \frac{e^2}{(2\pi)^3}\int d^3qd^3p(-\Pi(-(\mathbf{p}-\mathbf{q})^2)+\Pi(0))D_R(\mathbf{p}-\mathbf{q})\tilde{\psi}^*(\mathbf{p})\tilde{\psi}(\mathbf{q}). \quad (1.163)$$

We can write function $\bar{\Pi}$ as

$$\bar{\Pi}(p^2)-\bar{\Pi}(0) = -p^2\int_0^\infty \frac{\Pi(q^2)d(q^2)}{q^2(q^2-p^2)} \quad (1.164)$$

where

$$\Pi(q^2) = \frac{e^2}{12\pi}\left(1+\frac{2m^2}{q^2}\right)\sqrt{1-\frac{4m^2}{q^2}}\theta(\frac{q^2}{4}-m^2). \tag{1.165}$$

Changing the integration variable gives

$$E_{vac} = \frac{e^2}{(2\pi)^3}\int d^3q d^3k(-\Pi(-\mathbf{k}^2)+\Pi(0))D_R(\mathbf{k})\tilde{\psi}^*(\mathbf{q}+\mathbf{k})\tilde{\psi}(\mathbf{q}) \tag{1.166}$$

where $\mathbf{k} = \mathbf{p} - \mathbf{q}$. Moving to position space makes the calculation more intuitive:

$$\begin{aligned} E_{vac} &= e^2\int d^3k d^3x e^{-i\mathbf{k}\cdot\mathbf{x}}(-\Pi(-\mathbf{k}^2)+\Pi(0))D_R(\mathbf{k})\psi^*(\mathbf{x})\psi(\mathbf{x}) \\ &= e^2\int d^3k d^3x e^{-i\mathbf{k}\cdot\mathbf{x}}\left(\int_0^\infty \frac{\bar{\Pi}(q^2)d(q^2)}{q^2(\mathbf{k}^2+q^2)}\right)\psi^*(\mathbf{x})\psi(\mathbf{x}) \\ &= \int d^3x V_{VP}(x)\rho(\mathbf{x}) \end{aligned} \tag{1.167}$$

where

$$\rho(\mathbf{x}) = \psi^*(\mathbf{x})\psi(\mathbf{x}) \tag{1.168}$$

and the Uehling potential is

$$\begin{aligned} V_{VP}(x) &= e^2\int d^3k e^{-i\mathbf{k}\cdot\mathbf{x}}\int_0^\infty \frac{\bar{\Pi}(q^2)d(q^2)}{q^2(\mathbf{k}^2+q^2)} \\ &= -\frac{\alpha^2}{3\pi x}\int_4^\infty \frac{d(q^2)}{q^2}e^{-m_e q r}\left(1+\frac{2}{q^2}\right)\sqrt{1-\frac{4}{q^2}}. \end{aligned} \tag{1.169}$$

Since the Lamb shift is a difference between the 2P and the 2S states, we define

$$\rho \equiv \rho_{2P} - \rho_{2S}. \tag{1.170}$$

With this definition, our vacuum polarization contribution matches that of [9].

1.4.4.2 Muon vacuum polarization, self energy, and vertex correction

Since the muon Compton wavelength differs from the muonic hydrogen Bohr radius by about a factor of $1/\alpha$, we can make some approximations to the muon vacuum polarization contribution. We expand $\bar{\Pi}(q^2)$ for $q^2 << m_\mu^2$ and use the same approximations to our wave function shown above to arrive at the well known result:

$$\Delta E_{\mu vac} = -\frac{4\alpha^2}{15m_\mu^2}|\psi(0)|^2. \tag{1.171}$$

where $\psi(0)$ is the non relativistic position space wave function evaluated at the origin. The contribution to the Lamb shift is

$$L_{\mu vac} = -\frac{4\alpha^2}{15m_\mu^2}(|\psi_{2P}(0)|^2 - |\psi_{2S}(0)|^2) \tag{1.172}$$

$$= \frac{\alpha^5}{30\pi}\frac{\mu^3}{m_\mu^2} \tag{1.173}$$

For muonic hydrogen, this value is

$$L_{\mu vac} = 0.0168 \text{ meV}. \tag{1.174}$$

The last major contribution to the Lamb shift are the vertex and self-energy terms. We deal with the two terms in Eq. (1.153) separately:

$$L_{v,se} = T_1 + T_2, \tag{1.175}$$

where

$$T_1 = \frac{1}{(2\pi)^3} \int \frac{d^4q d^3p}{2E_p^{(2)}} T^e(p-q) D_R(p-q) \delta_{m_2}(q) \text{Tr}[\bar{f}_e(p,b)\gamma^\mu f_e(q,b)(\gamma_\mu)^T(\not{p}+m_2)^T] \tag{1.176}$$

$$T_2 = -\frac{\mu_e}{(2\pi)^3} \int \frac{d^4q d^3p}{2E_p^{(2)}} \bar{S}^e((p-q)^2) D_R(p-q) \delta_{m_2}(q)(p-q)_\nu \times \text{Tr}[\bar{f}_e(p,b) m_e^{\mu\nu} f_e(q,b)(\gamma_\mu)^T(\not{p}+m_2)^T]. \tag{1.177}$$

We neglect magnetic contributions and focus on the γ^0 terms. For the first term, keeping only the largest term in the trace gives

$$\text{Tr}[\bar{f}_e(p,b)\gamma^0 f_e(q,b)(\gamma^0)^T(\not{p}+m_2)^T] \approx 2m_2 g_L(q) g_L^*(p). \tag{1.178}$$

Expanding $T^e(p)$ in powers of $\frac{p}{m_1}$ and keeping only the first term in the series gives

$$T^e(\mathbf{p})D_R(\mathbf{p}) = \frac{e^2}{12\pi^2 m_1^2}[\log\frac{m_1}{m_{ph}} - \frac{23}{40}]. \tag{1.179}$$

We find for the first term

$$T_1 = \frac{4\alpha^2}{3}[\log\frac{m_1}{m_{ph}} - \frac{23}{40}]|g(0)|^2 \tag{1.180}$$

where we have used the large m_2 limit and $g(0)$ is the position space function evaluated at 0. Using the non-relativistic Schroedinger wave function for g(0), we find

$$T_1 = \frac{4}{3\pi}\frac{m\alpha^5}{n^3}[\log\frac{m_1}{m_{ph}} - \frac{23}{40}]\delta_{l,0} \tag{1.181}$$

Moving on to the second term, we once again focus on the γ^0 part:

$$\begin{aligned} T_2 = &- \frac{1}{(2\pi)^3 m_1}\int d^4q d^4p \bar{S}^e((p-q)^2)D_R(p-q)\delta_{m_2}(q)(p-q)^i \\ &\times \mathrm{Tr}[f_e^\dagger(p,b)\gamma^i f_e(q,b)(\gamma^0)^T(\not{p}+m_2)^T] \end{aligned} \tag{1.182}$$

In the large m_2 limit, this becomes

$$T_2 = - \frac{1}{(2\pi)^3 m_1}\int d^3q d^4p \bar{S}^e((p-q)^2)D_R(p-q)(p-q)^i \mathrm{Tr}[f_e^\dagger(p,b)\gamma^i f_e(q,b)\frac{1+\gamma^0}{2}]. \tag{1.183}$$

Transforming to position space, and using the lowest order approximation $\bar{S}^e(p) \approx \frac{\alpha}{2\pi}$, we find

$$T_2 = -\frac{\mu_e e\alpha}{8\pi^2}\int d^3x \frac{1}{|\mathbf{x}|}\mathrm{Tr}[\partial_i(f_e^\dagger(\mathbf{x})\gamma^i f_e(\mathbf{x}))\frac{1+\gamma^0}{2}].$$

We can make use of the large m_2 limit of the bound state equation, the position space version of Eq. (1.48), with only lowest order terms,

$$\gamma^i\partial_i f(x) = (\gamma^0 E_n - m)f(x) + V(x)\gamma^0 f(x)\frac{1+\gamma^0}{2}, \tag{1.184}$$

to simplify T_2. Right multiplying by the projection operator gives

$$\gamma^i\partial_i f(x)\frac{1+\gamma^0}{2} = (\gamma^0 E_n - m)f(x)\frac{1+\gamma^0}{2} + V(x)\gamma^0 f(x)\frac{1+\gamma^0}{2} \tag{1.185}$$

with the conjugate equation

$$\frac{1+\gamma^0}{2}\partial_i f^\dagger(x)\gamma^i = -\frac{1+\gamma^0}{2}f^\dagger(x)(\gamma^0 E_n - m) - V(x)\frac{1+\gamma^0}{2}f^\dagger(x)\gamma^0 \tag{1.186}$$

where

$$V(x) = -\frac{e^2}{|\mathbf{x}|} \tag{1.187}$$

Using these two equations, we simplify the second term to find

$$\begin{aligned} T_2 &= \frac{\mu_e e\alpha}{8\pi^2}\int d^3x \frac{1}{|\mathbf{x}|}\mathrm{Tr}[2\left(E_n+\frac{\alpha}{|\mathbf{x}|}\right)\bar{f}(\mathbf{x})f(\mathbf{x})\frac{1+\gamma^0}{2} - 2mf^\dagger(\mathbf{x})f(\mathbf{x})\frac{1+\gamma^0}{2}] \\ &\approx \frac{\mu_e e\alpha}{8\pi^2}\int d^3x \frac{1}{|\mathbf{x}|}[2\left(E_n+\frac{\alpha}{|\mathbf{x}|}\right)\bar{u}(\mathbf{x})u(\mathbf{x}) - 2mu^\dagger(\mathbf{x})u(\mathbf{x})] \end{aligned} \tag{1.188}$$

where $u(\mathbf{x})$ is the Dirac spinor for the electron. We can write the spinor as

$$u(\mathbf{x}) = \begin{pmatrix} \psi(\mathbf{x}) \\ -\frac{i}{2m}\boldsymbol{\sigma}\cdot\nabla\psi(\mathbf{x}) \end{pmatrix}, \tag{1.189}$$

where $\psi(\mathbf{x})$ satisfies the non-relativistic Schroedinger equation. Plugging this into T_2 and dropping terms with an explicit factor of α^2 in them gives

$$\begin{aligned} T_2 &\approx -\frac{\mu_e e\alpha}{8\pi^2}\int d^3x \frac{1}{|\mathbf{x}|}\frac{1}{2m}\boldsymbol{\sigma}\cdot\nabla\psi^*(\mathbf{x})\boldsymbol{\sigma}\cdot\nabla\psi(\mathbf{x}) \\ &= -\frac{\mu_e e\alpha}{8\pi^2}\int d^3x \frac{1}{|\mathbf{x}|}\left[\frac{\nabla^2}{2m}|\psi(\mathbf{x}|^2 - \frac{2i\mathbf{s}}{m}\nabla\psi^*(\mathbf{x})\times\nabla\psi(\mathbf{x})\right] \\ &= \frac{\mu_e e\alpha}{8\pi^2}\left[\frac{2\pi}{m}|\psi(0)|^2 + \frac{2\mathbf{L}\cdot\mathbf{s}}{m}\int d^3x\frac{|\psi(\mathbf{x})|^2}{|\mathbf{x}|^3}\right] \\ &= \frac{\mu_e e\alpha}{8\pi^2}\left[\frac{2\pi}{m}|\psi(0)|^2 + \frac{j(j+1)-l(l+1)-\frac{3}{4}}{m}\int d^3x\frac{|\psi(\mathbf{x})|^2}{|\mathbf{x}|^3}\right]. \end{aligned} \tag{1.190}$$

Plugging in the non-relativistic wave function and performing the integral results in

$$T_2 = \frac{1}{2\pi}\frac{m\alpha^5}{n^3}\frac{C_{l,j}}{2l+1} \tag{1.191}$$

where

$$C_{l,j} = \left\{ \begin{array}{ll} \frac{1}{l+1} & \text{for} \quad j = l + 1/2 \\ \\ -\frac{1}{l} & \text{for} \quad j = l - 1/2 \end{array} \right\}. \tag{1.192}$$

Since we already computed the muonic vacuum polarization contribution separately, we do not include it in our results here. We subtract the muonic vacuum polarization contribution from T_1 to find

$$\begin{aligned} T_1 &= \frac{4}{3\pi}\frac{\alpha^5}{n^3}\frac{\mu^3}{m^2}[\log\frac{m_1}{m_{ph}} - \frac{23}{40} + \frac{8}{40}]\delta_{l,0} \\ &= \frac{4}{3\pi}\frac{\alpha^5}{n^3}\frac{\mu^3}{m^2}[\log\frac{m_1}{m_{ph}} - \frac{15}{40}]\delta_{l,0}. \end{aligned} \tag{1.193}$$

After regularization (see [30] for details), we can write this in terms of the Bethe logarithm,

$$T_1 + T_{Reg} = \frac{4}{3\pi}\frac{\alpha^5}{n^3}\frac{\mu^3}{m^2}[\log\frac{m_1}{2k_0(2S)} + \frac{11}{24}]\delta_{l,0}. \tag{1.194}$$

(It is worth noting that these results match [9] up to order α^5; however, [30] has a $-\ln \mathrm{Ry}$ in the 2P energy shift, while [9] has a $+\ln \mathrm{Ry}$ in the 2S energy shift. This term is a result of the regularization process. For the 2P-2S Lamb shift, this difference doesn't matter, but it is an important distinction when other splittings are considered.) After regularization, the 2S and 2P shifts are

$$\Delta E_{2S} = T_1 + T_2 + T_{Reg} = \frac{4}{3\pi}\frac{\alpha^5}{8}\frac{\mu^3}{m^2}[\log\frac{m}{2k_0(2S)} + \frac{5}{6}] \tag{1.195}$$

and

$$\Delta E_{2P} = T_1 + T_2 + T_{Reg} = \frac{4}{3\pi}\frac{\alpha^5}{8}\frac{\mu^3}{m^2}[\log\frac{\mu\alpha^2}{2k_0(2P)} + \frac{3}{8}\frac{C_{l,j}}{2l+1}], \tag{1.196}$$

making the Lamb shift contribution

$$\begin{aligned} L_{v,se} &= \Delta E_{2P} - E_{2S} \\ &= \frac{4}{3\pi}\frac{\alpha^5}{8}\frac{\mu^3}{m^2}[\log\frac{k_0(2S)}{k_0(2P)} + \log\frac{\mu\alpha^2}{m} + \frac{3}{8}\frac{C_{l,j}}{2l+1} - \frac{5}{6}]. \end{aligned} \tag{1.197}$$

For the $2P_{1/2} - 2S_{1/2}$ we find

$$L_{v,se} = \frac{4}{3\pi}\frac{\alpha^5}{8}\frac{\mu^3}{m^2}[\log\frac{k_0(2S)}{k_0(2P)} + \log\frac{\mu\alpha^2}{m} - \frac{23}{24}]. \tag{1.198}$$

The Bethe logarithms are listed as

$$\log k_0(2S) = 2.8117698931205 \tag{1.199}$$

$$\log k_0(2P) = -0.0300167089. \tag{1.200}$$

With these values, we have

$$L_{v,se} = -0.679 \text{ meV} \tag{1.201}$$

and the sum of the two terms gives

$$L_{v,se} + L_{\mu vac} = -0.662 \text{ meV} \tag{1.202}$$

which is close to the result of [9] which is -0.668 meV. The discrepancy is caused by our dropping orders higher than $O(\alpha^5)$.

1.4.5 Higher order corrections to electron vacuum polarization

In searching for the 0.31 meV discrepancy, it seems sensible to examine corrections to the largest contribution to the Lamb shift. In muonic hydrogen, this is clearly the electron vacuum polarization, which is two orders of magnitude larger than any other contribution. We showed that the NQA vacuum polarization term reduces to the well known result when certain approximations are made. The projection operator on the right side of Eq. (1.161), $\frac{(\not{p}+m_2)^T}{2E_q^{(2)}}$, was simplified to the much simpler operator, $\frac{(1+\gamma^0)}{2}$, which simply projects out the upper left hand component of the wave function. We also did not calculate the magnetic contributions (γ^i terms). We expect both of these terms to be small, but a new correction just 0.15% of the largest vacuum polarization contribution can resolve the discrepancy. In the following subsections, we will determine if these terms are relevant.

1.4.5.1 Momentum space calculations

In the following subsection, we will examine corrections to the vacuum polarization from the full projection operator. We focus on calculating only the largest

corrections. We start with Eq. (1.161) without the magnetic terms, but keeping the full projection operator,

$$E_{vac} = \frac{e^2}{(2\pi)^3}\int \frac{d^3q d^3p}{4E_q^{(2)}E_p^{(2)}}(-\Pi((p-q)^2)+\Pi(0))D_R(p-q) \times \mathrm{Tr}[\bar{f}_e(p,b)\gamma^0 f_e(q,b)(\gamma^0)^T(\not{p}+m_2)^T]. \quad (1.203)$$

We take our wave function to be in the 2nd basis described in section 1.4.3, where the electron spin and orbital angular momentum are first coupled, then added to the proton spin. The trace in the Dirac basis is

$$\begin{aligned}&\mathrm{Tr}[\bar{f}_e(p,b)\gamma^0 f_e(q,b)(\gamma_0)^T(\not{p}+m_2)^T] \\ &= \chi^{F_z-J_z}\otimes \mathscr{Y}^{\dagger J_z}_{JL_a}(\hat{\mathbf{p}})g^*(p)A + \chi^{F_z-J_z}\otimes \mathscr{Y}^{\dagger J_z}_{JL_b}(\hat{\mathbf{p}})h^*(p)C \\ &\quad + \left(\frac{\sigma\cdot\mathbf{p}}{E_p+m_2}\chi^{J_z-F_z}\right)^*\otimes \mathscr{Y}^{\dagger J_z}_{JL_a}(\hat{\mathbf{p}})g^*(p)B + \left(\frac{\sigma\cdot\mathbf{p}}{E_p+m_2}\chi^{J_z-F_z}\right)^* \\ &\qquad \otimes \mathscr{Y}^{\dagger J_z}_{JL_b}(\hat{\mathbf{p}})h^*(p)D \end{aligned} \quad (1.204)$$

where

$$A = (E_p + m_2)\mathscr{Y}^{J_z}_{JL_a}(\hat{\mathbf{q}}) \otimes {\chi^{F_z - J_z}}^T g(q) + \mathscr{Y}^{J_z}_{JL_a}(\hat{\mathbf{q}}) \otimes \left(\frac{\sigma \cdot \mathbf{q}}{E_q + m_2}\chi^{J_z - F_z}\right)^T (\sigma \cdot \mathbf{p})^T g(q), \tag{1.205}$$

$$B = -\mathscr{Y}^{J_z}_{JL_a}(\hat{\mathbf{q}}) \otimes {\chi^{F_z - J_z}}^T (\sigma \cdot \mathbf{p})^T g(q) + (-E_p + m_2)\mathscr{Y}^{J_z}_{JL_a}(\hat{\mathbf{q}}) \otimes \left(\frac{\sigma \cdot \mathbf{q}}{E_q + m_2}\chi^{J_z - F_z}\right)^T g(q), \tag{1.206}$$

$$C = (E_p + m_2)\mathscr{Y}^{J_z}_{JL_b}(\hat{\mathbf{q}}) \otimes {\chi^{F_z - J_z}}^T h(q) + \mathscr{Y}^{J_z}_{JL_b}(\hat{\mathbf{q}}) \otimes \left(\frac{\sigma \cdot \mathbf{q}}{E_q + m_2}\chi^{J_z - F_z}\right)^T (\sigma \cdot \mathbf{p})^T h(q), \tag{1.207}$$

$$D = -\mathscr{Y}^{J_z}_{JL_b}(\hat{\mathbf{q}}) \otimes {\chi^{F_z - J_z}}^T (\sigma \cdot \mathbf{p})^T h(q) + (-E_p + m_2)\mathscr{Y}^{J_z}_{JL_b}(\hat{\mathbf{q}}) \otimes \left(\frac{\sigma \cdot \mathbf{q}}{E_q + m_2}\chi^{J_z - F_z}\right)^T h(q), \tag{1.208}$$

and to simplify the things we have taken

$$\mathscr{Y}^{J_z}_{JL_b}(\hat{\mathbf{p}}) = \frac{\sigma \cdot \mathbf{p}}{E_p + m_1}\mathscr{Y}^{J_z}_{JL_a}(\hat{\mathbf{p}}). \tag{1.209}$$

The first term of A in the large m_2 limit gives the result we calculated earlier for the electron vacuum polarization. In our approximation above, the Uehling potential did not have any angular dependence in $\mathbf{p}$, making analytical integration easier. Since we will be calculating in a more exact way, we will have terms with angular dependence if we follow the same method. We therefore employ a different method of calculating. We must first ensure that we arrive at the same results found above with our different method. As we did in section 1.3, we use a partial wave

expansion to expand the potential and keep everything in momentum space. We also keep the factor $\frac{E_p+m_2}{2E_q}$ rather than setting it to 1, as we did earlier. The main term is

$$E_{vac} = \frac{e^2}{(2\pi)^3}\int d^3q d^3p V(p-q)\sum_{J_z} |< FF_z|J, J_z; 1/2, F_z - J_z >|^2$$
$$\times \mathscr{Y}^{\dagger J_z}_{JL_a}(\hat{\mathbf{p}})\mathscr{Y}^{J_z}_{JL_a}(\hat{\mathbf{q}})g^*(p)g(q), \tag{1.210}$$

where

$$V(p-q) = \frac{(E_p+m_2)}{2E_q}(-\Pi(-(\mathbf{p}-\mathbf{q})^2) + \Pi(0))D_R(p-q)) \tag{1.211}$$
$$= \frac{(E_p+m_2)}{2E_p}\frac{e^2}{12\pi}\int_{4m^2}^{\infty}\frac{d(k^2)}{k^2(k^2+(p-q)^2)}\left(1+\frac{2m^2}{k^2}\right)\sqrt{1-\frac{4m^2}{k^2}}. \tag{1.212}$$

As we saw in section 1.3, we can use Eqs. (1.68-1.70) to expand the potential into partial waves, and use the orthogonality relations of the spin-angle functions to perform the angular integrals and simplify traces. Plugging the expansion into E_{vac}, performing the angular integrals using first the spherical harmonic orthogonality condition and then the spin angle function orthogonality condition gives

$$E_{vac} = \frac{2e^2}{\pi(2\pi)^3}\int dqdpp^2q^2V_L(p-q)g^*(p)g(q). \tag{1.213}$$

We will be numerically integrating to find the energy. Before, there was only one integral involved because we were able to integrate analytically for all but one, but here the inclusion of the $\frac{E_p+m_2}{2E_q^{(2)}}$ factor makes analytical integration more difficult,

so we are left with 3 numerical integrals. More numerical integrals will result in a less accurate answer, but we are simply trying to get an order of magnitude answer, accurate to just one or two decimal places for the vacuum polarization corrections. The corrections should be small enough to make further decimal places negligible. The kernel is finite everywhere, so there is no need for Lande subtraction. As before, we change the integral to a finite sum and take 200 integration points. We also employ the same substitutions as in section 1.3.9 to get rid of the mass dependence in the numerical integrals. We also use the same error analysis as section 1.3.6.

Numerically, we found the largest contribution from the vacuum polarization terms to be

$$\Delta E_{vac} = 203 \pm 2 \text{ meV}. \tag{1.214}$$

This compares well to the value found from the expression in [9] (which we found before through the NQA), 205.006 meV. Again, we did not expect the result of our numerical calculation to be precise because we only took 200 integration points and we had multiple numerical integrals, but it does seem to be accurate enough. Now that we know our numerical procedure will yield accurate results, we will use it to calculate corrections to the vacuum polarization energy.

1.4.5.2 Corrections from the projection operator

We can move on to estimating the size of some of the other vacuum polarization terms in Eq. (1.204) and calculating any significant terms. We can get an order

of magnitude estimate for a term by taking $p \sim \alpha\mu$, $E_p^{(i)} \sim m_i$, and comparing to the largest term. The second term in A is smaller than the first by about a factor of $\left(\frac{\alpha\mu}{m_2}\right)^2 \approx 5 \times 10^{-7}$. Including the factor multiplying B from the trace in Eq. (1.204), the first contribution from B is smaller than the largest term in A by the same factor. The second B term is even smaller. The terms in C and D are similar to those in A and B except with $L_a \to L_b$ and $g_L \to h_L$. This amounts to an additional factor of $\left(\frac{\alpha\mu}{m_\mu}\right)^2 \approx 4 \times 10^{-5}$. The first term in C is only smaller than the largest term in A by this factor. All other terms are significantly smaller than the largest term in A. These are very rough estimates and there are other factors involved that will determine the sizes of the contributions such as the overlap between the wave functions and the partial waves of the momentum space Uehling potential.

The above estimate motivates us to calculate the first term in C, which seems to be the next largest term. From the naive estimates, it would seem it is too small to resolve the muonic hydrogen Lamb shift discrepancy, but we calculate this term here to see if this turns out to be true. The energy associated with the term is

$$\begin{aligned} E_C = & \frac{e^2}{(2\pi)^3} \int d^3q d^3p V(p-q) \\ & \times \sum_{J_z J_z'} < FF_z|J, J_z; 1/2, F_z - J_z >< FF_z|J, J_z'; 1/2, F_z - J_z' > \\ & \times \mathscr{Y}^{\dagger J_z}_{JL_a}(\hat{\mathbf{p}}) \frac{\boldsymbol{\sigma} \cdot \mathbf{p}}{E_p^{(1)} + m_1} \frac{\boldsymbol{\sigma} \cdot \mathbf{q}}{E_q^{(1)} + m_1} \mathscr{Y}^{J_z}_{JL_a}(\hat{\mathbf{q}}) g^*(p) g(q), \end{aligned} \tag{1.215}$$

where we have used

$$\mathscr{Y}^{J_z}_{JL_a}(\hat{\mathbf{q}})h(p) \approx \frac{\boldsymbol{\sigma}\cdot\mathbf{p}}{E_p^{(1)}+m_1}\mathscr{Y}^{J_z}_{JL_b}(\hat{\mathbf{q}})g(p). \tag{1.216}$$

We need to calculate this term for both the $L_a = 1$, $J = 3/2$, $F = 2$, and $L_a = 0$, $J = 1/2$, $F = 1$ states. We are free to choose F_z since it will not effect the energies. We take $F_z = +F$ in both states because it simplifies the calculation by forcing J and the proton spin to be aligned in the +z direction. This simplifies the Clebsch-Gordan coefficients in the sum, leaving only one nonzero coefficient when $J_z = J'_z = F_z - 1/2$. Also, since we are dealing with the largest total angular momentum states for the given orbital angular momentum, the electron spin and orbital angular momentum must also be aligned. With our choice of F_z, this results in spin-angle functions with just a single term.

We start by calculating the 2S state, $L_A = 0$. In this state, we have $J_z = J'_z = S_{1z} = +1/2$. The energy is

$$E_{C|_{L_a=0}} = \frac{e^2}{(2\pi)^3}\int d^3q d^3p V(p-q)\frac{p}{E_p^{(1)}+m_1}\frac{q}{E_q^{(1)}+m_1} \times \mathscr{Y}^{\dagger 1/2}_{1/2,1}(\hat{\mathbf{p}})\mathscr{Y}^{1/2}_{1/2,1}(\hat{\mathbf{q}})g^*(p)g(q) \tag{1.217}$$

where we have used the identity

$$\boldsymbol{\sigma}\cdot\hat{\mathbf{p}}\mathscr{Y}^{J_z}_{1/2,0}(\hat{\mathbf{p}}) = -\mathscr{Y}^{J_z}_{1/2,1}(\hat{\mathbf{p}}). \tag{1.218}$$

Expanding the potential,

$$E_{C|_{L_a=0}} = \int d^3p d^3q \frac{2}{\pi} \sum_{l=0}^{\infty} \sum_{m_L=-L}^{L} V_L(p,q) Y^*_{Lm_L}(\hat{q}) Y_{Lm_L}(\hat{p}) \mathscr{Y}^{\dagger 1/2}_{1/2,1}(\hat{\mathbf{p}}) \mathscr{Y}^{1/2}_{1/2,1}(\hat{\mathbf{q}})$$
$$\times g_0(q) g_0^*(p)$$
$$= \int dp dq \frac{2p^2q^2}{\pi} V_1(p,q) g_0(q) g_0^*(p), \tag{1.219}$$

where we have absorbed some factors into the potential, i.e.

$$V(p,q) = \frac{p}{E_p^{(1)} + m_1} \frac{q}{E_q^{(1)} + m_1} \frac{(E_p^{(2)} + m_2)}{2E_p^{(2)}} (-\Pi(-(\mathbf{p}-\mathbf{q})^2) + \Pi(0)) D_R(p-q)) \tag{1.220}$$

and $V_1(p,q)$ is the $L = 1$ partial wave.

Moving on to the 2P state ($L_A = 1$), we have $J_z = J'_z = +3/2$ and an energy of

$$E_{C|_{L_a=1}} = \frac{e^2}{(2\pi)^3} \int d^3q d^3p V(p-q) \frac{p}{E_p^{(1)} + m_1} \frac{q}{E_q^{(1)} + m_1}$$
$$\times \mathscr{Y}^{\dagger 3/2}_{3/2,2}(\hat{\mathbf{p}}) \mathscr{Y}^{3/2}_{3/2,2}(\hat{\mathbf{q}}) g^*(p) g(q) \tag{1.221}$$

where we have used the identity

$$\boldsymbol{\sigma} \cdot \hat{\mathbf{p}} \mathscr{Y}^{J_z}_{3/2,1}(\hat{\mathbf{p}}) = -\mathscr{Y}^{J_z}_{3/2,2}(\hat{\mathbf{p}}). \tag{1.222}$$

Expanding the potential

$$E_{C|_{L_a=1}} = \int d^3p d^3q \frac{2p^2q^2}{\pi} V_2(p,q) g_1(q) g_1^*(p) \tag{1.223}$$

where $V_2(p,q)$ is the $L = 2$ partial wave of the potential.

We use the same numerical methods discussed in the previous subsection to evaluate the difference. Again we take 200 integration points. The result is

$$\Delta E_C = E_{C|_{L_a=1}} - E_{C|_{L_a=0}} = 5.43 \times 10^{-4} \text{ meV} \tag{1.224}$$

This is roughly one order of magnitude less than our crude estimate ($4 \times 10^{-5} \times 200$ meV $\approx 8 \times 10^{-3}$ meV) and about 3 orders of magnitude too small to resolve the 0.31 meV discrepancy. This result forces us to look elsewhere for corrections.

1.4.5.3 Corrections from the magnetic terms

In this section, we briefly investigate the magnetic corrections to electron vacuum polarization. We expect these terms to be small because they involve dipole moment factors with proton or lepton masses in the denominator, but it is worth analyzing in order to rule it out as a possible solution to resolving to discrepancy. We focus on the larger terms resulting from approximation of the projection operator

in the large m_2 limit,

$$E_{vmag} = -\frac{e^2}{(2\pi)^3}\int d^3q d^3p(-\Pi(-(\mathbf{p}-\mathbf{q})^2)+\Pi(0))D_R(\mathbf{p}-\mathbf{q}) \\ \times \mathrm{Tr}[\bar{f}_e(p,b)\gamma^i f_e(q,b)\gamma^{iT}\left(\frac{1+\gamma^0}{2}\right)]. \tag{1.225}$$

The trace can be expressed as

$$\begin{aligned} T &= \mathrm{Tr}[\bar{f}_e(p,b)\gamma^i f_e(q,b)\gamma^{iT}\left(\frac{1+\gamma^0}{2}\right)] \\ &= \sum_{J_z J_z'} < FF_z|J,J_z;1/2,F_z-J_z >< FF_z|J,J_z';1/2,F_z-J_z' > \\ &\times \left(\left(\mathscr{Y}_{JL}^{J_z\dagger}(\hat{p})\sigma^i\frac{\boldsymbol{\sigma}\cdot\mathbf{q}}{E_q^{(1)}+m_1}\mathscr{Y}_{JL}^{J_z}(\hat{q})\right)\left(\chi^{F_z-J_z T}\frac{(\boldsymbol{\sigma}\cdot\mathbf{q})^T}{E_q^{(2)}+m_2}\sigma^{iT}\chi^{F_z-J_z}\right)\right. \\ &+ \left.\left(\mathscr{Y}_{JL}^{J_z\dagger}(\hat{p})\frac{\boldsymbol{\sigma}\cdot\mathbf{p}}{E_p^{(1)}+m_1}\sigma^i\mathscr{Y}_{JL}^{J_z}(\hat{q})\right)\left(\chi^{F_z-J_z T}\frac{(\boldsymbol{\sigma}\cdot\mathbf{q})^T}{E_q^{(2)}+m_2}\sigma^{iT}\chi^{F_z-J_z}\right)\right)g_L^*(p)g_L(q). \end{aligned} \tag{1.226}$$

We could try to massage this a bit more to get it into a more tractable form, but it is easier to just plug in the relevant angular momenta and continue. We are only interested in two specific states, so this should not be too arduous. We choose the same azimuthal quantum numbers selected in the previous subsection to simplify

the Clebsch-Gordan coefficients. For the $L = 0$ case we have

$$
\begin{aligned}
T|_{L=0} = &\left(\left(\mathscr{Y}^{1/2\,\dagger}_{1/2,0}(\hat{p}) \sigma^i \frac{\boldsymbol{\sigma}\cdot\mathbf{q}}{E_q^{(1)}+m_1} \mathscr{Y}^{1/2}_{1/2,0}(\hat{q}) \right) \left({\chi^+}^T \frac{(\boldsymbol{\sigma}\cdot\mathbf{q})^T}{E_q^{(2)}+m_2} {\sigma^i}^T \chi^+ \right) \right. \\
&+ \left. \left(\mathscr{Y}^{1/2\,\dagger}_{1/2,0}(\hat{p}) \frac{\boldsymbol{\sigma}\cdot\mathbf{p}}{E_p^{(1)}+m_1} \sigma^i \mathscr{Y}^{1/2}_{1/2,0}(\hat{q}) \right) \left({\chi^+}^T \frac{(\boldsymbol{\sigma}\cdot\mathbf{q})^T}{E_q^{(2)}+m_2} {\sigma^i}^T \chi^+ \right) \right) g_0^*(p) g_0(q) \\
= &\left(\left((Y_0^0)^2 (-S^1(q)\sqrt{\frac{8\pi}{3}} Y_1^1(\hat{q}) + S^1(p)\sqrt{\frac{8\pi}{3}} Y_1^{-1}(\hat{p})) \right) \left(-S^2(q)\sqrt{\frac{8\pi}{3}} Y_1^1(\hat{q}) \right) \right. \\
&+ \left((Y_0^0)^2 (iS^1(q)\sqrt{\frac{8\pi}{3}} Y_1^1(\hat{q}) + iS^1(p)\sqrt{\frac{8\pi}{3}} Y_1^{-1}(\hat{p}))) \right) \left(iS^2(q)\sqrt{\frac{8\pi}{3}} Y_1^1(\hat{q}) \right) \\
&+ \left. \left((Y_0^0)^2 (S^1(q)\sqrt{\frac{4\pi}{3}} Y_1^0(\hat{q}) + S^1(p)\sqrt{\frac{4\pi}{3}} Y_1^0(\hat{p}))) \right) \left(S^2(q)\sqrt{\frac{4\pi}{3}} Y_1^0(\hat{q}) \right) \right) \\
&\qquad\qquad \times g_0^*(p) g_0(q) \\
= &\frac{S^2(q)}{3} [2 \left(-S^1(q) Y_1^1(\hat{q}) + S^1(p) Y_1^{-1}(\hat{p}) \right) \left(-Y_1^1(\hat{q}) \right) \\
&- 2 \left(S^1(q) Y_1^1(\hat{q}) + S^1(p) Y_1^{-1}(\hat{p}) \right) \left(Y_1^1(\hat{q}) \right) \\
&+ \left(S^1(q) Y_1^0(\hat{q}) + S^1(p) Y_1^0(\hat{p}) \right) \left(Y_1^0(\hat{q}) \right)] g_0^*(p) g_0(q), \qquad (1.227)
\end{aligned}
$$

where

$$
S^i(p) = \frac{p}{E_p^{(i)} + m_i}. \qquad (1.228)
$$

and for the $L = 1$ case we have

$$
\begin{aligned}
T_1 = &\left(\left((-S^1(q)\sqrt{\frac{8\pi}{3}}Y_1^1(\hat{q}) + S^1(p)\sqrt{\frac{8\pi}{3}}Y_1^{-1}(\hat{p})) \right) \left(-S^2(q)\sqrt{\frac{8\pi}{3}}Y_1^1(\hat{q}) \right) \right. \\
&+ \left((iS^1(q)\sqrt{\frac{8\pi}{3}}Y_1^1(\hat{q}) + iS^1(p)\sqrt{\frac{8\pi}{3}}Y_1^{-1}(\hat{p})) \right) \left(iS^2(q)\sqrt{\frac{8\pi}{3}}Y_1^1(\hat{q}) \right) \\
&+ \left. \left((S^1(q)\sqrt{\frac{4\pi}{3}}Y_1^0(\hat{q}) + S^1(p)\sqrt{\frac{4\pi}{3}}Y_1^0(\hat{p})) \right) \left(S^2(q)\sqrt{\frac{4\pi}{3}}Y_1^0(\hat{q}) \right) \right) Y_1^{1*}(\hat{p})Y_1^1(\hat{q}) \\
&\times g_1^*(p)g_1(q) \\
= &\frac{S^2(q)}{5}[4\left(-S^1(q)Y_1^{1*}(\hat{p})Y_2^2(\hat{q}) + S^1(p)Y_2^{-2}(\hat{p})Y_1^1(\hat{q})\right)\left(-Y_1^1(\hat{q})\right) \\
&- 4\left(S^1(q)Y_1^{1*}(\hat{p})Y_2^2(\hat{q}) + S^1(p)Y_2^{-2}(\hat{p})Y_1^1(\hat{q})\right)\left(Y_1^1(\hat{q})\right) \\
&+ \left(S^1(q)Y_1^{1*}(\hat{p})Y_2^1(\hat{q}) + S^1(p)Y_2^{-1}(\hat{p})Y_1^1(\hat{q})\right)\left(Y_1^0(\hat{q})\right)] \qquad (1.229)
\end{aligned}
$$

We could simplify these expressions further, expand the potential in partial waves, and perform the angular integrations, but at this point it is easy to estimate the sizes of these terms to determine if such calculations are worthwhile. Each term has a factor of $S^2(q)S^1(p)$ or $S^2(q)S^1(q)$, which is not surprising since we are dealing with magnetic terms. These terms are order $\frac{\alpha^2\mu^2}{m_\mu m_p} \approx 0.000005$ times the largest vacuum polarization term. This would amount to a contribution of about $0.000005 * 200 = 0.001$ meV, which is fairly insignificant. These corrections cannot account for the discrepancy.

1.4.6 Section summary

We discussed the NQA diagrams needed to calculate Lamb shift corrections. We showed how to simplify the diagrams to find other diagrams that resemble the usual Feynman Lamb shift diagrams. We discussed perturbation theory within our framework and selected a reasonable basis for our calculations. The results of our calculations were consistent with the expected electron vacuum polarization, muon vacuum polarization, vertex corrections and self energy corrections. We also analyzed some higher order corrections to the large electron vacuum polarization term in muonic hydrogen. We found that these corrections were not sufficient to account for the proton radius problem discrepancy.

Chapter 2: Bound States in Motion

2.1 Hydrogen in motion

We turn our attention to the effects of motion on bound states in the following section. Understanding bound state motion is important if any experimental scattering data involving bound states are to be used in search of the proton radius puzzle solution. While focusing on a QCD bound state such as the proton might be more relevant to the problem, we will be studying a simple QED bound state to illustrate how we can analyze bound state motion in the NQA framework.

2.1.1 Momentum space formulation

In this section, our goal is to arrive at an equation that shows the Lorentz contraction of a moving bound state while working in momentum space. This equation will be similar to that found in [33], but with different masses for the constituents. Although the results resemble each other, the derivations are quite different. We must first define the relative momentum by

$$q \equiv p - \kappa_2 b \tag{2.1}$$

where $\kappa_i = \frac{m_i}{M}$ and $M = m_1 + m_2$. In terms of the relative momentum, the proton has momentum $q+\kappa_2 b$ and the electron has momentum $b-p = -q+\kappa_1 b$. We use the notation $E_p^{(i)} = \sqrt{\mathbf{p}^2 + m_i^2}$ to distinguish between the energies of the two particles, and the subscripts $\|$ and $\perp$ to indicate components parallel and perpendicular to the bound state motion.

We begin with Eq. (1.47). We can left multiply by the inverse of the kinetic energy operator on both sides to get

$$f_e(p,b) = \frac{e^2}{(2\pi)^3}\frac{(\not{b}-\not{p}+m_1)}{(b-p)^2-m_1^2}\int d^4p'\gamma^\mu f_e(p',b)\delta_{m_2}(p')\gamma_\mu\left(\frac{1}{k^2}\right)(-\not{p}+m_2). \quad (2.2)$$

Manipulating the denominator outside of the integral, we find

$$\begin{aligned}
(b-p)^2 - m_1^2 &= (E - E_p^{(2)})^2 - (\mathbf{b}-\mathbf{p})^2 - m_1^2 \\
&= \epsilon^2 + 2\Delta E(\epsilon - E^{(2)}_{\mathbf{q}+\kappa_2\mathbf{b}}) - 2\epsilon E^{(2)}_{\mathbf{q}+\kappa_2\mathbf{b}} - \mathbf{b}^2 + 2\mathbf{b}\cdot(\mathbf{q}+\kappa_2\mathbf{b}) \\
&\quad + M^2(\kappa_2-\kappa_1) + O(\alpha^3) \\
&= \epsilon^2 + 2\epsilon\Delta E(1-\kappa_2) - 2\epsilon[\kappa_2\epsilon\left(1 + \frac{\left(\frac{\mathbf{q}}{\kappa_2}\right)^2 + \frac{2bq_\|}{\kappa_2}}{2\epsilon^2} - \frac{1}{8}\left(\frac{\frac{2bq_\|}{\kappa_2}}{\epsilon^2}\right)^2\right)] \\
&\quad + 2\mathbf{b}\cdot\mathbf{q} - (\mathbf{b}^2+M^2)(\kappa_1-\kappa_2) + O(\alpha^3) \\
&= -\frac{1}{\kappa_2}(\mathbf{q}_\perp^2 + \gamma^{-2}q_\|^2 - 2\kappa_1\kappa_2\Delta E\epsilon) \qquad (2.3)
\end{aligned}$$

where $\Delta E = E-\epsilon$, $\epsilon = \sqrt{\mathbf{b}^2+M^2}$, $\beta = \frac{\mathbf{b}}{\epsilon}$, and $\gamma = (1-\beta^2)^{-1/2}$. The denominator

of the integrand is

$$k^2 = k^{0\,2} - \mathbf{k}^2 = k^{0\,2} - \mathbf{k}_\perp^2 - k_\parallel^2.$$

We approximate $k^{0\,2}$ as

$$\begin{aligned} k^{0\,2} &= (E_p - E_{p'})^2 \\ &\approx [\kappa_2\epsilon\left(1 + \frac{(\frac{\mathbf{q}}{\kappa_2})^2 - \frac{2|\mathbf{b}|q_\parallel}{\kappa_2}}{2\epsilon^2}\right) - \kappa_2\epsilon\left(1 + \frac{(\frac{\mathbf{q}'}{\kappa_2})^2 - \frac{2|\mathbf{b}|q_\parallel{}'}{\kappa_2}}{2\epsilon^2}\right)]^2 \\ &= \left[\frac{|\mathbf{b}|(q_\parallel - q_\parallel{}')}{\epsilon}\right]^2 + O(\alpha^3) \\ &\approx (\beta k_\parallel)^2. \end{aligned}$$

Using this, we find

$$k^2 \approx -(\mathbf{k}_\perp^2 + \gamma^{-2}k_\parallel^2), \tag{2.4}$$

a result quoted earlier.

Inserting Eqs. (2.3) and (2.4) into (2.2) and doing the p'^0 integral gives

$$\begin{aligned} \frac{1}{\kappa_2}(\mathbf{q}_\perp^2 + \gamma^{-2}q_\parallel^2 - 2\kappa_1\kappa_2\Delta E\epsilon)f_e(p,b) = \frac{e^2}{(2\pi)^3}(\not{b} - \not{p}' + m_1)\int d^3p' \frac{1}{2E_{p'}^{(2)}}\frac{1}{\mathbf{k}_\perp^2 + \gamma^{-2}k_\parallel^2} \\ \times \gamma^\mu f_e(p',b)\gamma_\mu(-\not{p}' + m_2). \end{aligned} \tag{2.5}$$

We next follow the analysis of [33] and approximate

$$\begin{aligned}(\not{b}-\not{p}'+m_1)\gamma^\mu f_e(p',b)\gamma_\mu(-\not{p}'+m_2) &= 4E_p^{(2)}E_{b-p}^{(1)}\Lambda^+(\mathbf{b}-\mathbf{p})\gamma^\mu f_e(p',b)\gamma_\mu\Lambda^-(\mathbf{p}) \\ &= 4E_p^{(2)}E_{b-p}^{(1)}\frac{b^\mu}{\epsilon}f_e(p',b)\frac{b_\mu}{\epsilon}+O(\alpha) \\ &= 4E_p^{(2)}E_{b-p}^{(1)}\gamma^{-2}f_e(p',b). \qquad (2.6)\end{aligned}$$

where $\Lambda^\pm(\mathbf{p}) = \frac{\pm\gamma^0 E_{\mathbf{p}}\mp\gamma\cdot\mathbf{p}+m}{2E_{\mathbf{p}}}$. To lowest order in α, we can write $E_{b-p}^{(1)} = \kappa_1\epsilon$, $E_{p'}^{(2)} = E_p^{(2)} = \kappa_2\epsilon$. Using Eq. (2.6), our final equation has the form

$$\begin{aligned}\frac{1}{\kappa_2}(\mathbf{q}_\perp^2+\gamma^{-2}q_\parallel^2-2\kappa_1\kappa_2\Delta E\epsilon)f_e(p,b) &= \frac{2e^2\epsilon\kappa_1}{\gamma^2(2\pi)^3}\int d^3p'\frac{f_e(p',b)}{\mathbf{k}_\perp^2+\gamma^{-2}k_\parallel^2} \\ (\frac{1}{2\mu}(\mathbf{q}_\perp^2+\gamma^{-2}q_\parallel^2)-\Delta M)f_e(p,b) &= \frac{e^2}{\gamma(2\pi)^3}\int d^3p'\frac{f_e(p',b)}{\mathbf{k}_\perp^2+\gamma^{-2}k_\parallel^2} \qquad (2.7)\end{aligned}$$

where $\Delta M \equiv \gamma\Delta E$ and $\mu = \frac{m_1m_2}{m_1+m_2}$. The Lorentz contraction in the direction of motion is explicit in this equation. Our result reduces to that of [33] in the equal mass case.

2.1.2 Position space formulation

In the previous section, we worked only in momentum space and made non-relativistic approximations to find an equation that demonstrates the Lorentz contraction of the bound state in motion. In this section, we attempt a position space formulation of the same problem, but we will try to avoid making non-relativistic approximations for as long as possible. We will eventually find a position space equation for the bound state in a small boost limit.

In section 1.3.2, we determined how the Haag amplitude in momentum space must transform under a Lorentz transformation. We can use equation (1.35) to boost the amplitude to the CM frame:

$$f_{\alpha\beta}(k,b) = (\Lambda_{CM})^{-1}_{\alpha\delta}(\Lambda_{CM})^{-1}_{\beta\gamma} f_{\delta\gamma}(L_{CM}(k),(M,\mathbf{0})) \tag{2.8}$$

where

$$\begin{aligned} L_{CM}(k) &= (\gamma(k^0 - \beta\cdot\mathbf{k}), \mathbf{k} - \beta(\gamma k^0 - (\gamma-1)\frac{\beta\cdot\mathbf{k}}{\beta^2})) \\ &= \left(\frac{b^0k^0 - \mathbf{b}\cdot\mathbf{k}}{M}, \mathbf{k} - \frac{\mathbf{b}}{M}(k^0 - \frac{\mathbf{b}\cdot\mathbf{k}}{b^0+M})\right). \end{aligned} \tag{2.9}$$

The position space Haag amplitude is just the Fourier transform of the momentum space amplitude with full mass shell delta functions for the momenta of the amplitude. We can use equation (2.8) to write the position space amplitude in

terms of the rest frame amplitude:

$$
\begin{aligned}
f(x,x') &= (2\pi)^{-4}\int dkdb\delta_{m_2}(k)\delta_M(b)e^{-ik\cdot x}e^{-ib\cdot x'}f_e(k,b) \\
&= (2\pi)^{-4}\int dkdb\delta_{m_2}(k)\delta_M(b)e^{-ik\cdot x}e^{-ib\cdot x'}(\Lambda_{CM}(\mathbf{b}))^{-1}_{\alpha\delta}(\Lambda_{CM}(\mathbf{b}))^{-1}_{\beta\gamma} \\
&\qquad\qquad \times f_{e,\delta\gamma}(L_{CM}(k),(M,\mathbf{0})) \\
&= (2\pi)^{-4}\int dk'db\delta_{m_2}(k')\delta_M(b)e^{-iL^{-1}_{CM}(k')\cdot x}e^{-ib\cdot x'}(\Lambda_{CM}(\mathbf{b}))^{-1}_{\alpha\delta}(\Lambda_{CM}(\mathbf{b}))^{-1}_{\beta\gamma} \\
&\qquad\qquad \times f_{e,\delta\gamma}(k',(M,\mathbf{0})) \\
&= (2\pi)^{-4}\int \frac{d^3k'd^3b}{4E_{k'}E_b}e^{-iE_bt'}e^{i\mathbf{b}\cdot\mathbf{x}'}e^{-i\frac{-E_bE_{k'}+\mathbf{b}\cdot\mathbf{k}'}{M}t}e^{i(\mathbf{k}'+\frac{\mathbf{b}}{M}\left(-E_{k'}+\frac{\mathbf{b}\cdot\mathbf{k}'}{E_b+M}\right))\cdot\mathbf{x}} \\
&\qquad \times (\Lambda_{CM}(\mathbf{b}))^{-1}_{\alpha\delta}(\Lambda_{CM}(\mathbf{b}))^{-1}_{\beta\gamma}f_{e,\delta\gamma}(k',(M,\mathbf{0}))|_{k'^0=-E_{k'}} + 3 \text{ terms.} \quad (2.10)
\end{aligned}
$$

In the last line, we have only explicitly written the term where k' is on the negative mass shell and b is on the positive mass shell. This is the most important term, and the one we will be focusing on, but all of the following manipulations can be carried out on the other terms as well. We can now write the position space amplitude in a nicer form:

$$
f(x,x')_{\alpha\beta} = (2\pi)^2U(\mathbf{x},t;-i\nabla_{\mathbf{x}},-i\nabla_{\mathbf{x}'})_{\alpha\delta,\beta\gamma}[D(\mathbf{x}',t')f_{\delta\gamma}(\mathbf{x})], \qquad (2.11)
$$

where

$$
D(\mathbf{x}',t') = (2\pi)^{-3}\int \frac{d^3b}{2E_b}e^{-iE_bt'}e^{i\mathbf{b}\cdot\mathbf{x}'}, \qquad (2.12)
$$

$$f_{\delta\gamma}(\mathbf{x}) = \int \frac{d^3k'}{2E_{k'}} e^{i\mathbf{k}'\cdot\mathbf{x}} f_{\delta\gamma}(k', (M, \mathbf{0}))|_{k'^0 = -E_{k'}}, \tag{2.13}$$

and the boost operator is

$$U(\mathbf{x}, t; \mathbf{k}', \mathbf{b})_{\alpha\delta,\beta\gamma} = (2\pi)^{-3} e^{i\mathbf{x}\cdot\mathbf{S}(\mathbf{k}',\mathbf{b})} e^{-itT(\mathbf{k}',\mathbf{b})} (\Lambda_{CM}(\mathbf{b}))^{-1}_{\alpha\delta} (\Lambda_{CM}(\mathbf{b}))^{-1}_{\beta\gamma}, \tag{2.14}$$

where

$$\mathbf{S}(\mathbf{k}', \mathbf{b}) = \frac{\mathbf{b}}{M} \left(-E_{k'} + \frac{\mathbf{b}\cdot\mathbf{k}'}{E_b + M} \right), \tag{2.15}$$

$$T(\mathbf{k}', \mathbf{b}) = \frac{-E_b E_{k'} + \mathbf{b}\cdot\mathbf{k}'}{M}. \tag{2.16}$$

We have effectively "factored" the amplitude into an at rest wave function and the function $D(\mathbf{x}', t')$ with a boost dependent operator acting on both functions. In the non-relativistic framework, Galilean invariance can be used to factor the wave function into a rest frame function and a delta function,

$$f(\mathbf{x} - \mathbf{y}, \mathbf{x} - \mathbf{w}) = \delta(\mathbf{w} - \frac{\mathbf{x} + \mathbf{y}}{2}) F(\mathbf{x} - \mathbf{y}). \tag{2.17}$$

The next step in the non-relativistic formulation is to change coordinates to the relative and CM coordinates. The effects of the bound state momentum are decoupled from the relative motion of the constituents. In the relativistic situation, such a decoupling is impossible. Due to the nature of the Lorentz boost, it is impossible to completely decouple the bound state momentum from the relative momentum and

we are always left with terms that involve $\mathbf{b}\cdot\mathbf{k}$, a result of Eq. (2.9). Nevertheless, it may be useful to see what corrections emerge in this position space relativistic formulation.

The spinor boost Λ_{CM} can be written as

$$\Lambda_{CM} = exp(-\frac{i}{2}\omega_{\mu\nu}S^{\mu\nu}) \tag{2.18}$$

where

$$S^{\mu\nu} = \frac{i}{4}[\gamma^{\mu},\gamma^{\nu}] \tag{2.19}$$

and

$$\omega_{\mu\nu} = \begin{pmatrix} 0 & \beta_x & \beta_y & \beta_z \\ -\beta_x & 0 & 0 & 0 \\ -\beta_y & 0 & 0 & 0 \\ -\beta_z & 0 & 0 & 0 \end{pmatrix}. \tag{2.20}$$

In terms of the bound state momentum,

$$\Lambda_{CM} = exp(i\frac{\mathbf{b}\cdot\mathbf{S}^0}{E_b}). \tag{2.21}$$

The other well known way of writing the boost is

$$\Lambda_{CM} = \mathbf{1}\cosh(\frac{|\mathbf{b}|}{2E_b}) + G\sinh(\frac{|\mathbf{b}|}{2E_b}), \tag{2.22}$$

where

$$G = \hat{b} \cdot \begin{pmatrix} \vec{\sigma} & 0 \\ 0 & -\vec{\sigma} \end{pmatrix} \tag{2.23}$$

in the Weyl basis and

$$G = \hat{b} \cdot \begin{pmatrix} 0 & \vec{\sigma} \\ \vec{\sigma} & 0 \end{pmatrix} \tag{2.24}$$

in the Dirac basis.

The position space Haag expansion for the electron is

$$e_\alpha(x) = e^{in}_\alpha(x) + \int d^3y d^3z f_{\alpha\beta}(x-y, x-z) : (\bar{p}^{in}(y)\gamma^0)_\beta \overleftrightarrow{\partial}_{z^0} B^{in}(z) : \tag{2.25}$$

Since the purpose of the double arrowed derivative is to ensure that the B and f are on the same mass shell, we can write the second term as

$$T_2 = -2 \int d^3y d^3z f^{(-+)}_{\alpha\beta}(x-y, x-z) : (\bar{p}^{in}(y)\gamma^0)_\beta \overleftarrow{\partial}_{z^0} B^{(+)in}(z) : \tag{2.26}$$

where the "$-$" and "$+$" indicate which mass shell the momenta conjugate to the arguments of the function are on. It is easily verified that both expressions are equivalent. The reason for this manipulation will become clear in a moment. For simplicity, we will drop the "-" and "+" superscripts in the following. Using Eq.

(2.11), we can express the second term as

$$T_2 = -2(2\pi)^2 \int d^3y d^3z U(\mathbf{x}', x'^0; -i\nabla_{\mathbf{x}'}, -i\nabla_{\mathbf{x}''})_{\alpha\delta,\beta\gamma}[D(\mathbf{x}'', x''^0) f_{\delta\gamma}(\mathbf{x}')]|_{x'=x-y,x''=x-z}$$
$$\times : (\bar{p}^{in}(y)\gamma^0)_\beta \overleftarrow{\partial}_{z^0} B^{in}(z) :,$$
$$= i(2\pi)^2 \int d^3y d^3z D_1(\mathbf{x}-\mathbf{z}, x^0 - z^0) U(\mathbf{x}-\mathbf{y}, x^0 - y^0; i\nabla_{\mathbf{y}}, -i\nabla_{\mathbf{z}})_{\alpha\delta,\beta\gamma}$$
$$\times [f_{\delta\gamma}(\mathbf{x}-\mathbf{y}) B^{in}(\mathbf{z}, z^0)](\bar{p}^{in}(\mathbf{y}, y^0)\gamma^0)_\beta, \tag{2.27}$$

where

$$D_1(\mathbf{x}-\mathbf{z}, x^0 - z^0) = \frac{1}{(2\pi)^3} \int d^3b e^{-iE_b(x^0-z^0)} e^{i\mathbf{b}\cdot(\mathbf{x}-\mathbf{y})}. \tag{2.28}$$

The times in the Haag expansion do not matter. The equations are valid for any times we choose and the dynamics are not affected. We can use the arbitrary nature of the times to set $y^0 = z^0 = x^0$ and find

$$T_2 = i(2\pi)^2 \int d^3y (\bar{p}^{in}(\mathbf{y}, x^0)\gamma^0)_\beta$$
$$\times U(\mathbf{x}-\mathbf{y}, 0; i\nabla_{\mathbf{y}}, -i\nabla_{\mathbf{z}})_{\alpha\delta,\beta\gamma}[f_{\delta\gamma}(\mathbf{x}-\mathbf{y}) B^{in}(\mathbf{z}, x^0)]_{\mathbf{z}=\mathbf{x}}. \tag{2.29}$$

We are now in a position to use the NQA to find a bound state equation for a moving bound state in terms of an at rest wave function. To simplify things, we

take as our equation of motion the NQA-Coulomb equation,

$$(i\gamma^\mu\partial_\mu - m_1)e(x) = e_0^2\gamma^0\int d^3x' : \bar{p}^{in}(\mathbf{x}',t) : \gamma^0 : p^{in}(\mathbf{x}',t) : e(x)V(|\mathbf{x}-\mathbf{x}'|), \quad (2.30)$$

where

$$V(|\mathbf{x}-\mathbf{x}'|) = \frac{1}{|\mathbf{x}-\mathbf{x}'|}. \quad (2.31)$$

After Haag expanding, applying the above manipulations, and taking a partial Fourier transform, we find for the LHS part of the bound state equation to be

$$\begin{aligned}(LHS)_\alpha = {} & i(2\pi)^2 U(\mathbf{x}-\mathbf{y},0;i\nabla_{\mathbf{y}},\mathbf{b})_{\beta\delta,\sigma\gamma} \\ & \times((\gamma^0)_{\alpha\beta}T(i\nabla_{\mathbf{y}},\mathbf{b}) + (\vec{\gamma})_{\alpha\beta}\cdot\mathbf{S}(i\nabla_{\mathbf{y}},\mathbf{b}) \\ & - i(\vec{\gamma})_{\alpha\beta}\cdot\nabla_x - m_1 + (\gamma^0)_{\alpha\beta}E_{\mathbf{b}} + (\vec{\gamma})_{\alpha\beta}\cdot\mathbf{b})[f_{\delta\gamma}(\mathbf{x}-\mathbf{y})] \end{aligned} \quad (2.32)$$

The RHS of the bound state equation is

$$\begin{aligned}(RHS)_\alpha = {} & i(2\pi)^2\frac{g^2}{2}(\gamma^0)_{\alpha\beta}V(|\mathbf{x}-\mathbf{y}|)U(\mathbf{x}-\mathbf{y},0;i\nabla_{\mathbf{y}},\mathbf{b})_{\beta\epsilon,\xi\kappa}\{[f_{\epsilon\kappa}(\mathbf{x}-\mathbf{y})]\} \\ & E^{-1}_{i(\overleftarrow{\nabla}_y + i\mathbf{S}(i\overleftarrow{\nabla}_{\mathbf{y}},\mathbf{b}))}[(-\gamma^0 E_{i(\overleftarrow{\nabla}_y + i\mathbf{S}(i\overleftarrow{\nabla}_{\mathbf{y}},\mathbf{b}))} - i\vec{\gamma}\cdot(\overleftarrow{\nabla}_y + i\mathbf{S}(i\overleftarrow{\nabla}_{\mathbf{y}},\mathbf{b}) + m_2)(\gamma^0)]_{\sigma\xi} \end{aligned} \quad (2.33)$$

After canceling some common terms, our final equation is

$$
\begin{aligned}
&U(\mathbf{r},0;-i\nabla_{\mathbf{r}},\mathbf{b})_{\beta\delta,\sigma\gamma}((\gamma^0)_{\alpha\beta}(T(-i\nabla_{\mathbf{r}},\mathbf{b})+E_{\mathbf{b}}) \\
&\quad +(\vec{\gamma})_{\alpha\beta}\cdot(\mathbf{S}(-i\nabla_{\mathbf{r}},\mathbf{b})+\mathbf{b}-i\nabla_r)-m_1)[f_{\delta\gamma}(\mathbf{r})] \\
&=\frac{g^2}{2}(\gamma^0)_{\alpha\beta}V(r)U(\mathbf{r},0;-i\nabla_{\mathbf{r}},\mathbf{b})_{\beta\epsilon,\xi\kappa}\{[f_{\epsilon\kappa}(\mathbf{r})]\} \\
&E^{-1}_{i(-\overleftarrow{\nabla}_r+i\mathbf{S}(-i\overleftarrow{\nabla}_{\mathbf{r}},\mathbf{b}))}[(-\gamma^0 E_{i(-\overleftarrow{\nabla}_r+i\mathbf{S}(-i\overleftarrow{\nabla}_{\mathbf{r}},\mathbf{b}))}-i\vec{\gamma}\cdot(-\overleftarrow{\nabla}_r+i\mathbf{S}(-i\overleftarrow{\nabla}_{\mathbf{r}},\mathbf{b})+m_2)(\gamma^0)]_{\sigma\xi}.
\end{aligned}
\tag{2.34}
$$

When $\mathbf{b}=0$, this reduces to the position space version of Eq. (1.48),

$$
\begin{aligned}
&((\gamma^0)_{\alpha\beta}(M-E_{-i\nabla_r})-i(\vec{\gamma})_{\alpha\beta}\cdot\nabla_r-m_1)[f_{\beta\sigma}(\mathbf{r})] \\
&=\frac{g^2}{2}(\gamma^0)_{\alpha\beta}V(r)\{f_{\beta\xi}(\mathbf{r})\}E^{-1}_{i(-\overleftarrow{\nabla}_r)}[(-\gamma^0 E_{i(-\overleftarrow{\nabla}_r)}+i\vec{\gamma}\cdot\overleftarrow{\nabla}_r+m_2)(\gamma^0)]_{\sigma\xi}.
\end{aligned}
\tag{2.35}
$$

where $\mathbf{r}=\mathbf{x}-\mathbf{y}$. Eq. (2.33) involves complicated functions of derivatives. Finding an analytical solution to such an equation is most likely impossible. A numerical solution may be possible, but we have not attempted this yet. It may be useful to simplify the equation by looking at the small boost case. Dropping terms of $O(\mathbf{b^2})$

and higher, the bound state equation becomes

$$
\begin{aligned}
&((\gamma^0)_{\alpha\delta}(\left(\frac{-ME_{-i\nabla_r}-i\mathbf{b}\cdot\nabla_{\mathbf{r}}}{M}\right)+M)+(\vec{\gamma})_{\alpha\delta}\cdot(\frac{-E_{-i\nabla_r}\mathbf{b}}{M}+\mathbf{b}-i\nabla_r)-m_1\\
&-\mathbf{b}\cdot\left(i\frac{\mathbf{r}E_{-i\nabla_r}}{M}+\frac{\mathbf{G}_{\beta\delta}}{2M}+\frac{\mathbf{G}_{\sigma\gamma}}{2M}\right)((\gamma^0)_{\alpha\beta}(-E_{-i\nabla_r}+M)-i(\vec{\gamma})_{\alpha\beta}\cdot\nabla_r-m_1))[f_{\delta\gamma}(\mathbf{r})]\\
&=\frac{g^2}{2}(\gamma^0)_{\alpha\beta}V(r)(1-\mathbf{b}\cdot\left(i\frac{\mathbf{r}E_{-i\nabla_r}}{M}+\frac{\mathbf{G}_{\beta\epsilon}}{2M}+\frac{\mathbf{G}_{\xi\kappa}}{2M}\right))[f_{\epsilon\kappa}(\mathbf{r})]\\
&E^{-1}_{i(-\overleftarrow{\nabla}_r-i\frac{\mathbf{b}E_{-i\nabla_r}}{M})}[(-\gamma^0E_{i(-\overleftarrow{\nabla}_r-i\frac{\mathbf{b}E_{-i\nabla_r}}{M})}-i\vec{\gamma}\cdot(-\overleftarrow{\nabla}_r-i\frac{\mathbf{b}E_{-i\nabla_r}}{M})+m_2)(\gamma^0)]_{\sigma\xi} \quad (2.36)
\end{aligned}
$$

The terms with bound state momentum, $\mathbf{b}$, can be calculated perturbatively using numerical solutions to the rest frame bound state equation as the lowest order solution. After working in both position and momentum space, it seems that momentum space is the superior choice. The calculations in momentum space were simpler and there was no need for some of the contrived manipulations needed to arrive at the final result. The final equation is also more elegant in momentum space.

2.1.3 Section summary

We used the NQA to find an equation for a moving bound state consisting of two fermions of different masses. After some approximations, we cast this equation into a form where the Lorentz contraction was evident. This bound state equation matched that found through the Bethe-Salpeter procedure. We did not elaborate much on the final answer, i.e. explain how to put the Dirac structure back in or show how the frame dependence can be removed through rescaling variables, because such things are well discussed in [33]. The purpose of this section was simply to promote

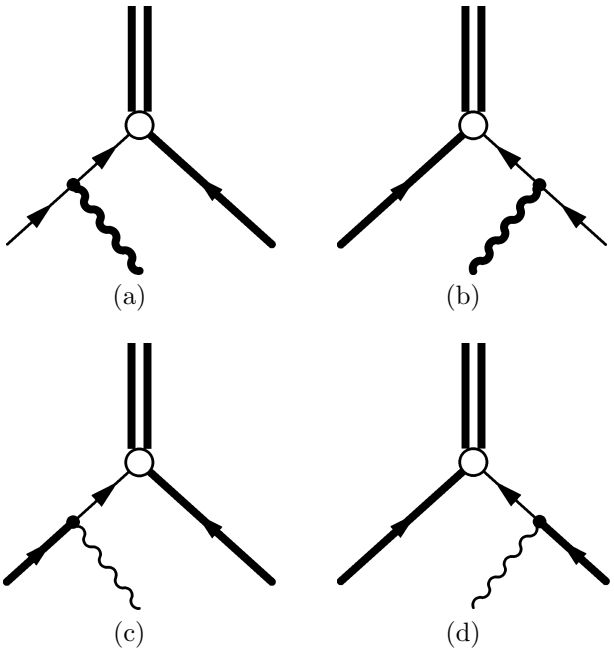

Figure 2.1: Graphs for the matrix element $< B|\psi_1(p_1)\psi_2(p_2)A^\mu(k)|0 >$. The left fermion line is the electron and the right fermion line is the proton in each diagram.

an alternative method for arriving at the same answer. Whether the N-Quantum was the simpler process in this case is debatable, but we feel it may be more useful in some other calculations involving bound states in motion. Integrating over the mass shell delta-functions generated by the on shell lines connected to amplitudes should be easier than the alternative in many cases. The N-Quantum also avoids the complications of the Bethe-Salpeter method discussed in the introduction. We also found a position space bound state equation by "factoring" the bound state amplitude into a rest frame wave function and a bound state operator. This equation reduced to the expected rest frame equation when $\mathbf{b} = 0$. Position space calculations were more complicated than momentum space.

The N-Quantum can also be used to calculate higher order Fock state contribu-

tions. These terms can be expressed in terms of the lower order amplitudes with some approximations. As an example, we can calculate the matrix element corresponding to the projection of the bound state onto the $ep\gamma$ Fock state, $M^\mu(p_1, p_2, k, \mathbf{b}) \equiv \langle B|\psi_{1\alpha}(p_1)\psi_{2\beta}(p_2)A^\mu(k)|0\rangle$. After using the equations of motion to approximate some of the higher order amplitudes in terms of lower order ones, Haag expanding the interacting fields and contracting all *in* fields, the result is

$$M^\mu = \frac{e}{(2\pi)^3}\delta^4(p_1 + p_2 + k - b)\Bigg\{(-\not{p}_1 + m_1)\gamma^\mu f_e(p_2, b)\left(\frac{\Theta_1(k, p_2)}{p_1^2 - m_1^2} - \frac{\Theta_1(p_1, p_2)}{k^2}\right) - f_p^T(p_1, b)(\gamma^\mu(\not{p}_2 + m_2))^T\left(\frac{\Theta_1(k, p_1)}{p_2^2 - m_2^2} - \frac{\Theta_1(p_1, p_2)}{k^2}\right)\Bigg\}|_{b^0 = E_{\mathbf{b}}} \tag{2.37}$$

where $\Theta_1(k_i, k_j) = \frac{1}{6}\delta_{m_i}(k_i)\delta_{m_j}(k_j)(1 + \theta(k_i^0)\theta(k_j^0) + \theta(-k_i^0)\theta(-k_j^0))$. The results could have been left in terms of higher order amplitudes for a more exact, but more difficult to calculate, solution. We could also find this expression by interpreting the diagrams shown in Figure 2.1 using the rules given in section 1.3.2 .

It would be interesting to use the N-Quantum procedure to see whether or not classical Lorentz contraction takes place in higher order Fock state amplitudes. This method can also be used to study other bound state models in which Lorentz covariance has been established. The subject of Lorentz covariance and bound states in motion has been studied in a number of papers already [34] [35] [36]. Some of the models within these works have interactions that lead to Lorentz invariant solutions [35], while others do not [36]. It would be interesting to analyze some of these models in the N-quantum framework, and determine which interactions result in Lorentz contracting solutions. We hope that this paper has shown the utility of

the N-quantum procedure in studying such models, and we plan to use it to gain a better understanding of bound state motion in future work.

Chapter 3: Treatment of Soft Photons

3.1 Soft photons

The following work can be found in [37]. There are open questions about the description of charged particles in theories with long range interactions connected with massless fields and particles. For example, the asymptotic (in and out) states and fields of QED do not exist because of the long range Coulomb interaction. In this paper we construct a clothed field for a charged particle in QED. We show that the asymptotic limits exist for this clothed field.

In a pioneering paper, Kulish and Faddeev [38] showed that terms in the interaction of QED that have an annihilation and a creation operator of a charged particle give nonvanishing contributions in the limits $t \to \pm\infty$. These contributions come from the coupling of soft photons to the charged particles, and produce a branch cut at the (renormalized) mass of the charged field in the Källén-Lehmann (KL) weight of the two-point function, instead of a delta function. The analogous problem in the Feynman propagator is that there is a branch cut instead of a pole at the mass of the charged fields. Because of this branch cut, the asymptotic limits that would define the in and out fields for the charged fields do not exist. In addition these branch cuts produce infrared (IR) divergences in scattering amplitudes.

Lavelle and McMullen [39] gave a method to clothe charged fields to create a gauge-invariant charged field that can be used to define asymptotic fields. The KL weight of their clothed field has a delta function singularity at the mass of the charged particle. They also showed that the scattering amplitudes constructed with their clothed fields are free of IR divergences.

Dirac [40] and Creutz [41] constructed a composite gauge invariant field,

$$\psi_f(x) \equiv \exp[-ie \int d^4y f^\mu(x-y) A_\mu(y)] \psi(x) \tag{3.1}$$

for the field of the charged particles. Dirac noted the existence of several choices for $f^\mu(x-y)$ that fulfill the gauge invariance condition, but are unphysical. He argued the correct choice of $f^\mu(x-y)$ is the one that produces the correct electric field.

We also note the work of Stefanovich [42], who reformulated QED to eliminate ultraviolet (UV) infinities in the S-matrix and Hamiltonian, and discussed applications to bound states. He used the approach of [43] to find a finite Hamiltonian that is equivalent, for scattering, to the usual QED Hamiltonian.

In this paper, in contrast to [43], which eliminated the entire trilinear term in their scalar model, we eliminate only the soft photon part of the terms that give nonvanishing contributions in the limits $t \to \pm\infty$. This is the minimal reformulation of the Hamiltonian that allows the asymptotic limits for the in and out fields to exist. The interaction terms with soft photons are the terms that produce a branch point at the mass of the charged particle rather than a delta function in the KL weight (or a pole in the Feynman propagator). We show that the two-point function of the

clothed charged field has an isolated singularity at the mass of the charged particle.

Our calculation gives a two-body interaction between charged particles associated with soft photons of momentum less that a given value, which, for illustration, we chose to be αm_e.

3.1.1 Preliminaries

We repeat the discussion of [38] to show why the terms with a creation and an annihilation operator of the charged particle together with a soft photon operator (which we call the problematic terms) produce a branch cut in the KL weight. For example, if the charged field represents the electron, the square of the mass of an electron produced on the vacuum by $b^\dagger(\mathbf{p})a_\mu^\dagger(\mathbf{k})$ is

$$m_e^2 + 2(\sqrt{\mathbf{p}^2 + m_e^2}|\mathbf{k}| - \mathbf{p}\cdot\mathbf{k}) \to m_e^2, \mathbf{k} \to 0.$$

Thus this state does not have a discrete mass. The two-point function of the charged field will have a branch point at the square of the mass of the charged particle instead of an isolated singularity. When we eliminate the soft photons with momentum $|\mathbf{k}| \leq \alpha m_e$ from the electron field, the square of the mass of $b^\dagger(\mathbf{p})a_\mu^\dagger(\mathbf{k})$ is greater than $m_e^2 + 2(\sqrt{\mathbf{p}^2 + m_e^2} - \mathbf{p}\cdot\hat{\mathbf{k}})\alpha m_e$; thus there is a gap between the mass of the electron and the mass of the lowest electron-photon state. The quantitative size of the gap is not important; only the existence of a finite gap is necessary to provide a discrete mass for the charged particle.

We noted that only certain terms in the interaction Hamiltonian destroy the

gap. The problematic terms survive when we take the asymptotic limits $t \to \pm\infty$ and prevent the existence of a gap above m_e^2 in the KL weight. These are the terms we remove with our clothing operator. To do this, we absorb the soft photons for $|\mathbf{k}| < \alpha m_e$ in the definition of the electron operator, removing the low-momentum part of the terms in the trilinear interaction that do not produce (or annihilate) pairs, but keeping the remaining part of the electron-photon interaction.

We begin with the QED Hamiltonian, $H = H_0 + H_I$. The free Hamiltonian is just $H_0 = H_{0f} + H_{0ph}$ where

$$H_{0f} = \int \frac{d^3p}{(2\pi)^{3/2}} E_p (b_p^{s\dagger} b_p^s + d_p^{s\dagger} d_p) \tag{3.2}$$

$$H_{0ph} = -\int \frac{d^3k}{(2\pi)^{3/2}} |\mathbf{k}| a_{\mu k}^\dagger a_k^\mu \tag{3.3}$$

where $E_p = \sqrt{\mathbf{p}^2 + m_e^2}$ and the creation and annihilation operators have the usual commutation relations

$$\{b_p^s, b_k^{r\dagger}\} = (2\pi)^{3/2} \delta^3(\mathbf{p} - \mathbf{k}) \delta^{rs} \tag{3.4}$$

$$[a_{\mu p}, a_{\nu k}^\dagger] = -(2\pi)^{3/2} \delta^3(\mathbf{p} - \mathbf{k}) g_{\mu\nu}, \tag{3.5}$$

and the interaction Hamiltonian is

$$H_I(t) = -e \int d^3x A_\mu(x) \bar{\psi}(x) \gamma^\mu \psi(x). \tag{3.6}$$

The creation and annihilation operators depend on three-momenta and spin; the sum

over repeated spin indices is implied. We do not include renormalization counter terms because they are irrelevant for the issues of this section. We divide our Hamiltonian,

$$H = H_{0f} + H_{0ph_{soft}} + H_{0ph_{hard}} + H_{I_{soft}} + H_{I_{hard}} \tag{3.7}$$

where

$$H_{0ph_{soft}} = -\int_0^{\alpha m_e} \frac{d^3k}{(2\pi)^{3/2}} |\mathbf{k}| a^\dagger_{\mu k} a^\mu_k, \tag{3.8}$$

$$H_{0ph_{hard}} = -\int_{\alpha m_e}^{\infty} \frac{d^3k}{(2\pi)^{3/2}} |\mathbf{k}| a^\dagger_{\mu k} a^\mu_k, \tag{3.9}$$

and similarly $H_{I_{soft}}$ and $H_{I_{hard}}$, written in momentum space, involve integrals over small and large photon momenta, respectively. When the asymptotic limit is taken, only the soft photon part of the interaction Hamiltonian will survive.

The asymptotic limit of this Hamiltonian has been discussed in both [38] and [39] and we only give a brief summary here. We expand the fields in the usual way

$$\psi(x) = \int \frac{d^3p}{(2\pi)^3} \frac{1}{\sqrt{2E_p}} \sum_s (b^s_p u^s(p) \exp(-ip\cdot x) + d^{s\dagger}_p v^s(p) \exp(ip\cdot x)) \tag{3.10}$$

$$A_\mu(x) = \int \frac{d^3k}{(2\pi)^3} \frac{1}{\sqrt{2|\mathbf{k}|}} (a_{\mu k} \exp(-ik\cdot x) + a^\dagger_{\mu k} \exp(ik\cdot x)). \tag{3.11}$$

With these expansions, we find eight terms in (3.6), each with some time dependence of the form $\exp(if(E)t)$, where $f(E)$ involves sums and differences of energies . We wish to know which terms will be significant and which terms will vanish in the

asymptotic limit. In this limit, $t \to \pm\infty$, therefore $f(E)$ must go to 0 or else the term will not vanish. Only terms where $f(E) = \pm(E_{p+k} - E_p \pm |\mathbf{k}|)$ can survive the limit because for $|\mathbf{k}| \approx 0$, $f(E) \approx 0$. The resulting Hamiltonian is

$$H_{Ias}(t) = -\frac{e}{(2\pi)^{3/2}} \int \frac{d^3k d^3p}{\sqrt{2|\mathbf{k}|}E(p)} p^\mu (\exp(-i\frac{p\cdot k}{E(p)}t)\rho^\dagger(p,k)a_{\mu k} + \exp(i\frac{p\cdot k}{E(p)}t)\rho(p,k)a^\dagger_{\mu k}) \tag{3.12}$$

where

$$\rho(p,k) = \sum_s (b^{s\dagger}_{p-k} b^s_p - d^{s\dagger}_{p-k} d^s_p) \tag{3.13}$$

and we have used the small-k limit to simplify the energy sums in the exponentials: $E_{p-k} - E_p + |\mathbf{k}| \approx \frac{p\cdot k}{E_p}$ and we dropped k in $E(p-k)$ in the denominator. We also set $\mathbf{k} = \mathbf{0}$ in the Dirac wave functions so that the wave functions do not appear in $\rho(p,k)$. We plan to clothe the whole Hamiltonian in a later paper; however here we focus on the asymptotic Hamiltonian, the free fermion Hamiltonian and the soft part of the free photon Hamiltonian.

3.1.2 The clothing transformation

Following [43], we introduce clothed operators related by a unitary clothing operator generated by S, to the bare operators in the interaction picture Hamiltonian. (We will call this unitary clothing operator S for short.) We define a clothed

operator $\mathbf{O}$ as

$$\mathbf{O} = \exp(iS) O \exp(-iS). \tag{3.14}$$

where O is the bare operator. We denote clothed operators with bold type. Because the clothing operator is unitary, clothed operators obey the same commutation relations given in (3.4) and (3.5) as the bare ones. The clothed Hamiltonian as a function of clothed operators is equal to the bare Hamiltonian as a function of unclothed operators [43],

$$\mathbf{H}(\mathbf{b}, \mathbf{b}^\dagger, \mathbf{d}, \mathbf{d}^\dagger, \mathbf{a}, \mathbf{a}^\dagger) = H(b, b^\dagger, d, d^\dagger, a, a^\dagger). \tag{3.15}$$

Since the clothing operator commutes with itself, it can be written as a function of clothed or bare fields:

$$S(\mathbf{b}, \mathbf{b}^\dagger, \mathbf{d}, \mathbf{d}^\dagger, \mathbf{a}, \mathbf{a}^\dagger) = S(b, b^\dagger, d, d^\dagger, a, a^\dagger). \tag{3.16}$$

We use

$$\begin{aligned} \mathbf{H}(\mathbf{b}, \mathbf{b}^\dagger, \mathbf{d}, \mathbf{d}^\dagger, \mathbf{a}, \mathbf{a}^\dagger) &= \exp(-iS) H(\mathbf{b}, \mathbf{b}^\dagger, \mathbf{d}, \mathbf{d}^\dagger, \mathbf{a}, \mathbf{a}^\dagger) \exp(iS) \\ &= H(\mathbf{b}^\dagger, \mathbf{b}, \cdots) - i[S, H(\mathbf{b}^\dagger, \mathbf{b}, \cdots)] + \frac{(-i)^2}{2!}[S, [S, H(\mathbf{b}^\dagger, \mathbf{b}, \cdots)]] + \dots \end{aligned} \tag{3.17}$$

to find the clothed Hamiltonian, where the bold fields represent clothed fields, the bold **H** represents a clothed Hamiltonian, and $H(\mathbf{b}^\dagger, \mathbf{b}, \cdots)$ is the bare Hamiltonian as a function of the clothed fields. This relation is easily verified by inserting $1 = \exp(-iS)\exp(iS)$ on both sides of each bare operator in the Hamiltonian. We assume S has an expansion in powers of α and (3.17) is a valid perturbative expansion.

The soft photon part of the asymptotic trilinear term is what interferes with the definition of in and out fields. Therefore we define our clothing to cancel only the soft photon part of this term, and further, only to the order α that we are calculating. All integrals over photon momenta below are taken only over the range $\{k = 0, \alpha m_e\}$.

To remove the soft photon part of the asymptotic trilinear interaction we require S to satisfy

$$-i[S, H_0(\mathbf{b}^\dagger, \mathbf{b}, \cdots)] = -H_{Ias}(\mathbf{b}^\dagger, \mathbf{b}, \cdots). \tag{3.18}$$

From (3.17), this will create the needed cancellation. We use the equation of motion for S in the interaction picture,

$$i\frac{dS}{dt} = [S, H_0] = -iH_{Ias}(\mathbf{b}^\dagger, \mathbf{b}, \cdots), \tag{3.19}$$

to derive an expression for S:

$$\begin{aligned} S(t) &= -\int dt H_{Ias}(\mathbf{b}^\dagger, \mathbf{b}, \cdots) \\ &= \frac{ie}{(2\pi)^{3/2}} \int \frac{d^3k d^3p}{\sqrt{2|\mathbf{k}|}} \frac{p^\mu}{p\cdot k} (\exp(-i\frac{p\cdot k}{E(p)}t)\rho^\dagger(p,k)a_{\mu k} - \exp(i\frac{p\cdot k}{E(p)}t)\rho(p,k)a^\dagger_{\mu k}). \end{aligned} \tag{3.20}$$

This clothing operator is nearly identical to the soft component of the "distortion operator" of [39].

We find the order in α of terms involving integrals over k with an upper limit of αm_e. Due to this limit, the photon creation and annihilation operators carry a power of $\alpha^{-3/2}$ (See Appendix B). The lowest order term of the free fermion Hamiltonian, which does not involve a k integral, is $O(\alpha^0)$. The soft part of the free photon Hamiltonian is $O(\alpha^1)$; the asymptotic interaction is $O(\alpha^{3/2})$. Each power of S contributes $O(\alpha^{1/2})$. We compute our clothed Hamiltonian to $O(\alpha^2)$.

We also used (3.15) to find the clothed Hamiltonian by writing the bare operators of the original (bare) Hamiltonian in terms of clothed fields. The relation between the clothed and bare operators is

$$\mathbf{b}^s_p = exp(iS) b^s_p exp(-iS) \tag{3.21}$$

$$\mathbf{a}^\mu_k = exp(iS) a^\mu_k exp(-iS). \tag{3.22}$$

To first order in S,

$$\mathbf{b}_p^s = b_p^s - i[b_p^s, S] \tag{3.23}$$

$$\mathbf{a}_k^\mu = a_k^\mu - i[a_k^\mu, S]. \tag{3.24}$$

After performing the commutators, we find

$$\mathbf{b}_p^s = b_p^s + \frac{e}{(2\pi)^{3/2}} \int \frac{d^3k}{\sqrt{2|\mathbf{k}|}} (\frac{p^\mu}{p\cdot k} b_{p-k}^s a_{\mu k} - \frac{\bar{p}^\mu}{\bar{p}\cdot k} b_{p+k}^s a_{\mu k}^\dagger) \tag{3.25}$$

$$\mathbf{a}_{\mu k} = a_{\mu k} - \frac{e}{(2\pi)^{3/2}\sqrt{2|\mathbf{k}|}} \int \frac{d^3p}{p\cdot k} p_\mu (b_{p-k}^{s\dagger} b_p^s - d_{p-k}^{s\dagger} d_p^s). \tag{3.26}$$

where $\bar{p} \equiv (p^0, \mathbf{p}+\mathbf{k})$. Since the clothing operator S commutes with itself, it is easy to invert the clothing operation to get the bare fields in terms of clothed fields:

$$b_p^s = \mathbf{b}_p^s - \frac{e}{(2\pi)^{3/2}} \int \frac{d^3k}{\sqrt{2|\mathbf{k}|}} (\frac{p^\mu}{p\cdot k} \mathbf{b}_{p-k}^s \mathbf{a}_{\mu k} - \frac{\bar{p}^\mu}{\bar{p}\cdot k} \mathbf{b}_{p+k}^s \mathbf{a}_{\mu k}^\dagger) \tag{3.27}$$

$$a_{\mu k} = \mathbf{a}_{\mu k} + \frac{e}{(2\pi)^{3/2}\sqrt{2|\mathbf{k}|}} \int \frac{d^3p}{p\cdot k} p_\mu (\mathbf{b}_{p-k}^{s\dagger} \mathbf{b}_p^s - \mathbf{d}_{p-k}^{s\dagger} \mathbf{d}_p^s) \tag{3.28}$$

3.1.3 Calculation of the clothed Hamiltonian

In this section we use (3.17) to clothe the Hamiltonian to $O(\alpha^2)$. We can use (3.18) to simplify the procedure (proof of (3.18) for our explicit operators is given in Appendix C). Since we calculate to $O(\alpha^2)$, we insert (3.18) into (3.17) and combine

terms to find

$$\begin{aligned}\mathbf{H}(\mathbf{b},\mathbf{b}^\dagger,\mathbf{d},\mathbf{d}^\dagger,\mathbf{a},\mathbf{a}^\dagger) &= H_{\mathbf{b}^\dagger,\mathbf{b},\cdots} - i[S, H_{\mathbf{b}^\dagger,\mathbf{b},\cdots}] + \frac{(-i)^2}{2!}[S,[S, H_{\mathbf{b}^\dagger,\mathbf{b},\cdots}]] \\ &= H_{0f} + H_{0ph} - i[S, H_{Ias}] + \frac{(-i)^2}{2!}[S, -iH_{Ias}] \\ &= H_{0f} + H_{0ph} - \frac{i}{2}[S, H_{Ias}], \end{aligned} \tag{3.29}$$

where we have dropped the term involving two commutators of S with H_{Ias} because it is higher order in α. The Hamiltonians in (3.29) are all functions of clothed fields. By design, we no longer have a trilinear term to order α^2. All that is left to find the clothed Hamiltonian is to find $[S, H_{Ias}]$. Since both S and H are trilinear expressions in operators and have two terms each, the calculation is cumbersome. For this reason, we will leave out much of the details. We first define

$$\frac{i}{2}[H_{Ias}, S] \equiv H_{self} + H_{qu}, \tag{3.30}$$

where H_{self} is the bilinear self energy term and H_{qu} represents the quartic interaction terms. Before computing the commutator, we write the H_{Ias} and S in a simpler way:

$$H_{Ias} = -\frac{e}{(2\pi)^{3/2}} \int \frac{d^3k d^3p}{\sqrt{2|\mathbf{k}|}E_p} p^\mu (A_\mu + A_\mu^\dagger) \tag{3.31}$$

$$S_{Ias} = \frac{ie}{(2\pi)^{3/2}} \int \frac{d^3k' d^3p'}{\sqrt{2|\mathbf{k}|'}} \frac{p'^\nu}{p' \cdot k'} (A'_\nu - A'^\dagger_\nu) \tag{3.32}$$

where

$$A_\mu = (\mathbf{b}_p^{s\dagger}\mathbf{b}_{p-k}^s - \mathbf{d}_p^{s\dagger}\mathbf{d}_{p-k}^s)\mathbf{a}_{\mu k} \tag{3.33}$$

$$A'_\nu = (\mathbf{b}_{p'}^{s\dagger}\mathbf{b}_{p'-k'}^s - \mathbf{d}_{p'}^{s\dagger}\mathbf{d}_{p'-k'}^s)\mathbf{a}_{\nu k'}. \tag{3.34}$$

Now the operator part of the commutator is

$$\begin{aligned}[A_\mu + A_\mu^\dagger, A'_\nu - A'^\dagger_\nu] &= [A_\mu, A'_\nu] - [A_\mu, A'^\dagger_\nu] + [A_\mu^\dagger, A'_\nu] - [A_\mu^\dagger, A'^\dagger_\nu] \\ &= ([A_\mu, A'_\nu] + [A_\mu, A'_\nu]^\dagger) - ([A_\mu, A'^\dagger_\nu] + [A_\mu, A'^\dagger_\nu]^\dagger) \end{aligned} \tag{3.35}$$

The only commutators we need to compute are $[A_\mu, A'_\nu]$ and $[A_\mu, A'^\dagger_\nu]$. We take hermitian conjugates to find the other two terms. The first commutator is

$$\begin{aligned}[A_\mu, A'_\nu] = (2\pi)^{3/2}[&\delta^3(\mathbf{p} - \mathbf{k} - \mathbf{p}')(\mathbf{b}_p^{s\dagger}\mathbf{b}_{p'-k'}^s + \mathbf{d}_p^{s\dagger}\mathbf{d}_{p'-k'}^s) \\ &- \delta^3(\mathbf{p}' - \mathbf{k}' - \mathbf{p})(\mathbf{b}_{p'}^\dagger\mathbf{b}_{p-k} + \mathbf{d}_{p'}^\dagger\mathbf{d}_{p-k})]\mathbf{a}_{\mu k}\mathbf{a}_{\nu k'}, \end{aligned} \tag{3.36}$$

and the second commutator is

$$\begin{aligned}[A_\mu, A'^\dagger_\nu] = (2\pi)^{3/2}[&-(2\pi)^{3/2}(\mathbf{b}_p^\dagger\mathbf{b}_{p'} + \mathbf{d}_p^\dagger\mathbf{d}_{p'})\delta^3(\mathbf{p} - \mathbf{p}') \\ &+ \mathbf{b}_p^\dagger\mathbf{b}_{p'-k'}^\dagger\mathbf{b}_{p-k}\mathbf{b}_{p'} + \mathbf{d}_p^\dagger\mathbf{d}_{p'-k'}^\dagger\mathbf{d}_{p-k}\mathbf{d}_{p'} \\ &+ \mathbf{b}_p^\dagger\mathbf{b}_{p-k}\mathbf{d}_{p'-k'}^\dagger\mathbf{d}_{p'} + \mathbf{d}_p^\dagger\mathbf{d}_{p-k}\mathbf{b}_{p'-k'}^\dagger\mathbf{b}_{p'}]\delta^3(\mathbf{k} - \mathbf{k}')g_{\mu\nu} \\ &+ [(\mathbf{b}_p^\dagger\mathbf{b}_{p'} + \mathbf{d}_p^\dagger\mathbf{d}_{p'})\delta^3(\mathbf{p} - \mathbf{k} - \mathbf{p}' + \mathbf{k}') \\ &- (\mathbf{b}_{p'-k'}^\dagger\mathbf{b}_{p-k} + \mathbf{d}_{p'-k'}^\dagger\mathbf{d}_{p-k})\delta^3(\mathbf{p} - \mathbf{p}')]\mathbf{a}_{\nu k'}^\dagger\mathbf{a}_{\mu k}. \end{aligned} \tag{3.37}$$

Collecting terms bilinear in operators, we find the self-energy correction term

$$H_{self} = e^2 m_e^2 \int \frac{d^3p d^3k}{2|\mathbf{k}|} \frac{1}{E_p p \cdot k} (\mathbf{b}_p^\dagger \mathbf{b}_p + \mathbf{d}_p^\dagger \mathbf{d}_p).$$

We will ignore this term in the next section and assume our energy is renormalized. Note that our clothing does not induce any photon self-energy correction term.

Collecting the remaining terms, it is clear H_{qu} will be a sum of terms involving $b^\dagger b^\dagger bb$, $b^\dagger baa$, $b^\dagger ba^\dagger a^\dagger$, $b^\dagger ba^\dagger a$, all preceding terms with $b \to d$, and $b^\dagger bd^\dagger d$. No terms involving the photon creation or annihilation operators survive to $O(\alpha^2)$. The only dependence on these operators in the clothed Hamiltonian will be in the free photon part. We have decoupled the soft photons. The final quartic interaction Hamiltonian is

$$H_{qu} = -\frac{e^2}{2(2\pi)^{3/2}} \int d^3k d^3p d^3p' K(\mathbf{k}, \mathbf{p}, \mathbf{p}') [(\mathbf{b}_p^{s\dagger} \mathbf{b}_{p'-k}^{r\dagger} \mathbf{b}_{p-k}^s \mathbf{b}_{p'}^r + (\mathbf{b} \to \mathbf{d})) + (\mathbf{b}_p^{s\dagger} \mathbf{b}_{p-k}^s \mathbf{d}_{p'-k}^{r\dagger} \mathbf{d}_{p'}^r + \mathbf{b} \leftrightarrow \mathbf{d})] \quad (3.38)$$

where

$$K(\mathbf{k}, \mathbf{p}, \mathbf{p}') = \frac{p \cdot p' (E_{p'} p + E_p p') \cdot k}{2|\mathbf{k}| E_p E_{p'} p \cdot k p' \cdot k} \quad (3.39)$$

This quartic interaction is the contribution to the asymptotic interaction, H_{Ias}, from soft photons with momentum less than αm_e.

3.1.4 Equation of motion

With the clothed Hamiltonian, we can find the equations of motion for the clothed interacting creation and annihilation operators. We start by defining

$$\mathbf{b}^s(\mathbf{p},t) \equiv \mathbf{b}^s_p \exp(-iEt). \tag{3.40}$$

We will find the Heisenberg equation of motion for this momentum and time dependent field. We begin by finding the commutator of $\mathbf{b}^s_p$ with the clothed Hamiltonian. The commutator with the free Hamiltonian is trivial

$$[\mathbf{b}^s_p, H_0] = E_p \mathbf{b}^s_p, \tag{3.41}$$

and the commutator with the first quartic term in (3.38) is

$$\begin{aligned}
[\mathbf{b}^s_q, H_{qu}|_1] &= -\frac{e^2}{2(2\pi)^3}\int d^3k d^3p (K(\mathbf{k},\mathbf{q},\mathbf{p})\mathbf{b}^{r\dagger}_{p-k}\mathbf{b}^s_{q-k}\mathbf{b}^r_p \\
&\qquad\qquad - K(\mathbf{k},\mathbf{p},\mathbf{q}+\mathbf{k})\mathbf{b}^{r\dagger}_p\mathbf{b}^r_{p-k}\mathbf{b}^s_{q+k}) \\
&= \frac{e^2}{2(2\pi)^3}\int d^3k d^3p (K(\mathbf{k},\mathbf{q},\mathbf{p}) + K(-\mathbf{k},\mathbf{p}-\mathbf{k},\mathbf{q}-\mathbf{k}))\mathbf{b}^{r\dagger}_{p-k}\mathbf{b}^r_p\mathbf{b}^s_{q-k}.
\end{aligned} \tag{3.42}$$

The commutator with the second quartic term in the Hamiltonian vanishes trivially. The commutator with the third and fourth quartic terms are

$$\begin{aligned}[\mathbf{b}^s_q, H_{qu}|_{3,4}] &= -\frac{e^2}{2(2\pi)^3}\int d^3k d^3p (K(\mathbf{k},\mathbf{q},\mathbf{p})\mathbf{b}^s_{q-k}\mathbf{d}^{r\dagger}_{p-k}\mathbf{d}^r_p \\ &\qquad + K(\mathbf{k},\mathbf{p},\mathbf{q}+\mathbf{k})\mathbf{b}^s_{q+k}\mathbf{d}^{r\dagger}_p\mathbf{d}^r_{p-k}) \\ &= -\frac{e^2}{2(2\pi)^3}\int d^3k d^3p (K(\mathbf{k},\mathbf{q},\mathbf{p}) + K(-\mathbf{k},\mathbf{p}-\mathbf{k},\mathbf{q}-\mathbf{k}))\mathbf{b}^s_{q-k}\mathbf{d}^{r\dagger}_{p-k}\mathbf{d}^r_p.\end{aligned} \tag{3.43}$$

Using the above commutators, our equation of motion is

$$i\frac{d\mathbf{b}^s(\mathbf{q},t)}{dt} = E_q\mathbf{b}^s(\mathbf{q},t) + \frac{e^2}{2(2\pi)^3}\int d^3k d^3p\, T(\mathbf{k},\mathbf{q},\mathbf{p})\boldsymbol{\rho}(\mathbf{p},\mathbf{k},t)\mathbf{b}^s(\mathbf{q}-\mathbf{k},t) \tag{3.44}$$

where

$$T(\mathbf{k},\mathbf{q},\mathbf{p}) = K(\mathbf{k},\mathbf{q},\mathbf{p}) + K(-\mathbf{k},\mathbf{p}-\mathbf{k},\mathbf{q}-\mathbf{k}). \tag{3.45}$$

Since the clothed Hamiltonian is symmetric under $b \leftrightarrow d$ interchange, we find the equation of motion for d by interchanging b and d in (3.44),

$$i\frac{d\mathbf{d}^s(\mathbf{q},t)}{dt} = E_q\mathbf{d}^s(\mathbf{q},t) - \frac{e^2}{2(2\pi)^3}\int d^3k d^3p\, T(\mathbf{k},\mathbf{q},\mathbf{p})\boldsymbol{\rho}(\mathbf{p},\mathbf{k},t)\mathbf{d}^s(\mathbf{q}-\mathbf{k},t) \tag{3.46}$$

We now find a perturbative solution to these equations in powers of e^2. We

begin by expanding the time dependent operator

$$\mathbf{b}^s(\mathbf{q},t) = \mathbf{b}^{s\ in}(\mathbf{q},t) + e^2\mathbf{b}^{(2)s}(\mathbf{q},t) + e^4\mathbf{b}^{(4)s}(\mathbf{q},t) + \dots \tag{3.47}$$

$$\mathbf{d}^s(\mathbf{q},t) = \mathbf{d}^{s\ in}(\mathbf{q},t) + e^2\mathbf{d}^{(2)s}(\mathbf{q},t) + e^4\mathbf{d}^{(4)s}(\mathbf{q},t) + \dots \tag{3.48}$$

The first term in the expansion is the annihilation operator for an asymptotic in field, which obeys the free equation of motion. The time dependence of the higher order terms is unknown at this point, but we can assign them time dependence of the form $\exp(-iE^{(n)}t)$, where $E^{(n)}$ is the energy associated with the nth order and will be determined during our perturbative approach, i.e.

$$\mathbf{b}^{(n)s}(\mathbf{q},t) \equiv \mathbf{b}^{(n)s}(\mathbf{q})\exp(-iE^{(n)}t). \tag{3.49}$$

To solve (3.44) and (3.46), we use (3.47) and (3.48) for $\mathbf{b}$ and $\mathbf{d}$ and collect terms of the same power in e. Since we have already identified the first term with the in field annihilation operator, we know its time dependence is $\exp(-iE_qt)$, and therefore at $O(e^0)$, we have an identity,

$$E_q\mathbf{b}_q^{s\ in} = E_q\mathbf{b}_q^{s\ in}. \tag{3.50}$$

At $O(e^2)$, we find

$$(E^{(2)} - E_q)\mathbf{b}^{(2)s}(\mathbf{q},t) = \frac{e^2}{2(2\pi)^3}\int d^3k d^3p\; T(\mathbf{k},\mathbf{q},\mathbf{p})\boldsymbol{\rho}^{in}(\mathbf{p},\mathbf{k},t)\mathbf{b}^{s\,in}(\mathbf{q}-\mathbf{k},t) \tag{3.51}$$

$$(E^{(2)} - E_q)\mathbf{b}^{(2)s}(\mathbf{q}) = \frac{e^2}{2(2\pi)^3}\int d^3k d^3p\; T(\mathbf{k},\mathbf{q},\mathbf{p})\boldsymbol{\rho}^{in}(\mathbf{p},\mathbf{k})\mathbf{b}^{s\;in}_{\mathbf{q}-\mathbf{k}} \times \exp(i(E^{(2)} - (E_p + E_{q-k} - E_{p-k}))t) \tag{3.52}$$

where

$$\boldsymbol{\rho}^{in}(\mathbf{p},\mathbf{k},t) \equiv \mathbf{b}^{s\,in\dagger}(\mathbf{p}-\mathbf{k},t)\mathbf{b}^{s\,in}(\mathbf{p},t) - \mathbf{d}^{s\,in\dagger}(\mathbf{p}-\mathbf{k},t)\mathbf{d}^{in\,s}(\mathbf{p},t). \tag{3.53}$$

There is no time dependence on the left hand side of (3.52), so the time dependence on the right hand side must vanish, i.e. $E^{(2)} = E_p + E_{q-k} - E_{p-k}$. Using this in the equation gives

$$\mathbf{b}^{(2)s}(\mathbf{q}) = \frac{e^2}{2(2\pi)^3}\int d^3k d^3p \frac{T(\mathbf{k},\mathbf{q},\mathbf{p})\boldsymbol{\rho}^{in}(\mathbf{p},\mathbf{k})\mathbf{b}^{s\;in}_{\mathbf{q}-\mathbf{k}}}{E_p + E_{q-k} - E_{p-k} - E_q}. \tag{3.54}$$

where we have again kept only the lowest order in k to arrive at (3.54). We find the equation for d by taking $b \leftrightarrow d$. Calculating to $O(e^4)$ is more laborious, and beyond the scope of this paper. It requires computing a sum of terms, in each of which all the creation and annihilation operators are taken to be in fields except for one, which is taken to be the $O(e^2)$ term. Since the $O(e^2)$ term has two terms itself,

there are 12 terms before any contractions take place. This calculation can be done, but it is not necessary for this work.

We have found an expansion of the clothed interacting fermion annihilation operator (and creation operator if we take the Hermitian conjugate of (3.47)) in terms of normal ordered in field operators, which annihilate the vacuum and obey the free equation of motion. This expansion does not involve any photon operators, nor will it at any order, because of the form of the clothed Hamiltonian.

One thing that is worth studying is the clothed two-point function,

$$< \Omega | \{ \bar{\boldsymbol{\psi}}_\alpha(x), \boldsymbol{\psi}_\beta(y) \} | \Omega > . \tag{3.55}$$

where

$$\boldsymbol{\psi}_\alpha(x) = \exp(iS) \psi(x) \exp(-iS). \tag{3.56}$$

The clothed field can be expanded in terms of the clothed operators and the expansion has the same form as (3.10). We can then expand the clothed interacting operators in terms of clothed in field operators via (3.47) and (3.48), inserting (3.54) where necessary. From (3.54), we see that the second order contribution is expressed in terms of normal ordered in field creation and annihilation operators which annihilate the vacuum; therefore, they do not contribute to the two-point function. Even if we include higher order terms, they will be normal ordered operators, and also will not contribute to the two-point function. We still have a contribution from the

leading order in field which gives the usual pole at the mass of the fermion squared, but all other terms vanish once we have absorbed the soft photons in the definition of the electron operator. We still need to take the "hard" part of the Hamiltonian, in which a trilinear term still exists, into account. This part of the Hamiltonian creates a branch cut in the spectral density beginning after some gap. We can determine the size of this gap kinematically. The invariant mass of the lowest order multi-particle state is

$$\begin{aligned} q^2 &= (E_p + |\mathbf{k}|)^2 - (\mathbf{p} + \mathbf{k})^2 \\ &= m_e^2 + 2|\mathbf{k}|(E_p - \mathbf{p} \cdot \hat{\mathbf{k}}) \end{aligned} \tag{3.57}$$

where $\hat{\mathbf{k}}$ is a unit vector in the direction of the photon momentum. Our "hard" photons must have $|\mathbf{k}| > \alpha m_e$, so as long as $|\mathbf{p}| < \infty$, there exists a gap

$$q^2 - m_e^2 = 2|\mathbf{k}|(E_p - \mathbf{p} \cdot \hat{\mathbf{k}}) \tag{3.58}$$

We have suppressed the distribution aspects of our calculations. From the point of view of distribution theory, our formulas should be taken as distributions and should be integrated with a function from a Schwartz space [44] such as $\mathcal{S}$. Then sets of measure zero or values in the limit of momenta becoming infinitely large are not relevant. Thus it is not relevant that if p and k are parallel, i.e. $\hat{\mathbf{p}} \cdot \hat{\mathbf{k}} = 1$, the gap above mass m^2 can vanish, since in the large $|\mathbf{p}|$ limit the gap goes as $m^2|\mathbf{k}|/|\mathbf{p}|$.

3.1.5 Section summary

We reformulated the Hamiltonian of QED to eliminate the part of the asymptotic interaction, H_{Ias}, with soft photons that produces a branch cut at the mass of the electron. The clothed charged fields have absorbed the soft photons that prevented the proper definition of in and out fields. The reformulated charged fields have a gap between the mass shell single-particle singularity and the many-particle branch cut in the KL weight. The effects of soft photons that originally appeared in the trilinear interaction terms now appear in quadrilinear interaction terms. These quadrilinear interaction terms do not produce a branch cut in the KL weight, and we expect that they will not lead to infrared divergences in scattering amplitudes.

We used our clothed Hamiltonian to find an equation of motion for the clothed creation and annihilation operators. After finding these equations, we solved them perturbatively in powers of e^2. From this process, we were able to find an expansion of the clothed interacting operators in terms of in field operators that annihilate the vacuum. The $O(e^2)$ terms of the expansion contain normal ordered in field creation and annihilation operators with at least one annihilation and one creation operator. Higher order terms will also be normal ordered. Due to this normal ordering, these higher order terms did not contribute to the clothed two-point Green's function. The combination of the normal ordering and the lack of photon operators in the expansions shown in (3.47) and (3.48) produces a gap between the mass shell singularity at m_e^2 and the beginning of the multi-particle branch cut in the KL weight. From our calculations we have found the lowest-order contribution to the

two-particle interaction from soft photons.

3.2 Conclusion

We have studied the lowest order NQA bound state equation, calculated some Lamb shift correction terms, examined the effects of motion on bound states, and constructed clothed fields that reduce to the correct *in* and *out* fields in the asymptotic limit while producing soft photon interaction corrections when included in a theory. In sections 1.3 and 1.4, we directly looked for any additional corrections to the $2S - 2P$ splitting that could account for the proton radius discrepancy. In the next two sections, we discussed two factors that may be relevant to the proton radius problem in the future. We briefly recapitulate each section here and discuss each part's relevance to Pohl's discovery.

In section 1.3, we used the NQA to find a bound state equation and solved the equation numerically. The results did not yield any significant differences from Dirac-Coulomb energies. It is clear that simply calculating lowest order energies using a more appropriate bound state equation will not account for the discrepancy. We did not attempt to solve the original pair of coupled integral equations, Eqs. (1.41) and (1.42). While a numerical solution of these equations should not be difficult, and comparison to our simplified equation, Eq. (1.47) would give us more insight into the NQA, it is unlikely to solve the proton radius problem. We also found the contribution of the opposite mass shell term. This contribution was negligible.

Section 1.4 is most directly related to Pohl's discovery. We found the NQA

diagrams needed to calculate the Lamb shift and calculated some of them. Our simplified results were consistent with the expected vacuum polarization, vertex correction, and self energy terms. We did not find any additional terms that could account for the discrepancy in the NQA framework. We did not calculate the crossed and uncrossed two-photon exchange diagrams or any proton structure dependent terms. Such terms are obviously important to the problem we are investigating, but it is unlikely that the results of such calculations would deviate from the usual results. We also looked into some higher order corrections to the largest Lamb shift term, electron vacuum polarization. We found that corrections from the projection operator and magnetic terms were insignificant.

In section 2, we used the NQA to investigate the effects of motion on a bound state. We found that our weakly bound state exhibited Lorentz contraction along the direction of motion. It would be interesting to examine the effects of motion on higher order Haag amplitudes. Although we analyzed a QED bound state, it is possible that a QCD bound state such as the proton contracts in a similar way when in motion. Such considerations are necessary when attempting to extract the proton radius from electron scattering experiments and compare to the rest frame radius.

In section 3, we studied the effects of clothing fields in a Hamiltonian. Understanding how to construct fields that approach the proper *in* and *out* fields used in the Haag expansion is vital to the NQA process. In this section, we found that our clothing eliminated a trilinear interaction Hamiltonian term and produced a soft photon quadrilinear interaction term. It may be worthwhile to calculate a similar

term within the framework of the NQA in QED and determine if such a term has any significant effect on energy levels.

The proton radius problem is still an unresolved issue. In this thesis, we have developed a foundation for investigating QED effects related to this problem using the NQA. Our approach is one of many different potential solutions. As more progress is made towards the resolution of such an elusive puzzle, many different possibilities are being ruled out by experimental data and theoretical considerations. While it is possible that corrections within the framework of the NQA are insufficient to account for the 0.31 meV discrepancy, there are still many potential factors to be investigated with this procedure. Additionally, outside of the proton radius problem, the NQA is a versatile method for studying bound state properties with some distinct advantages over alternative frameworks. These advantages include three dimensional covariant equations, only having one off-shell constituent at a time, and the independent introduction of constituent masses. In the case of a bound state where one or more constituents are very nearly on-shell, the NQA is an excellent framework for deriving spectator bound state equations. When all constituents are off-shell, the NQA can still be a powerful tool for finding a coupled bound state equations for wavefunctions.

It is the author's opinion that the resolution of the proton radius discrepancy will come from a reevaluation of proton structure dependent terms. The muon is closer to the proton in muonic hydrogen than the electron is in electronic hydrogen, thus it is more sensitive to proton structure effects. Mohr's innovative model [23] could be a step in the right direction. As it is, it is oversimplified and adjustments

need to made for it to be consistent with experimental bounds, but it seems like a very good starting point. The QED calculations are well known, and our findings verify that they are accurate. Introducing new particle interactions seems to be a last resort effort after all other possible explanations are ruled out.

The utility of the NQA has not yet been fully explored. We have discussed only a few of its applications in this thesis, and even those applications can be developed further. There are still many unresolved problems associated with bound states, and the NQA may prove to be a valuable tool in probing these issues in the future.

J=0

L=0, S=0

L'= \ S'=	1
1	-1

J=1

L=0, S=1

S'=

L'=	0	1
1	$\frac{1}{\sqrt{3}}$	$-\sqrt{\frac{2}{3}}$

L=1, S=0

S'=

L'=	1
0	$\frac{1}{\sqrt{3}}$
2	$-\sqrt{\frac{2}{3}}$

L=1, S=1

S'=

L'=	1
0	$-\sqrt{\frac{2}{3}}$
2	$-\sqrt{\frac{1}{3}}$

L=2, S=1

L'= \ S'=	0	1
1	$-\sqrt{\frac{2}{3}}$	$-\frac{1}{\sqrt{3}}$

J=2

L=1, S=1

L'= \ S'=	0	1
2	$\sqrt{\frac{2}{5}}$	$-\sqrt{\frac{3}{5}}$

L=2, S=0

L'= \ S'=	1
1	$\sqrt{\frac{2}{5}}$
3	$-\sqrt{\frac{3}{3}}$

L=2, S=1

L'= \ S'=	1
1	$-\sqrt{\frac{3}{5}}$
3	$-\sqrt{\frac{2}{5}}$

Chapter B: α power counting

We have integrals of the form

$$\int_0^{\alpha m} d^3k F(\mathbf{k}) a_\mu(\mathbf{k}).$$

We need a consistent way to keep track of the order in α of such an expression. Since k is restricted to the range $[0, \alpha m]$, we expect that this integral is $O(\alpha^3)$ times the power of α in $F(\mathbf{k})$, if we neglect $a_\mu(\mathbf{k})$ in our power counting. If we take a commutator between our integral and $a_\nu^\dagger(\mathbf{p})$, we find

$$[\int_0^{\alpha m} d^3k F(\mathbf{k}) a_\mu(\mathbf{k}), a_\nu^\dagger(\mathbf{p})] = -g_{\mu\nu} F(\mathbf{p})$$

where $\mathbf{p}$ is also restricted to the range $[0, \alpha m]$. This term seems to be of the same order in α as $F(\mathbf{p})$. Thus, if we ignore the αm dependence of $a_\mu(\mathbf{k})$, we have lost a factor of α^3.

To take account of the αm dependence of $a_\mu(\mathbf{k})$, we change the range of $\mathbf{k}$ from $[0, \alpha m]$ to $[0, 1]$ in a new variable $\hat{\mathbf{k}} = (\alpha m)^{-1}\mathbf{k}$. Then the integral becomes

$$(\alpha m)^3 \int_0^1 d^3\hat{\mathbf{k}} F(\alpha m \hat{\mathbf{k}}) a_\mu(\alpha m \hat{\mathbf{k}})$$

The commutation relations for operators with such arguments are

$$[a_\mu(\alpha m\hat{\mathbf{k}}), a^\dagger_\nu(\alpha m\hat{\mathbf{p}})] = -g_{\mu\nu}\delta(\alpha m(\hat{\mathbf{k}} - \hat{\mathbf{p}}))$$

$$[(\alpha m)^{3/2}a_\mu(\alpha m\hat{\mathbf{k}}), (\alpha m)^{3/2}a^\dagger_\nu(\alpha m\hat{\mathbf{p}})] = -g_{\mu\nu}\delta^3(\hat{\mathbf{k}} - \hat{\mathbf{p}})$$

$$[\hat{a}_\mu(\hat{\mathbf{k}}), \hat{a}^\dagger_\nu(\hat{\mathbf{p}})] = -g_{\mu\nu}\delta^3(\hat{\mathbf{k}} - \hat{\mathbf{p}})$$

where we have defined $\hat{a}_\mu(\hat{\mathbf{k}}) = (\alpha m)^{3/2}a_\mu(\mathbf{k})$, and we see that $\hat{a}_\mu$ satisfies the usual commutation relations. Now our integral can be written as

$$(\alpha m)^{3/2}\int_0^1 d^3\hat{k}F(\alpha m\hat{\mathbf{k}})\hat{a}_\mu(\hat{\mathbf{k}})$$

and it is clear that our integral is $O(\alpha^{3/2})$ times the power of α in $F(\alpha m\hat{\mathbf{k}})$. Now if we commute with $a^\dagger_\nu(\mathbf{p}) = (\alpha m)^{-3/2}\hat{a}^\dagger_\nu(\hat{\mathbf{p}})$, we find

$$[(\alpha m)^{3/2}\int_0^1 d^3\hat{k}F(\alpha m\hat{\mathbf{k}})\hat{a}_\mu(\hat{\mathbf{k}}), (\alpha m)^{-3/2}\hat{a}^\dagger_\nu(\hat{\mathbf{p}})] = -g_{\mu\nu}F(\alpha m\mathbf{p})$$

and the power counting is consistent. Each $a_\mu(\mathbf{k})$ and $a^\dagger_\mu(\mathbf{k})$ effectively carries a power of $(\alpha m)^{-3/2}$.

A quicker way to see this is to note that if we take $\hbar = 1$, the free Hamiltonian is $H = \int d^3k|\mathbf{k}|a^\dagger_\mu(\mathbf{k})a^\mu(\mathbf{k})$; since the dimensions of H and $|\mathbf{k}|$ are the same, a and $a^\dagger$ must each carry dimensions $\mathbf{k}^{-3/2}$.

Chapter C: Checking (3.18) explicitly

We check (3.18) explicitly in here. We focus on the $\mathbf{b}^\dagger\mathbf{b}$ part of the free fermion Hamiltonian because the $\mathbf{d}^\dagger\mathbf{d}$ part is clothed in the same way. The commutator of S with $H_{0f}|_b$, where $H_{0f}|_b$ is the $\mathbf{b}^\dagger\mathbf{b}$ term, is

$$[S, H_{0f}|_b] = -\frac{ie}{(2\pi)^{3/2}} \int \frac{d^3k d^3p}{\sqrt{2|\mathbf{k}|}} \frac{p^\mu}{p\cdot k} [\mathbf{b}_p^\dagger \mathbf{b}_{p-k} \mathbf{a}_{\mu k}(E_p - E_{p-k}) + \mathbf{b}_{p-k}^\dagger \mathbf{b}_p \mathbf{a}_{\mu k}^\dagger (E_p - E_{p-k})]$$

$$= -\frac{ie}{(2\pi)^{3/2}} \int \frac{d^3k d^3p}{\sqrt{2|\mathbf{k}|}} \frac{p^\mu}{p\cdot k} \frac{\mathbf{p}\cdot\mathbf{k}}{E_p} [\mathbf{b}_p^\dagger \mathbf{b}_{p-k} \mathbf{a}_{\mu k} + \mathbf{b}_{p-k}^\dagger \mathbf{b}_p \mathbf{a}_{\mu k}^\dagger] + O(\alpha^{5/2}). \tag{C.1}$$

We used $k \sim \alpha m$ to simplify the difference in energies. The lowest order term in this difference contributes a factor of α, making this commutator $O(\alpha^{3/2})$, rather than $O(\alpha^{1/2})$, as we might have expected. The commutator of S with the $d^\dagger d$ part of the free fermion Hamiltonian is identical up to a negative sign after taking $b \to d$. Combining the two parts, we find

$$[S, H_{0f}] = -\frac{ie}{(2\pi)^{3/2}} \int \frac{d^3k d^3p}{\sqrt{2|\mathbf{k}|}} \frac{p^\mu}{p\cdot k} \frac{\mathbf{p}\cdot\mathbf{k}}{E_p} [\boldsymbol{\rho}^\dagger(p,k)\mathbf{a}_{\mu k} + \boldsymbol{\rho}(p,k)\mathbf{a}_{\mu k}^\dagger]. \tag{C.2}$$

The commutator of S with the free photon Hamiltonian is straightforward:

$$[S, H_{0ph}] = \frac{ie}{(2\pi)^{3/2}} \int \frac{d^3k d^3p}{\sqrt{2|\mathbf{k}|}} |\mathbf{k}| \frac{p^\mu}{p \cdot k} (\mathbf{a}_{\mu k} \boldsymbol{\rho}^\dagger(p,k) + \mathbf{a}^\dagger_{\mu k} \boldsymbol{\rho}(p,k)), \tag{C.3}$$

The sum of the two terms multiplied by $-i$ is

$$-i[S, H_0] = -i \left(\frac{ie}{(2\pi)^{3/2}} \int \frac{d^3k d^3p}{\sqrt{2|\mathbf{k}|}} \left(\frac{E_p|\mathbf{k}| - \mathbf{p} \cdot \mathbf{k}}{E_p} \right) \frac{p^\mu}{p \cdot k} (\mathbf{a}_{\mu k} \boldsymbol{\rho}^\dagger(p,k) + \mathbf{a}^\dagger_{\mu k} \boldsymbol{\rho}(p,k)) \right)$$

$$= \frac{e}{(2\pi)^{3/2}} \int \frac{d^3k d^3p}{E_p \sqrt{2|\mathbf{k}|}} p^\mu (\mathbf{a}_{\mu k} \boldsymbol{\rho}^\dagger(p,k) + \mathbf{a}^\dagger_{\mu k} \boldsymbol{\rho}(p,k))$$

$$= -H_{Ias}.$$

which confirms (3.18).

Chapter D: NQA diagrams

The following pages show examples of NQA Lamb shift diagrams.

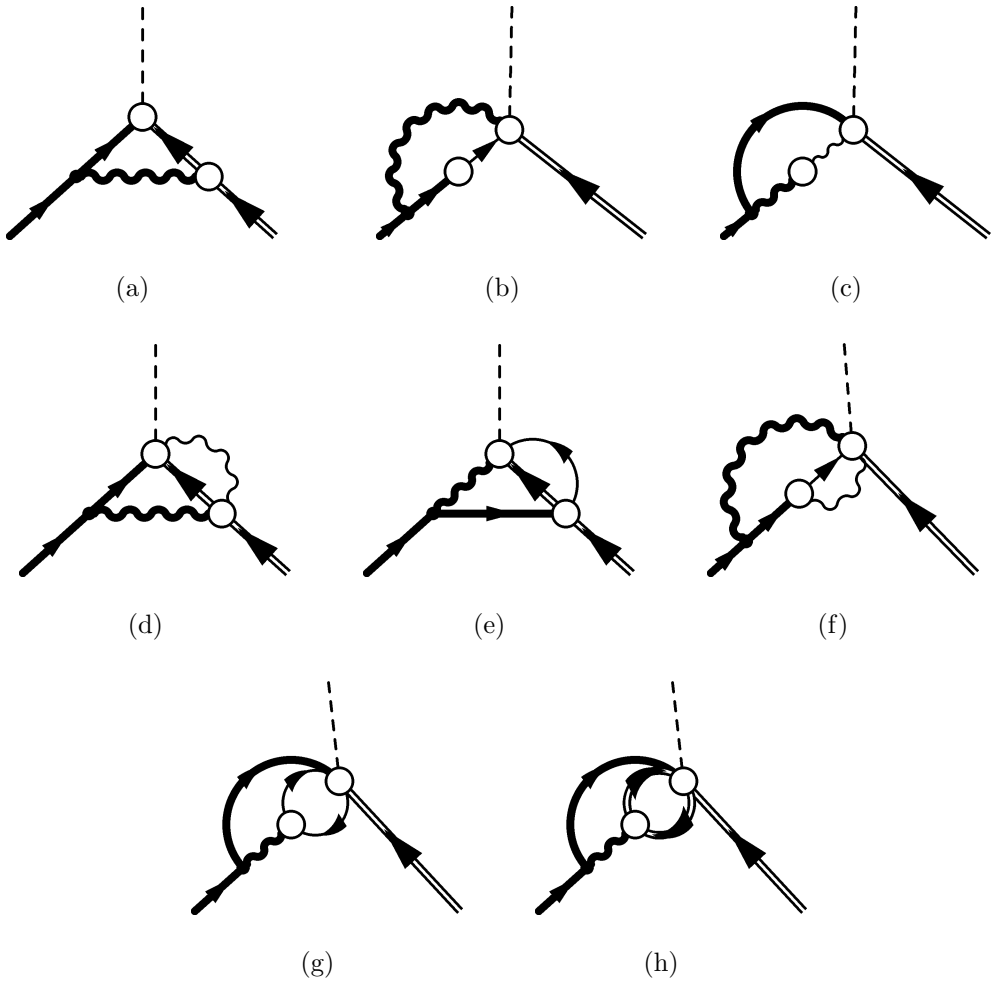

Figure D.1: Graphs for the right hand side of the electron equation of motion. Heavy lines are off-shell and light lines are on-shell. The dashed line represents the bound state (hydrogen atom). The empty circle represents the amplitude f_e in (a) and f_p in (b). The left fermion line is the electron and the right line is the proton. Similar graphs exist for the proton equation.

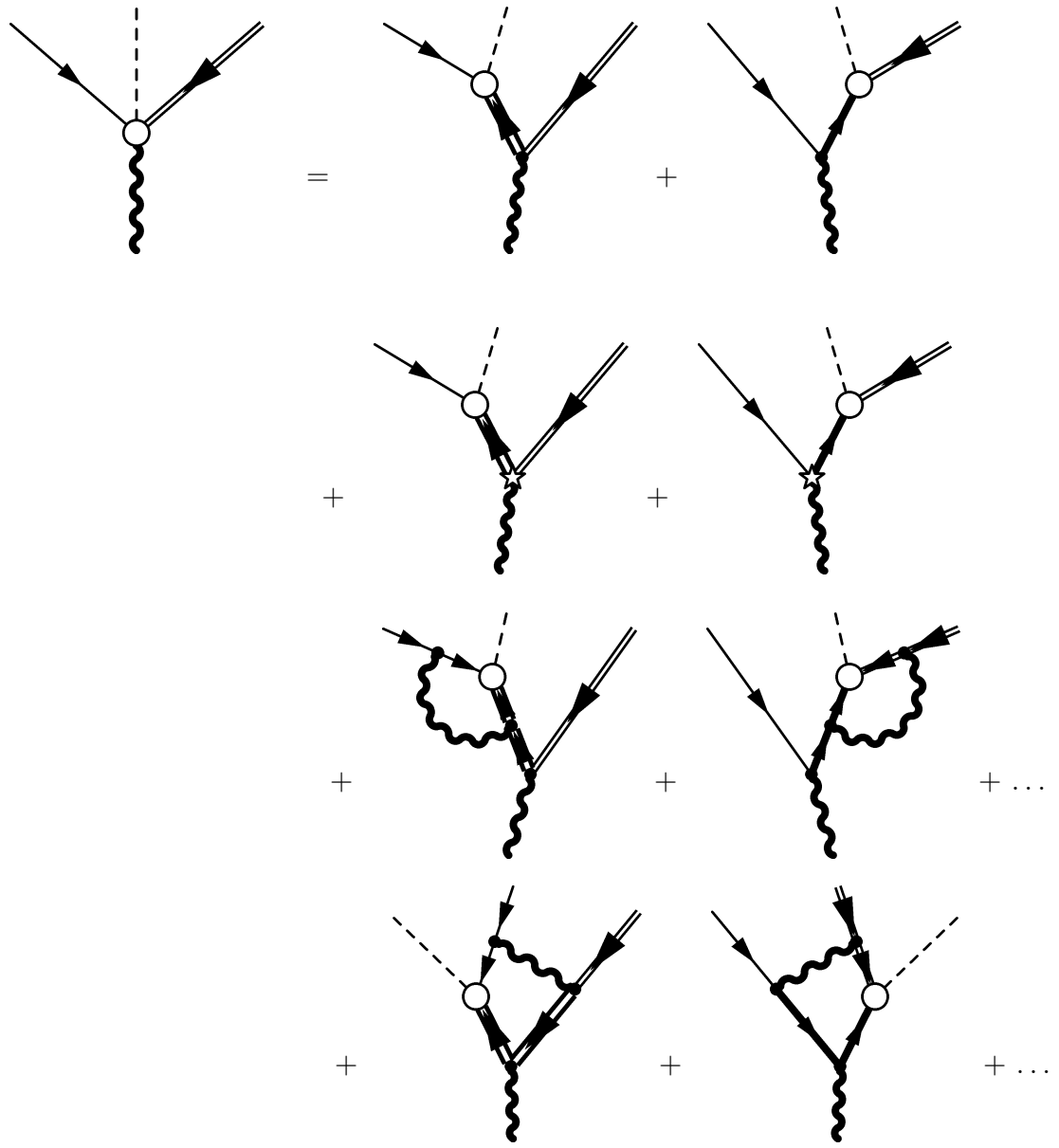

Figure D.2: Expansions of photon amplitude. The pentagram vertex is expanded in Figure D.3.

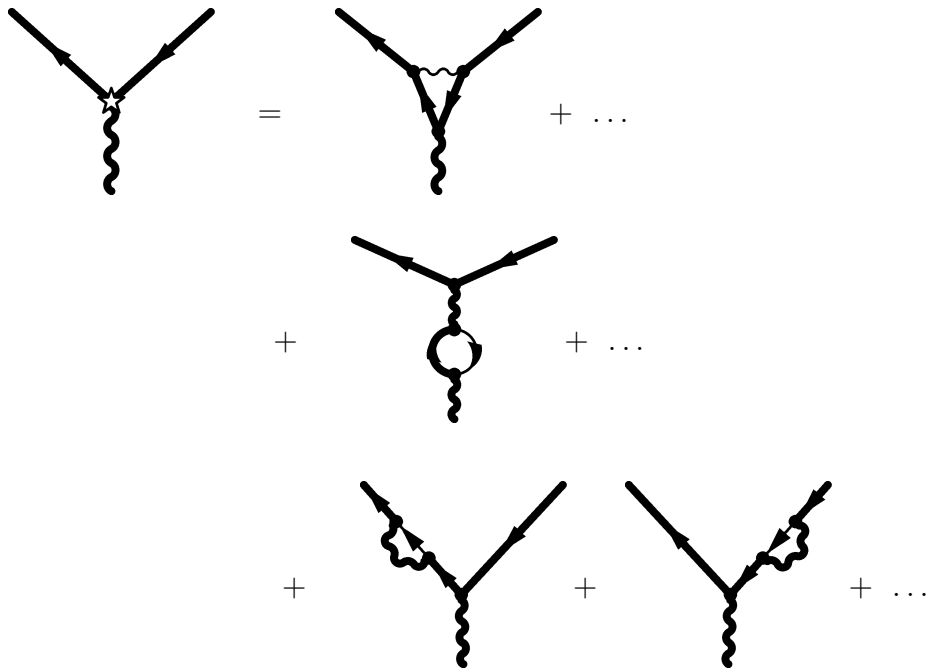

Figure D.3: Expansions of pentagram vertex. These are higher order corrections to the fundamental vertex. The external lines are not necessarily on shell or electron lines. The direction in time of the particles also does not matter.

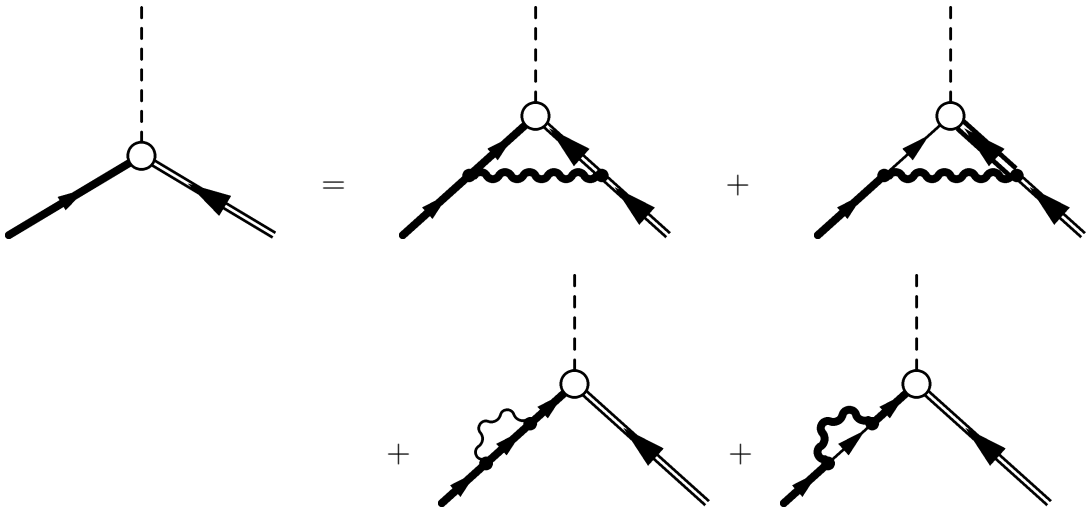

Figure D.4: Lowest order graphs.

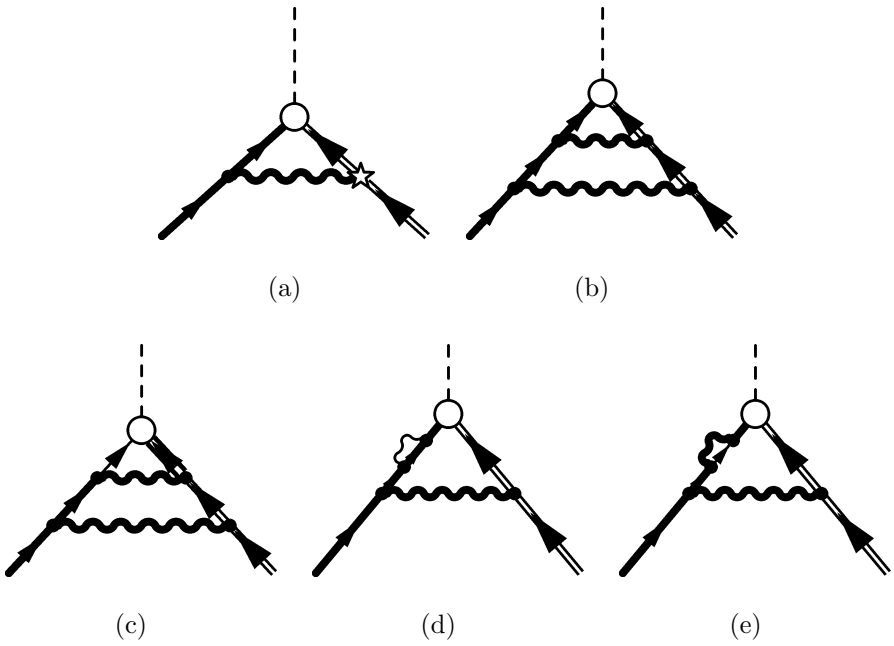

Figure D.5: NLO graphs from a.

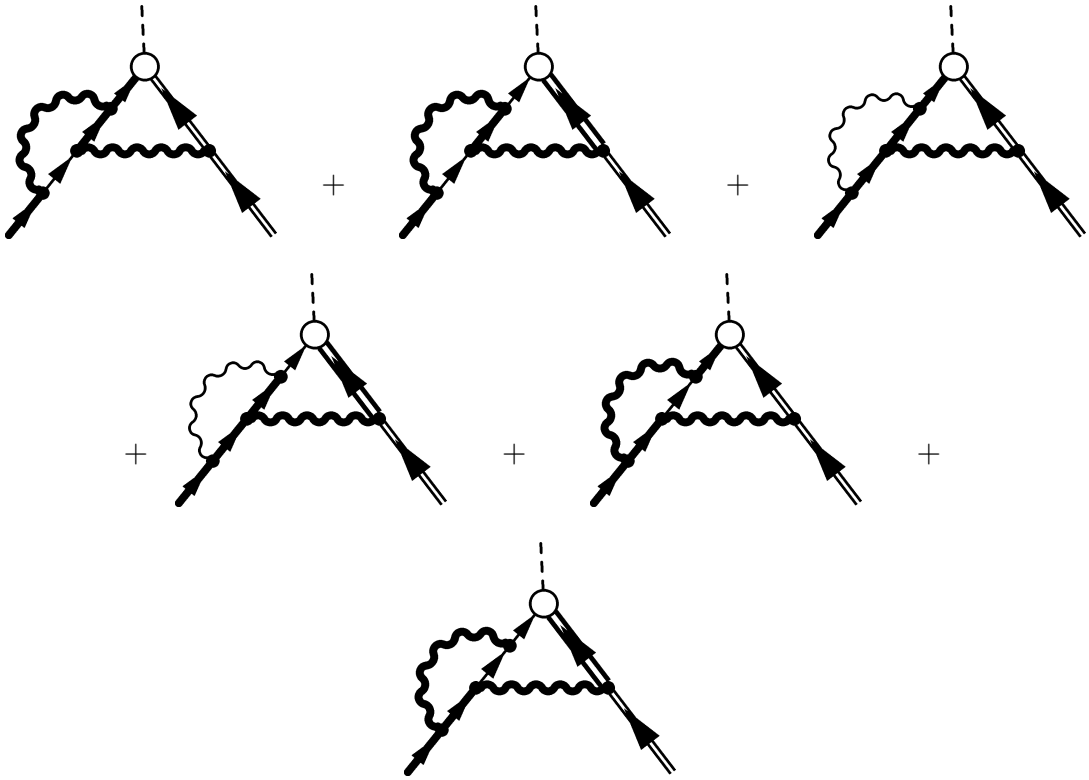

Figure D.6: All lepton vertex correction diagrams.

Bibliography

[1] R. Haag, K. Dan Vidensk. Selsk. Mat-Fys. Medd. **29** (12) 1 (1955).

[2] O. W. Greenberg, R. Ray, F. Schlumpf. Phys.Lett. **B353** 284 (1995).

[3] O. W. Greenberg, P. K. Mohapatra. Phys. Rev. **D34** 1136 (1986).

[4] O. W. Greenberg. Phys. Rev. **D47** 331 (1993).

[5] O.W. Greenberg, R. J. Genolio. Phys. Rev. **150** (1966).

[6] A. Raychaudhuri, Phys. Rev. **D 18**, 4658 (1978)

[7] O.W. Greenberg, Phys. Rev. **D17** 2576 (1966).

[8] H. Garcilazo, A. Valcarce, F. Fernandez, Phys. Rev. **C63** 035207 (2001).

[9] K. Pachuki, Phys. Rev. **A53** 2092 (1995).

[10] K. Pachuki, Phys. Rev. **A60** 3593 (1999).

[11] E. Borie, Phys. Rev. **A71** 032508 (2005).

[12] J. L. Friar, Ann. Phys. **122**, 151 (1979).

[13] O.W. Greenberg and S. Cowen,Phys. Rev. **A87** 042516 (2013).

[14] R. Pohl, et al, Nature **466**, 213 (2010).

[15] J. D. Carroll, A. W. Thomas, J. Rafelski, G. A. Miller, Phys Rev. **A 84** 012506 (2011)

[16] U. D. Jentschura, Ann. Phys. **326**, 500 2011.

[17] D. Robson, arXiv:1305.4552 [nucl-th].

[18] A. Antognini, et al, Science **339**, 417 (2013).

[19] C Carlson, V Nazaryan, K Griffioen. Phys Rev A83, 042509 (2011).

[20] V Barger, C W Chiang, W Y Keung, D Marfatia. PRL 106, 153001 (2011).

[21] D. Chen, Y, Dong, Phys. Rev. **C87**, 045209 (2013).

[22] M Gorchtein, F Llanes-Estrada, A Szczepaniak, Phys. Rev. **A87**, 052501 (2013).

[23] P Mohr, J. Griffith, J. Sapirstein, Phys. Rev. **A87**, 052511 (2013).

[24] L. Wang, W. Ni, Mod. Phys. Lett. **A 28**, 1350094, (2013).

[25] O.W. Greenberg, Phys. Rev. **139**, B1038 (1965); erratum, Phys. Rev. **156**, 1742 (1967).

[26] A. Raychaudhuri, "On the application of the N-quantum approximation to bound state problems," *University of Maryland Thesis* (1977), pp 1-101.

[27] E. Salpeter and H.A. Bethe, Phys. Rev. **84**, 1232 (1951).

[28] J. W. Norbury, K.M. Maung, D. E. Kahana. Phys. Rev. **A 50**, 2075 (1994).

[29] A. P. Martynenko, Phys. Rev. **A 71**, 2005.

[30] G. Källén, *Quantum Electrodynamics*, (Springer, New York, 1972).

[31] G.P. Lepage, Phys. Rev. **A 16**, 863 (1977).

[32] L.S. Dulyan, R.N. Faustov, Theor. Math. Phys. **22**, 220 (1973).

[33] M. Jarvinen. Phys. Rev. **D71**, 085006 (2005).

[34] W. Glockle and Y. Nogami, Phys. Rev. **D35**, 3840 (1987).

[35] W. Glockle, Y. Nogami, and I. Fukui, Phys. Rev. **D35**, 584 (1987).

[36] X. Artru, Phys. Rev. **D29**, 1279 (1984).

[37] O.W. Greenberg and S. Cowen, Int. J. Mod. Phys. Int. **A 27**, 1250133 (2012).

[38] P. P. Kulish and L. D. Faddeev, *Teor. Mat. Fiz.* **4**, 153 (1970).

[39] M. Lavelle and D. McMullan, *Ann. Phys.* **282**, 471 (2000), arXiv:hep-ph/9909257v2.

[40] P. A. M. Dirac, *Can. J. Phys.* **33**, 650 (1955).

[41] M. Creutz, *Ann. Phys.* **117**, 471 (1979).

[42] E. V. Stefanovich, *Ann. Phys.* **292**, 139 (2001).

[43] O.W. Greenberg and S.S. Schweber, *Nuovo Cimento* **8**, 378 (1958).

[44] L. Schwartz, *Theorie des distributions* (Hermann & Cie, Paris 1966).